Master Thesis

Trend analysis of the runoff patterns in Central and Northern Europe: Identification of changes in magnitude and timing.

Authors

Akrivi Alexandraki

Supervisors

Markus Hrachowitz

Gerrit Schoups

Faculty of Civil Engineering

MSc Water Management Delft University of Technology

Acknowledgements

Two years back, after working as a civil engineer in an environmental assessment office in Athens, I made a big decision to learn more. So, I came to the Technical University in Delft. In my first year, I really enjoyed studying Water Management and the projects were exciting, like working and living in Ghana for almost two months.

Also, during my studies I met some interesting people there who inspired me a lot. Two of these inspiring people were Markus and Gerrit, and I want to thank them. They didn't just help me with my thesis work, but they also made a personal impact on me. Markus is full of energy and enthusiasm. He got me interested in hydrology and helped me focus on really understanding it deeply, instead of just passing the courses. I also owe a big thank you to Gerrit. He's a really generous professor and he's always there to support all of the students. He was available all the time and helped me out whenever I had questions. Both professors made me feel comfortable asking anything, which was really important for me.

I couldn't have come this far or done my research without my family's support. My mom, dad, and younger sister have been there for me consistently. But I want to give special thanks to my parents. They're both highly educated, and they could have studied abroad, but because of financial reasons, they couldn't. Even so, they continued their studies in Greece, imparting upon their children the ethos that "learning never ceases."

I also want to thank my partner, Kostas. He's been by my side through thick and thin, especially since we're in a foreign country. We support each other and are working together to make our dreams real.

Last but not least, a big shoutout to all my friends. I can't leave anyone out because they've all been there for me. We've had fun, gone on trips, and helped each other through tough times. These moments mean a lot to me, and I'm really thankful for them.

Delft, September 2023

Akrivi Alexandraki

Abstract

In today's world, extreme flooding and drought events are becoming increasingly common globally. These challenges arise from various factors, with climate change and changes in land use being among the most significant contributors.

While numerous studies have explored the combined impact of climate change and land use on streamflow, there is a research gap when it comes to analyzing historical data for changes in the magnitude and timing of discharge peaks and low-flow periods. To address this gap, this MSc Thesis investigates river discharge in five European countries: Belgium, Germany, France, Luxembourg, and the Netherlands.

To analyze potential patterns and variations in magnitude changes, trend analyses were conducted for annual and monthly mean daily flows. Non-parametric methods such as Sen's slope and the Mann-Kendall test were employed to calculate trends in average, maximum, and minimum daily flows at both yearly and monthly levels. The issue of autocorrelation in discharge flows was also addressed by using a modified version of the Mann-Kendall test for stations with autocorrelated data. Furthermore, the possible shifts in the timing of discharge peaks and low-flow periods were examined. We employed statistical tools such as statistical entropy, Kullback-Leibler divergence, and various descriptive statistics to determine if there have been changes in the month with the highest flow over the years.

The study's results generally align with existing research. Regarding annual discharges, for average and maximum analyses, stations with decreasing trends were predominantly found in the North, East, and central parts of the study area (Germany), while the North-West exhibited stations with significant increasing trends in most cases (North France).

In yearly minima discharge flows, the patterns were aligned with average and maximum analyses; however, additional stations showed decreasing trends, which were located in Belgium. In the monthly analysis, positive trends were primarily observed during winter months (February, December, and January), while April and March showed decreasing trends in most cases (monthly average and maxima analyses), with a few exceptions in minimum daily flows.

Notably, more than 50% of the stations exhibited shifts in the month when they experienced maximum and minimum discharge, particularly between 1980-2000 and 2000-2021. This finding suggests potential avenues for future research.

Keywords –Trend analysis, Statistical analysis, Mann Kendall, Sen's slope, Autocorrelated data

Contents

List of Figures

List of Tables

1 Introduction

Today, Europe faces critical challenges with river flooding, droughts, and their worsening due to climate change and land use impacts. These issues not only threaten the environment but also have far-reaching economic and societal consequences. Climate change has already altered in an extent the hydrological cycle, affecting precipitation, evaporation, and temperature patterns, leading to significant changes in discharge volumes (Lehner et al., 2006). Additionally, human activities like urbanization, deforestation, and agriculture expansion can disrupt natural drainage patterns, altering discharge volumes.

To address these challenges, climate adaptation is crucial. Before implementing adaptation strategies, a comprehensive understanding of the hydrological system is essential. This knowledge provides a vital foundation for informed predictions and improved preparedness.

These considerations motivate this Master's thesis. The introductory chapter begins with an extensive literature review, leading to the problem statement. Based on this problem, we formulate research questions, concluding with an overview of the study's structure.

1.1 Literature review

In the literature review, the impact of climate variations and land use on discharge pattern changes, particularly in terms of magnitude and timing, is investigated. The review begins by defining climate change terminology and its influence on the hydrological cycle. Subsequently, an analysis of various studies explores the impact of global warming on discharge flows and projections of temperature and precipitation patterns in European countries. Land cover dynamics and land use changes in Europe are also assessed. At the conclusion of the literature review, we summarize existing research findings and projections to understand the academic consensus on European discharge changes due to climate and land use.

1.1.1 Climate change & Hydrological Impacts

1.1.1.1 Climate change

Climate change, widely debated, holds varying definitions. The Framework Convention on Climate Change (FCCC) defines it as alterations in climate due to human behavior, notably the increase in greenhouse gases intensifying the natural greenhouse effect (United Nations, 1992). This is expected to cause additional warming and potential adverse consequences for both natural ecosystems and humanity (United Nations, 1992). In contrast, the Intergovernmental Panel on Climate Change (IPCC) defines climate change as modifications in climate patterns over time, regardless of natural or human causes (Roger A. Pielke, 2004). While climate change has natural components, human activities over the past two centuries have exacerbated it, extending its influence on various sectors, including the hydrological cycle (Connors et al., 2021).

1.1.1.2 Hydrological cycle

The hydrological cycle, or water cycle, involves interconnected processes that move water between Earth's reservoirs (Kuchment, 2004). Key hydrological processes include evaporation, transpiration, precipitation, runoff, sublimation, infiltration, snowmelt, interception, subsurface flow, and capillary rise. Solar energy drives evaporation, turning water into vapor, which later condenses to form clouds and falls as precipitation, such as rain, snow, or hail (Kuchment, 2004).

Evaporation and precipitation are crucial in the water cycle. The "Law of conservation of mass" (Eq. 1.1) is fundamental mathematical way to express these processes. It underlines the principle behind the movement of water through evaporation and precipitation (Kuchment, 2004).

$$\text{Inflow} - \text{Outflow} = \text{Storage Change} \tag{1.1}$$

In analyzing critical hydrological processes, such as precipitation, basin evaporation, runoff, and changes in storage (surface waters, soil moisture, groundwater, intercepted water), we create the continuity equation (Eq. 1.2) for a river basin, as outlined by Kundzewicz

(2008).

$$\text{Precipitation} - \text{Evaporation} - \text{Runoff} = \text{Storage Change} \tag{1.2}$$

Global warming affects evaporation and precipitation through temperature changes (1.3). This equation shows that temperature impacts atmospheric water-holding capacity, influencing evaporation and precipitation (Kundzewicz, 2008).

$$\frac{de_s(T)}{e_s(T)} = \frac{L}{R \cdot T^2} dT \tag{1.3}$$

Where:

$e_s(T)$: Saturated vapor pressure of water vapor at temperature T.

L : Latent heat of vaporization, representing the energy needed for water to vaporize.

R : Gas constant, a fundamental constant in physics and chemistry.

T : Temperature at which the equation is evaluated (in Kelvins, K).

$de_s(T)$: Change in saturated vapor pressure with respect to temperature.

dT : Small change in temperature over which the change is evaluated.

1.1.1.3 Changes in Temperature Patterns

As already mentioned, the increased temperature caused by global warming plays a pivotal role in influencing evaporation and precipitation patterns. Temperature fluctuations have historically been influenced by natural factors, notably changes in Earth's orbital path. However, the contemporary warming trend, initiated in the mid-1800s, stands out as a distinct phenomenon primarily driven by human activities, particularly the release of heat-trapping gases like carbon dioxide, methane, and nitrous oxide during the Industrial Revolution (Santer et al., 2003). These human-induced emissions have contributed to a significant global temperature rise of approximately 1.1°C (IPCC, 2022).

Especially Europe experienced a substantial temperature rise, averaging +0.5°C per decade between 1991 and 2021, double the global average (Organisation, 2022), (Twardosz et al., 2021). Regional variations exist, with central and northern Europe showing higher trends, while Western Europe expects relatively lower temperature increases (Twardosz et al., 2021; European Environment Agency, 2023a).

Mediterranean countries now exceed global mean warming, with projections suggesting continued high warming trends (Linares et al., 2020b) (European Environment Agency, 2023a). Eastern Europe has seen an increase in warm extremes, particularly during winter (Vyshkvarkova and Sukhonos, 2022).

1.1.1.4 Changes in Precipitation Patterns

Atmospheric warming can lead to both increased and decreased precipitation due to its complex nature (European Environment Agency, 2023a; Kundzewicz, 2008). This complexity results in significant variability and uncertainty in projections across different regions.

Research suggests central Europe may experience more intense rainfall events, but North German lowlands have seen increased aridification (Zeder and Fischer, 2020; Weigel et al., 2022).

In the Mediterranean Basin, extended dry seasons and heatwaves may reduce rainfall (Linares et al., 2020a). Predictive models vary, with some indicating a 12% decrease in winter precipitation in southern Europe (Deser et al., 2017). The central north-eastern Mediterranean Sea region could see more frequent, heavy, and severe precipitation events (Georgoulias et al., 2022).

Western Europe saw increased precipitation until the 1950s, followed by a decline and recovery (Kundzewicz, 2008). North France may experience a moderate increase in precipitation (Terray and Boé, 2013).

1.1.2 Changes in Land Use & Land Cover

When investigating hydrological processes, it is essential not only to consider the effects of climate change but also to evaluate the significance of land cover and its alterations, which play a substantial role in shaping discharge volumes. Land use encompasses a spectrum of human activities within specific geographical regions, such as agriculture, forestry, urban development, entrepreneurial initiatives, and environmental preservation. Recognizing the interplay between these factors is integral to comprehending the dynamics of hydrological systems and their responses to changing conditions (Winkler et al., 2021).

1.1.2.1 Land Use Changes & Hydrological Impacts

A multitude of alterations in land cover and land use have exerted profound influences on hydrological patterns. Below, we enumerate key land changes and scrutinize their impact on discharge volumes:

1. **Deforestation:** The ability of the ground to absorb and store water is diminished when forests and other types of vegetation are destroyed. Increased runoff, soil erosion, and decreased groundwater recharge may result from this. As a result, during periods of rainfall and during dry spells, the discharge quantities in streams and rivers may change (Winkler et al., 2021).

2. **Agriculture activities:** The ability of the land to hold water may change as agricultural activities are expanded, such as when natural landscapes are turned into farmland. Surface runoff and discharge volumes may rise as a result of land use changes, especially in regions with extensive irrigation systems or a shift in the sorts of crops grown there (European Environment Agency, 2017).

3. **Urbanization:** Rainfall infiltration into the earth is reduced when natural landscapes are transformed into urban areas with impermeable surfaces like highways and buildings. This causes an increase in surface runoff, which causes rainstorm events to produce greater and faster discharge volumes. Flooding that is both more frequent and severe can be attributed to urbanization (European Environment Agency, 2017), (Winkler et al., 2021).

4. **Reservoir construction:** A river's seasonal flow patterns can be altered by dams. It is possible for water behind a dam to be discharged when it normally wouldn't. The timing of high and low flows may be impacted, which may have an effect on downstream users and aquatic ecosystems (Rottler et al., 2020).

5. **Wetland loss:** The drainage of wetlands has multifaceted consequences. On one hand, it leads to diminished surface water levels within wetland ecosystems, potentially jeopardizing the water supply for the diverse plant and animal species

reliant on these habitats. On the other hand, this practice can trigger a decline in local groundwater levels, causing a reduction in the volume of water stored underground. The repercussions extend beyond the wetlands themselves, as lowered groundwater reserves can have a broader impact on water availability in the surrounding areas, making the management of wetlands and their associated hydrological systems a critical aspect of environmental conservation (Bring et al., 2022).

1.1.2.2 European Land Cover

The European Environment Agency provides information from Land Monitoring Service of Copernicus and Corine Land Cover Classes (European Environment Agency, 2023b) for European Union Member countries. The EU Countries displayed distinct land cover patterns for 2018, as visualized in the bar chart below (Figure 1.1). The largest expanse of land is enveloped by forests and semi-natural areas, constituting the prevailing majority (almost 49%). Agricultural regions span nearly 42%, while artificial surfaces claim approximately 4%.

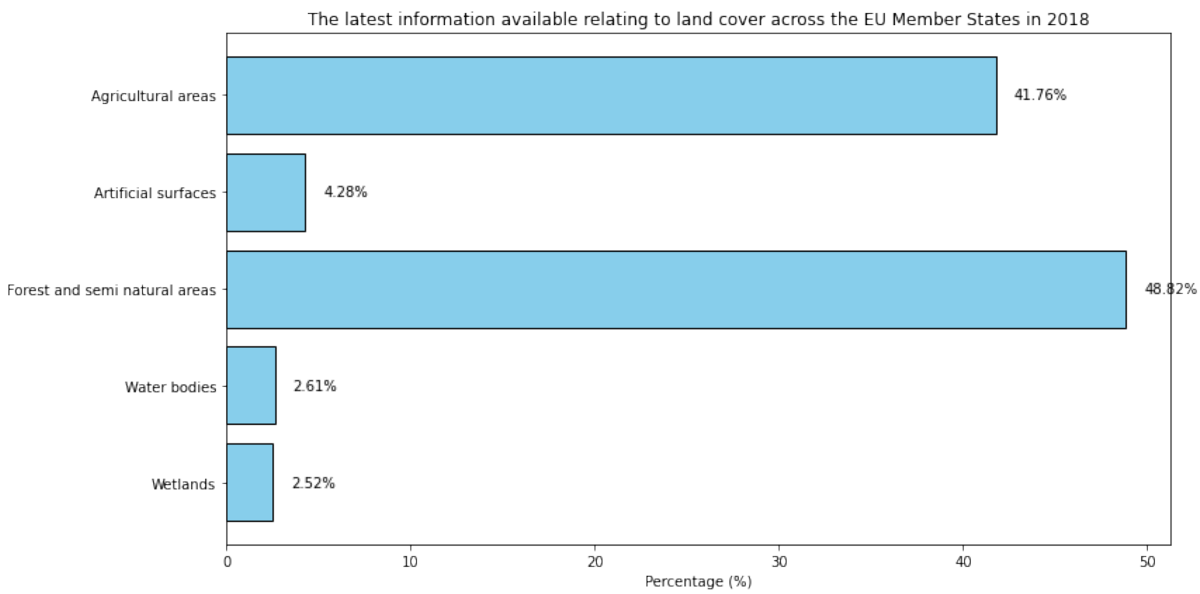

Figure 1.1: Land cover across European countries for the year of 2018 (European Environment Agency, 2023b).

In the forthcoming tables, we delve into the intricate landscape of land cover in European countries and the transformations it underwent from 2000 to 2018 (European Environment

Agency, 2023b). These tables encompass detailed percentages for five specific European countries, the focal points of our ongoing study.

First, table 1.1 features five predominant land use categories derived from Corine data: Agricultural areas, Artificial surfaces, Forest and semi-natural areas, Wetlands and Water bodies for 2018. Additionally, whenever open-access information maps are available, the table contains geographical information pinpointing the location of each land cover category. This comprehensive overview facilitates a holistic understanding of the land cover and utilization within each country (European Environment Agency, 2023b).

Table 1.1: Land Use Statistics for Europe and Belgium, France, Germany, Luxembourg, and Netherlands (2018) (European Environment Agency, 2023b).

Country	**Artificial surfaces (%)**	**Agricultural areas (%)**	**Forest and semi-natural areas (%)**	**Wetlands (%)**	**Water bodies (%)**
Belgium	**20.91** (mainly around Brussels, north part of the country and center)	**56.93**	**21.12** (mainly in the South)	**0.36** (mainly in North and South East)	**0.68**
France	**6.00** (around Paris, and North and east part)	**58.65**	**33.76** (almost in the whole country, less in North and West)	**0.70** (South-East and West)	**0.89**
Germany	**9.37** (West, South East, North)	**56.50**	**31.30** (almost in the whole country)	**1.25** (North)	**1.59**
Luxembourg	**10.57** (almost the whole country)	**52.55** (almost the whole country)	**36.51** (almost the whole country)	**0.02** (no information)	**0.35**
Netherlands	**13.75** (mainly in the west part of the country and in the South)	**59.70** (almost equally distributed around the country)	**10.76** (mainly in the center, less amount in the South-West and North-East)	**7.15** (North-East and South-East)	**8.65**

Second, the table (Table 1.2) serves as a compelling visual representation of the shifts in land cover over an extensive 18-year period, spanning from 2000 to 2018, across five prominent European countries. The featured percentages offer a clear indicator of the dynamic direction of these changes, whether they lean towards a positive or negative percentage. For instance, consider Belgium, which witnessed a decline of 0.07% in its agricultural land cover from 2000 to 2018. This is further exemplified by the fact that in 2018, agricultural areas accounted for 56.93% of the landscape, while in 2000, this figure stood slightly higher at 57.21%. All these nuanced transformations are meticulously charted within Table 1.2.

Table 1.2: Land Use Change Differences (2000 - 2018) (European Environment Agency, 2023b).

Area	Artificial surfaces	Agricultural areas	Forest and semi natural areas	Wetlands	Water Bodies
Belgium	-0.09%	-0.07%	-0.19%	-0.29%	-0.64%
France	0.00%	-0.15%	0.12%	-0.40%	-0.18%
Germany	0.30%	-0.60%	-0.23%	0.01%	-0.45%
Luxembourg	0.42%	0.90%	0.00%	0.02%	-0.35%
Netherlands	0.58%	-2.14%	0.00%	-2.70%	-0.76%

1.1.3 Changes in Discharge Patterns

1.1.3.1 Influences on Discharge Patterns: Climate and Land Cover Changes

As previously noted, understanding discharge patterns requires considering not only climate fluctuations (Hanus et al., 2021b) but also various other parameters, such as land cover and land use alterations (Petrow and Merz, 2009), which impact runoff dynamics. Specifically, climate and land use changes influence both the discharge magnitude and the timing of peak flow occurrences.

1.1.3.2 Magnitude and Timing Shifts

In terms of climate dynamics, regions characterized by elevated altitudes and colder climates witness an increase in river flow due to rising temperatures, leading to amplified snowmelt. Conversely, regions with milder climates, where the water cycle primarily hinges on rainfall and evaporation, experience changes in flow magnitude primarily linked to alterations in precipitation levels (Blöschl et al., 2017, 2019).

From a land use perspective, alterations in land cover, often in concert with climate variations, frequently result in shifts in discharge magnitude. For example, research by Ward et al. (2008) underscores how changes in forest types can impact evaporation and transpiration rates, culminating in higher mean discharge and increased flood frequency. This study also highlights a strong correlation between deforestation and heightened mean discharge. Additionally, modifications like shifts in crop types can influence discharge patterns (Ward et al., 2011). Urbanization plays a significant role in Europe. Increased impermeable surfaces, combined with reduced evaporation rates in certain cold areas, have resulted in substantial increases in streamflow (Teuling et al., 2019).

The timing of peak flows holds equal importance. Climate change has precipitated shifts in the timing of snowmelt and river floods. Elevated temperatures have triggered earlier spring snowmelt floods in northeastern Europe, while delayed winter storms, linked to polar warming, have postponed winter floods along the North Sea and specific Mediterranean coastal areas. Anticipated earlier soil moisture peaks have led to advanced winter floods, underscoring the far-reaching influence of climate change on flood timing across a continental scale (Blöschl et al., 2017, 2019).

1.1.3.3 Discharge Magnitude Trends in Europe

In 2021, across Europe, river discharge demonstrates a prevailing pattern of decreasing trends, consistently remaining below the historical average for approximately two-thirds of the year, as reported by the European State of Climate and Copernicus (Copernicus EMS/ECMWF., 2021). Nonetheless, it is essential to acknowledge the trends in river flows (Copernicus EMS/ECMWF., 2021). The subsequent section elucidates the intricate variations in river discharge across diverse regions of the continent.

In northwestern Europe, an upward trend in flood discharges has emerged, with nearly 69% of monitoring stations reporting an average local increase of approximately +2.3% per decade (Blöschl et al., 2019). This trend aligns with findings by Bertola et al. (2020) for the same region. Notably, changes in land cover over the past century in northwestern Europe, including an increase in coniferous forests, have contributed to higher mean discharge and increased flood frequency (Ward et al., 2008). Furthermore, data from the Copernicus Climate Change Service indicates that in 2021, July witnessed recordbreaking river discharge levels, coinciding with unprecedented flooding events. Historically, during the winter months, February and January were recognized as the peak periods for river discharges within the reference period spanning from 1991 to 2020 (Copernicus EMS/ECMWF., 2021). Additionally, future projections suggest that the mean 50-year discharge for northwest Europe will surpass historical levels due to the combined effects of climate change and land use changes (Ward et al., 2011).

In contrast, southern Europe has witnessed decreasing trends in floods due to diminished precipitation and heightened evaporation, resulting in fewer flood occurrences in medium and large catchments (Blöschl et al., 2019). These negative trends align with findings in the study by Bertola et al. (2020).

Central Europe, particularly Germany, has experienced heightened drought probabilities, especially during summers, because of reduced rates of Standardized Precipitation Evaporation and transpiration Index (SPEI) values (Al-Qubati et al., 2023). Notably, the diminishing trends in flood behavior within Germany are concentrated primarily in the eastern part of the country, specifically within the Elbe catchment (Petrow and Merz, 2009). Regarding urban areas of Germany, it is supported that they have to manage severe floods because of the reduced infiltration capacity (Bronstert et al., 2002). This observed increase in trends finds further corroboration in additional studies that investigated a comparable time frame in Germany. These studies revealed a consistent pattern of increasing trends within the period from 1960 to 2010. The ascertainment of this trend was achieved through a meticulous trend analysis employing non-parametric methods (Blöschl et al., 2019). Furthermore, in central Europe, we observe decreasing trends in flood peak records due to the construction of dams and river training initiatives. These efforts are primarily aimed at regulating river flow and generating hydropower, which have an impact on discharge volumes (Villarini et al., 2011).

Eastern Europe has also seen decreasing trends (Blöschl et al., 2019), particularly in snow cover and snowmelt due to warmer temperatures, resulting in reduced flood occurrences. However, the extent of these negative trends in eastern Europe is contingent upon catchment size, as emphasized by Bertola et al. (2020).

1.2 Problem Statement & Research Objective

As evident from the extensive literature review, climate change and land cover alterations have significantly impacted discharge volumes in Europe. Projections underscore the urgency of further investigation into this subject.

Despite the importance of grasping the effects of climate change on European discharge volumes, a research gap exists, particularly concerning the timing and magnitude of annual and monthly extremes in historical data across the continent (Hanus et al., 2021a).

Moreover, in the present study, we employ the most current data available, extending up to 2021, to meticulously manage historical data. Data management is important not only to understand the current discharge magnitude and timing of peaks and minima, but also can be possibly used as the basis for other research, such as predictive hydrological models, in order to test their results.

Given these considerations, our primary research motivation is to examine historical discharge data from Northern and Central European catchments. Our goal is to contribute to a more profound understanding of magnitude trends and potential shifts in peak and low flow timings within specific European catchment areas.

1.3 Research Question

Based on the aforementioned issue and the objective of managing historical discharge data while exploring potential alterations in magnitude and timing, the following research questions arise, accompanied by sub-questions aimed at refining the inquiries addressed within the present study.

Are there any historical changes in the discharge patterns in specific European catchments?

Sub-questions:

- Are there any trends in magnitude (increasing or decreasing) of the runoff (average, maximum and minimum) of the examined catchments based on the given dataset (yearly analysis of data)? Which month contributes more to changes (monthly analysis of data)?

- Are there any changes in the timing of the runoff of the examined catchments (change of the month when the maximum and minimum flow happens during the year)?

1.4 Outline

To address the research question, this MSc Thesis follows a structured approach, commencing with an extensive literature review (1.1) in the Introduction chapter (1).

The subsequent chapter (2), titled "Background Information," provides information about the case study area. It includes a geographical description of the area (2.1), location of the discharge stations and details about data availability (2.2).

The Methodology chapter (3) provides a detailed insight into the research methods used throughout this study. It offers a thorough explanation of the various levels of analysis: yearly (4.1.1) and monthly analysis (3.1.3). These explanations involve calculating average, maximum, and minimum discharge values to identify potential changes in magnitude. Moreover, the methods used for investigating possible shifts in timing are also analyzed. Additionally, the chapter includes information on the methods employed for trend analysis (3.3) and statistical analysis (3.4). These analyses were conducted using a Python code specifically developed for this study's data analysis. This detailed methodology equips readers with a clear understanding of the upcoming results, which are presented in the subsequent chapter (4).

Looking ahead, the obtained results are examined in the Results chapter (4), and a thorough discussion follows in the Discussion chapter (5). This meticulous examination culminates in the Conclusion chapter (6), where definitive responses to the primary research question, accompanied by answers to pertinent sub-questions, are presented, along with valuable recommendations for future research.

2 Background Information

2.1 Case study area

The current MSc thesis aims to manage a large number of stations measuring mean daily flows in cubic meters per second (m^3/sec). There are a total of 1185 stations covering an area of approximately approximately 2293829.915 square kilometers (km^2). The stations are located in five countries: Belgium, Germany, France, Luxembourg, and the Netherlands. Specifically, they are situated in various regions in Belgium and Luxembourg, the southeastern part of the Netherlands (near Maastricht), the northern and eastern parts of France, and the central and eastern-southern parts of Germany. Additional information about the case study area and the location of the stations can be found on the accompanying Map 2.1 in which the circles correspond to each station.

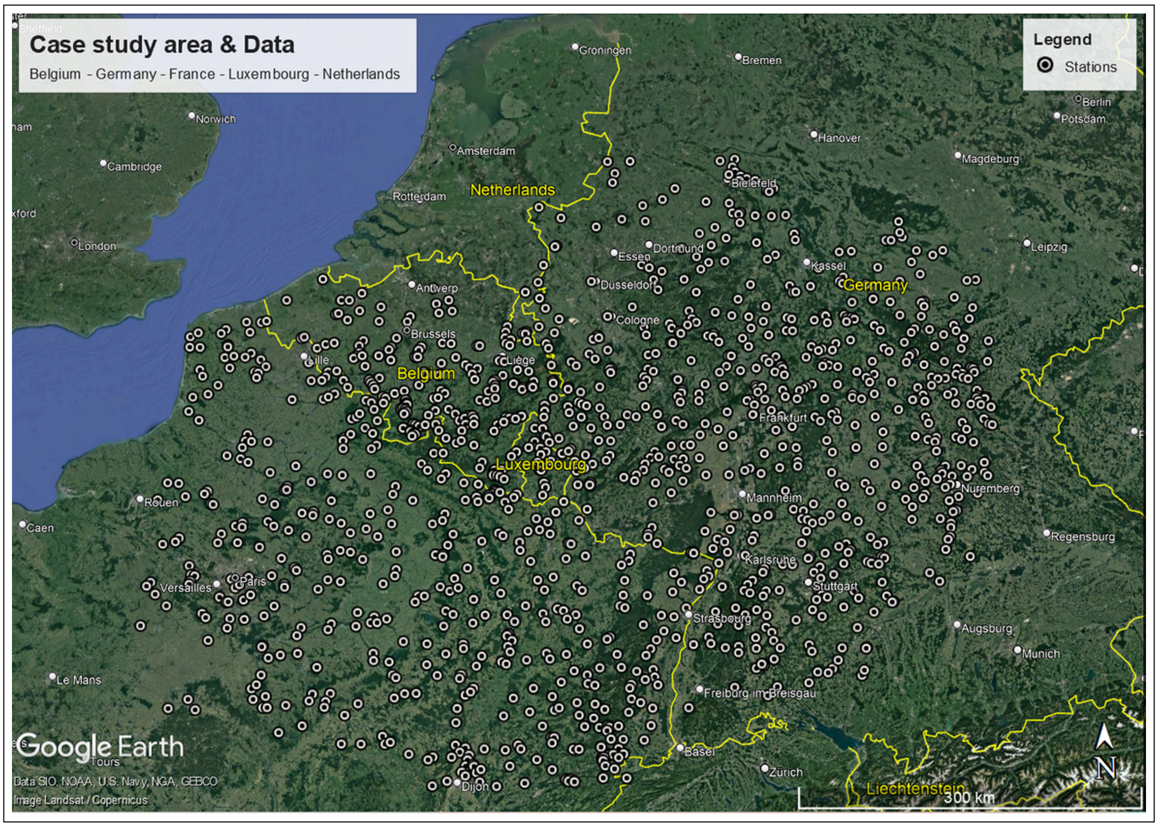

Figure 2.1: Stations located in five different countries: Belgium, Germany, France, Luxembourg, and the Netherlands.

2.1.1 Digital Elevation Map

To gain insights into the region's elevation, a Digital Elevation Map (DEM) analysis was conducted using QGIS (Map 2.2), an Open Source Geographic Information System. DEM data, sourced from EARTHDATA (NASA), was used to create elevation maps. The spatial resolution of the DEM is 90m. This revealed the variations of the location of the stations within the study area, ranging from ground level to almost 1000 m. Notably, the Northern region and parts of North East Germany, Netherlands, North Belgium, and North Eastern France have low elevations, while central and southern Germany, along with South East France, exhibit elevations reaching 968 m.

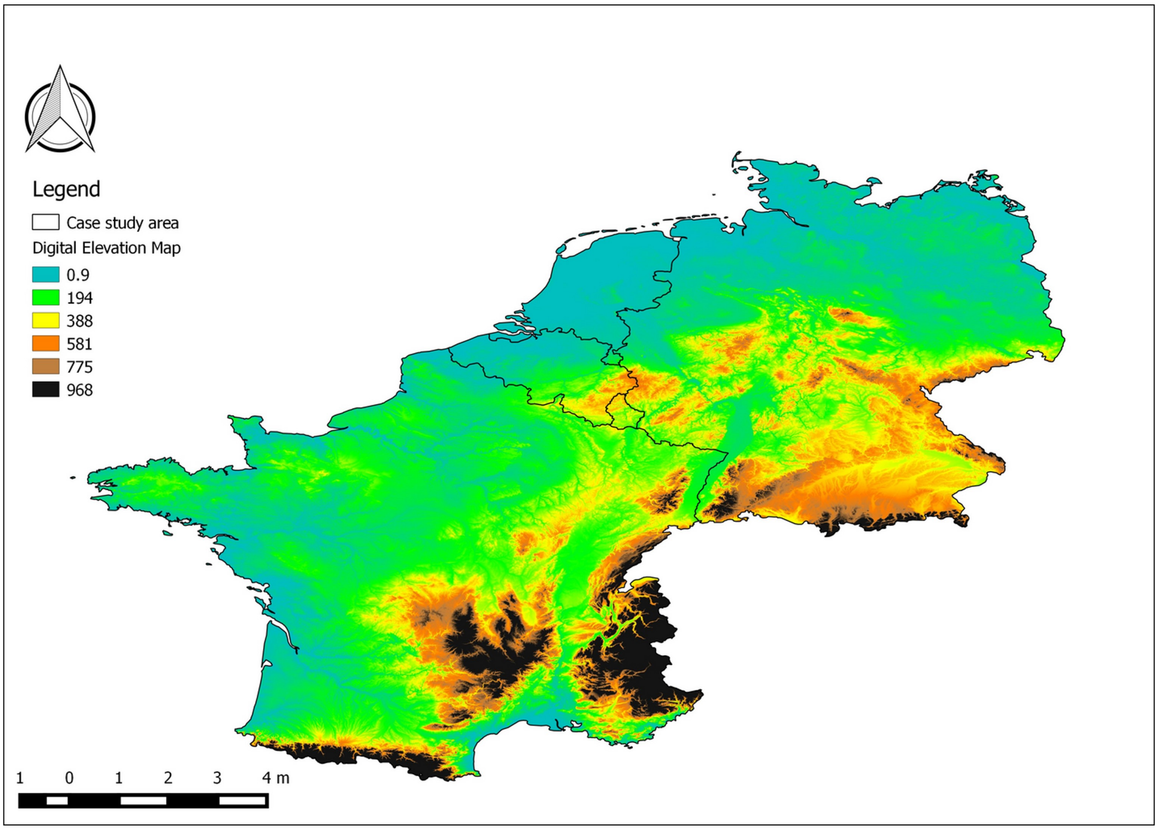

Figure 2.2: Digital Elevation Map: the orange to black colors correspond to higher elevations (from 581 up to almost 1000 m), the blue to yellow colors correspond to lower elevations (from ground level up to almost 400 m).

2.1.2 Catchment areas

Furthermore, it is essential to understand the geographical extent and boundaries of these basins. Table 2.1 provides an overview of the catchment areas, ranging from the smallest to the largest, measured in square kilometers (km^2), for each country. Additionally, the table 2.1 includes the count of catchments within each country as valuable information.

Table 2.1: The ranges of the catchment areas in different countries:

Country	Catchment area km^2	Number of catchment
Belgium	1 to 23000	99
Germany	6 to 159300	348
France	8.13 to 64200	239
Luxembourg	70.03 to 4231.80	10
Netherlands	27.11 to 160800	9

Furthermore, the delineation of watersheds plays a crucial role in understanding the case study area. To achieve this, we leveraged a Digital Elevation Map and customized code developed by Heberger, enabling us to delineate over 1000 watersheds. The code was tailored to handle the 1185 stations within the case study area. We harnessed Python and the API offered by the Global Watersheds web app at mghydro.com (Matthew Heberger, n.d.) to automate the watershed delineation process. The results are visualized in Map 2.3. Notably, the stations in this study area are closely situated, resulting in overlapping catchment areas. The map boasts a resolution of 90 meters, with distinctively colored circles representing basin outlets. These circles share the same color as their corresponding basins but appear darker for enhanced clarity.

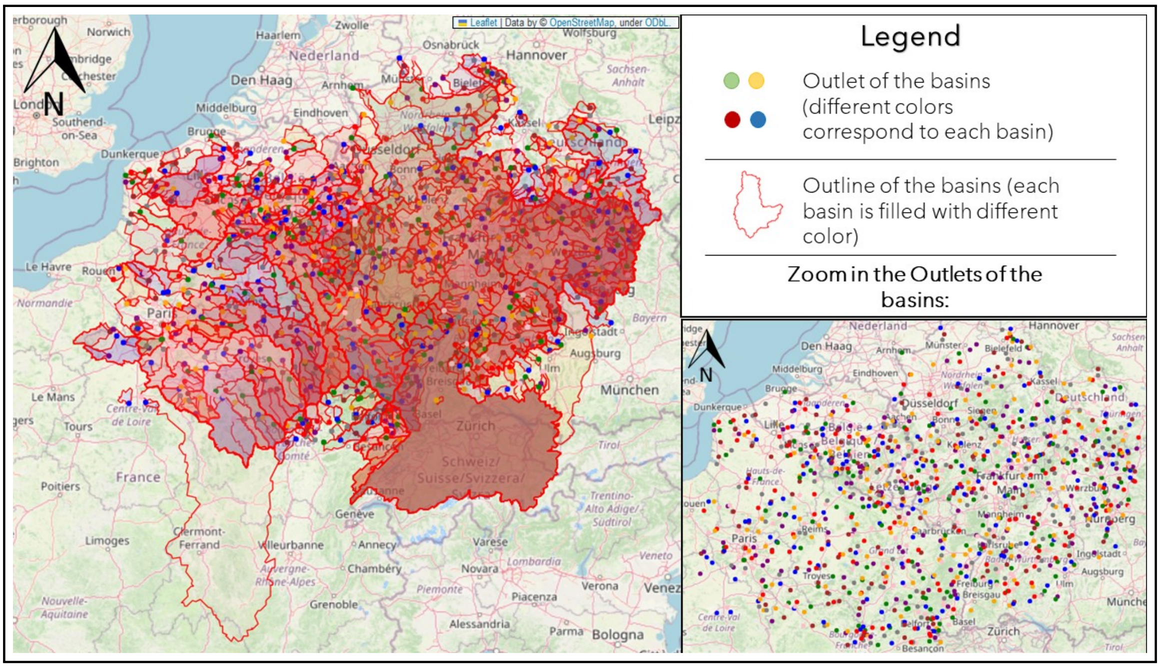

Figure 2.3: Delineation of the watershed: the colorful points denote the basin outlets, while the red polygons represent the basins themselves. Each basin is distinguished by its distinct color.

2.2 Data Availability

As already mentioned, the discharge volumes representing the mean daily flow in cubic meters per second (m^3/sec) are obtained from various country-specific sources. For Belgium, the dataset is accessible through the providers "Hydrometrie Wallonie" (Service Public de Wallonie, n.d.) and "Waterinfo Belgium" (Belgian Federal Public Service for Public Health, Food Chain Safety and Environment, n.d.). Germany provides its dataset via the provider "Pegelportal" (Landesamt für Umwelt, Naturschutz und Geologie Mecklenburg-Vorpommern, n.d.). In the case of France, the dataset is made available through the provider "Hydro Eau France" (Ministry for the Ecological Transition, France, n.d.). Luxembourg's dataset can be obtained from the provider "Inondations Luxembourg" (Ministère de l'Environnement, du Climat et du Développement durable, Luxembourg, n.d.). Lastly, the dataset for the Netherlands is obtainable through the provider "Rijkswaterstaat" (Rijkswaterstaat, Ministry of Infrastructure and Water Management, Netherlands, n.d.). It should be noted that precise information is available regarding the exact locations of all the stations, including their longitude and latitude coordinates. Additionally, comprehensive data is provided for the station ID, the Gauge name, the associated stream, and the corresponding catchment area.

To account for varying data availability, a summary Table 2.2 was created. This table displays the average data period and the associated station count per country. Examining these time spans is crucial for identifying variations and patterns. However, the specific data availability is as follows:

1. Belgium 1975-2021
2. France 1987-2021
3. Germany 1922-2021
4. Luxembourg 2002 - 2021
5. Netherlands 1901 (only one station) - 2021

Table 2.2: Average time periods per country:

Country	Average period of years	Number of stations
Belgium	1987-2021	168
France	1983-2021	423
Germany	1962-2021	565
Luxembourg	2002-2021	19
Netherlands	1967-2021	10

3 Methodology

In this chapter, the analysis of mean daily flows (m^3/sec) on both yearly and monthly scales is explored. The primary objective is to address two sub-questions: one related to potential changes in discharge magnitude and the other regarding shifts in timing. Specific time spans are established, and various trend analysis and statistical methods are employed to achieve these objectives. The chapter serves a dual purpose. Firstly, it sets the groundwork by defining distinct time periods, allowing for meaningful comparisons in subsequent analyses. Secondly, it provides a comprehensive description of the methods used for examining changes in magnitude and timing of flow patterns. These analyses serve as the foundation for answering the research questions.

The chapter's organization is as follows. It begins with an outline of the established time frames, which are essential for meaningful data comparisons. Subsequently, it delves into the methodology used for the yearly analysis of mean daily flows. Following this, a detailed examination of the methodology employed in analyzing monthly mean daily flows is provided. The core of the chapter encompasses the analysis of non-parametric statistical methods like Sen's slope, Mann Kendall, and Modified Mann Kendall to explore trends and account for autocorrelation in the data. Finally, the chapter concludes with an overview of the statistical methods used to address the sub-research question related to possible changes in timing.

3.1 Magnitude perspective

3.1.1 Time spans

The variability in measurement timeframes, as highlighted in the Section 2.2, necessitates the establishment of consistent time periods for robust trend and statistical analysis across the entire case study area. This ensures comparability and the detection of potential trends. The following time spans were examined, along with the corresponding station counts:

- 20 years of analysis: 2002 - 2021. Available data 1185 stations.
- 40 years of analysis: 1982 - 2021. Available data 725 stations.

- 60 years of analysis: 1962 - 2021. Available data 266 stations.
- 80 years of analysis: 1942 - 2021. Available data 106 stations.

Beyond data management, these time spans are selected to capture trends that might otherwise be overlooked. A trend from the last 20 years could differ from the broader 40-year analysis. This challenge is clearly illustrated in Figure 3.1, where there is no evident trend for the entire 40-year analysis period; however, there is a noticeable increasing trend for the last 20 years. This graph underscores the significance of time spans in trend detection. It is important to note that the graph is theoretical and intended for visual understanding; it does not contain real data.

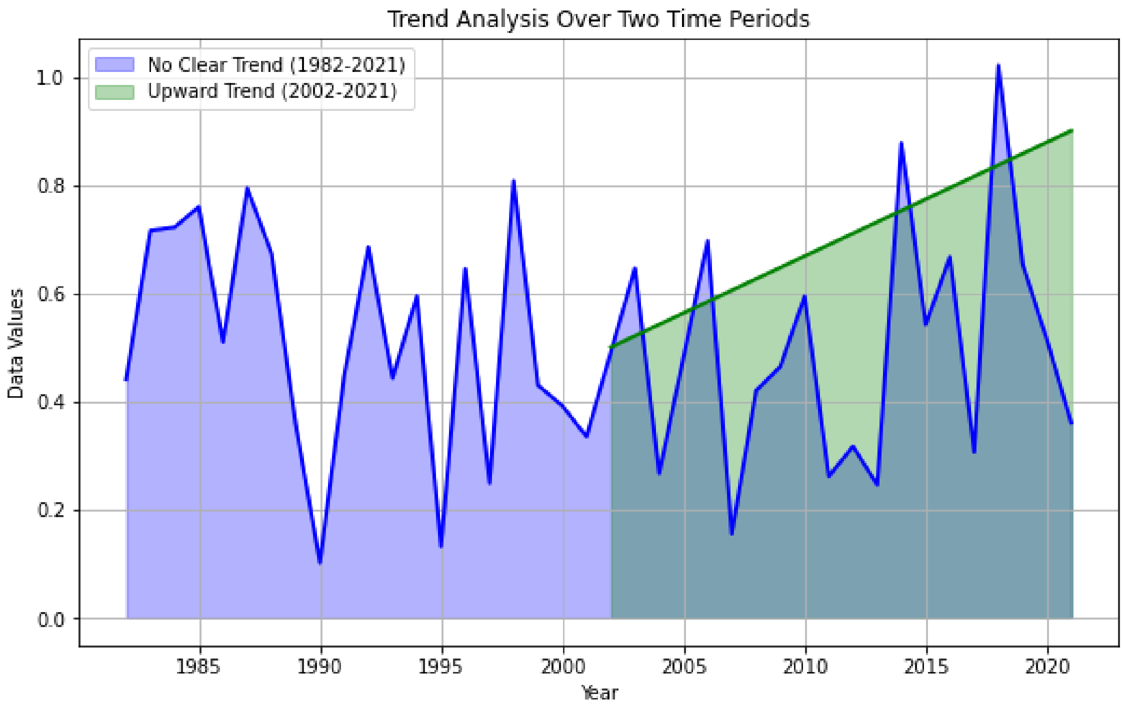

Figure 3.1: Time spans as a solution to capturing trends effectively: While the last 20 years exhibit a clear trend, the entire 40-year analysis period lacks a discernible trend.

3.1.2 Yearly analysis

The yearly analysis encompasses three distinct calculations. Firstly, the average yearly analysis computes the mean daily flow's (m^3/sec) annual average value. Secondly, the maximum yearly analysis identifies the maximum mean daily flow (m^3/sec) for each year, while the minimum yearly analysis determines the minimum mean daily flow (m^3/sec) for each year. These calculations are performed individually for each station, resulting in separate time series representing the average, maximum, and minimum values per year.

It is important to note that the graph presented here is purely theoretical and does not contain real data. The graph illustrates that Station with ID 9 possesses time series data for maximum, average, and minimum mean daily flows in m^3/sec. These time series serve as the foundation for calculating trend lines and the rate of change in the continue.

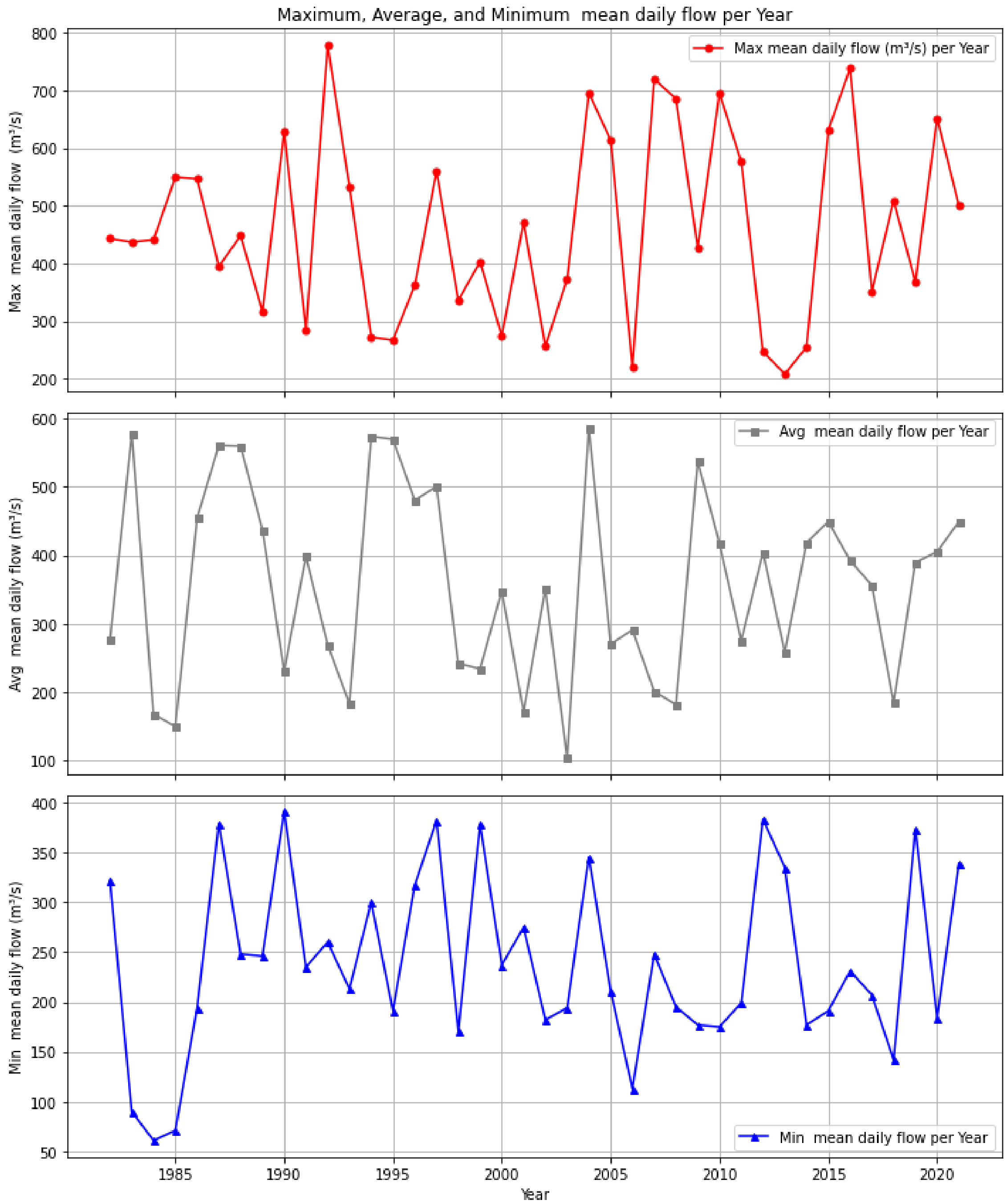

Figure 3.2: The graph displays time series data for maximum, average, and minimum mean daily flows per year for Station ID 9, spanning a 40-year analysis period from 1982 to 2021.

However, m^3/sec is important to be expressed mm/year and also the results need to be normalized with the catchment's areas. This is significant in order the results to correspond with the reality. Thus, the data expressed in m^3/sec changed in mm per year by dividing each value with the catchment area in km^2.

The trends of the yearly time series are calculated with the Modified Mann Kendall or Mann Kendall and the Sen's slope (non-parametric methods), as they in detail analysed in the following section, for all the analyses (average, maxima and minima). Each analysis has a reason why is conducted. First, the average analysis is done in order to take the overall image of the case study area and its trends. Second, the maxima and minima yearly analysis are conducted in order to understand the possible trends of the extremes which result in magnitude changes.

To sum up, the main goals of the yearly analysis are listed below:

- Calculation for each station the time series for its average, maxima and minima discharge in mm/year for the different time spans as they are analysed above.
- Calculation of the trends of all the stations in different time spans.
- Calculation of the number of stations with increasing and decreasing trends.
- Identification of the possible patterns and/or changes through the different time spans (location of the increasing/decreasing trends and connection of the elevation of the stations with the trends).
- Comparisons of the different distributions of the rate of change in mm/year of different time spans.

3.1.3 Monthly analysis

The monthly analysis, similar to the yearly analysis discussed earlier, aims to examine trend lines for each month at different stations over the years. It focuses on determining the trend of each month for all of the stations for different time spans and for different analyses (average, maxima, and minima).

For the average mean daily flow in the monthly analysis, the process involves calculating the average value for each month of each year. This calculation provides insight into the typical monthly mean daily flow trends. Moreover, the maxima and minima values of the monthly analysis identify the maximum and minimum values of mean daily flow per month, respectively. This allows for a detailed examination of extreme values during specific months. These time series are akin to the theoretical Graph 3.3, which illustrates the time series for one station with ID 9 over a 20-year period. It particularly highlights the time series for two months: January and August (the values in the graph are not actual data but serve as an illustration).

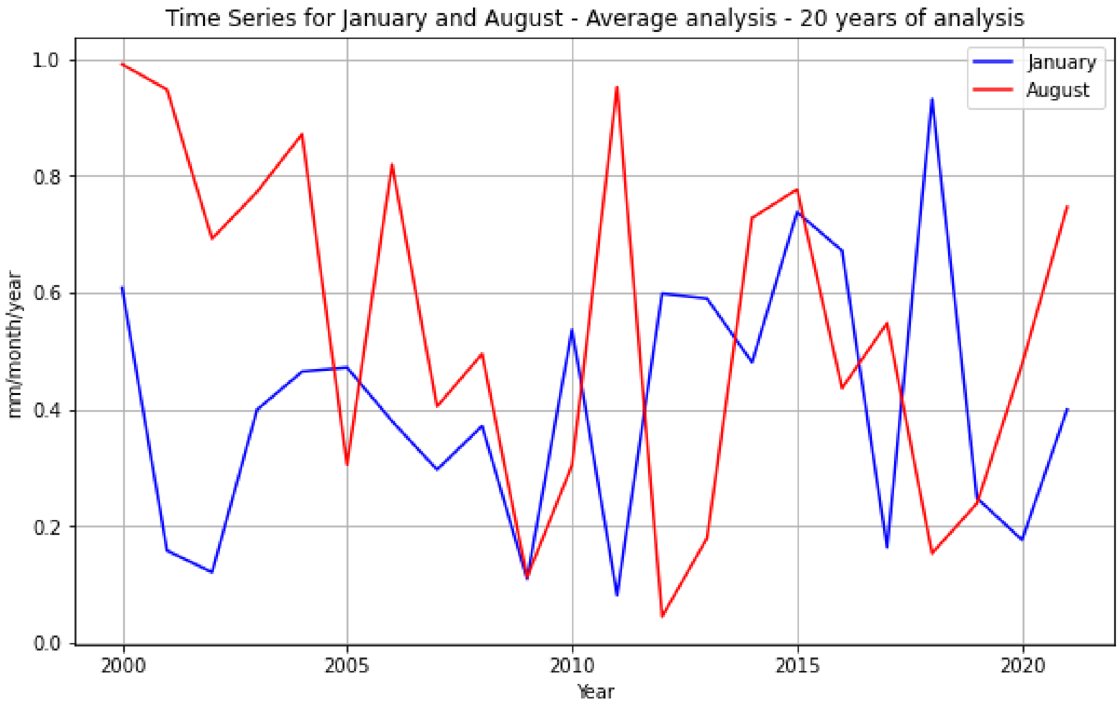

Figure 3.3: The graph displays time series data for a specific station over two months: January and August, spanning from 2000 to 2021. Similar time series data is calculated for all stations across various analyses (average, maxima and minima) and time spans.

Furthermore, it is crucial to note that the values obtained in the analysis are normalized with respect to the catchment area. Specifically, the measurement values from mean daily flows, initially expressed in m^3/sec, are divided by the catchment area of each station and then expressed in mm/month/year. This normalization ensures that the results are comparable across different stations and accurately reflect the influence of catchment size on discharge trends.

Based on the time series data for each month and station, trend lines are computed for various time spans and different analyses, including average, maxima, and minima. The purpose of the average analysis is to provide an overall perspective on the monthly trends in discharge, especially focusing on identifying the months with the most positive and most negative trends among the study area's stations. Additionally, analyzing trends in extreme values is crucial for understanding the consistency of hydrological patterns during these specific months. By examining both average and extreme values, it becomes possible to assess whether there are noticeable trends or significant variations in discharge for particular months over time.

However, within the realm of monthly analysis, an essential challenge arises due to the considerable volume of data. This dataset encompasses 1185 stations (for the last 20 years), each with data for 12 months for various analyses (average, maxima, and minima).

To address the aforementioned challenge, the study divides the entire case study area into ten distinct groups. It's worth noting that different time frames of analysis yield varying numbers of stations with available data. Consequently, in the context of the 20-year analysis, each group is designed to include approximately 100 stations, with geographical proximity as the only criterion for group clustering. In the case of the 40, 60, and 80 years of analysis, the number of station groups is relatively lower due to the smaller dataset. However, the criterion for grouping stations based on their geographical proximity remains consistent across all time frames.

The clustering method employed for this purpose utilizes machine learning tools, particularly the K-means algorithm (James et al., 2023). More precisely, K-means clustering, a machine learning technique, categorizes data points into clusters based on similarities, minimizing variance within each cluster and maximizing differences between clusters. This method simplifies large hydrological datasets by organizing stations efficiently. By applying K-means and machine learning, researchers uncover hidden patterns and relationships in hydrological data, deepening insights into processes and variations across regions and time spans. K-means enhances data visualization, aiding decision-making in hydrology and beyond.

The clustering method utilizes the K-means algorithm, which groups stations based on geographical proximity. Mathematically, K-means seeks to minimize the following objective function:

$$J(c, \mu) = \sum_{i=1}^{k} \sum_{j=1}^{n} \|x_j - \mu_i\|^2 \tag{3.1}$$

Where $J(c, \mu)$ represents the sum of squared distances between data points x_j and cluster centroids μ_i, k is the number of clusters, and n is the number of data points. K-means assigns data points to clusters by updating centroids iteratively until convergence. This approach aids in station grouping and geographical analysis, contributing to hydrological research and decision support.

In summary, the objectives of the monthly analysis encompass the following key aspects:

- Calculation for each station, for each month the corresponding time series for different time spans(20, 40, 60, 80) and analyses (average, maxima and minima).
- Calculation of the trends of all the stations, for each month, for different time spans and all the analyses (average, maxima and minima), by using Mann Kendall, Modified Mann Kendall and Sen's slope for the monthly values.
- Clustering the stations in groups -based on their location- and connection of the month with the highest (most positive) rate of change in mm/month/year and the lowest (most negative) rate of change in mm/month/year discharge with the location of the groups of stations.
- Calculation of the average contribution of each month to the rate of change -for average, maxima and minima analyses- which month has the highest and the lowest trend on average for each of analysis.

3.2 Timing perspective

3.2.1 Time spans

In the context of timing analyses, in addition to the previously mentioned time spans discussed in the magnitude analysis 3.1.1, a more detailed examination is conducted for the 40-year analysis period (1982-2021). Consequently, this aforementioned time frame is further subdivided into two distinct intervals: 1982-2000 and 2001-2021. These subdivisions facilitate a more profound exploration of potential variations, with a particular focus on the last 20 years.

3.2.2 Analysis

In the context of timing analysis, the annual assessment exclusively concentrates on extreme values, specifically maxima and minima. The objective here is not to perform trend analysis, but rather to investigate months with maximum and minimum values, as well as any potential changes in these months over time. With time series data for maxima and minima already available for each station, as depicted in Figure 3.2, precise dates for the occurrence of maximum and minimum values are recorded for each year and station.

For stations across various time spans, this process results in the compilation of a table, similar to the theoretical example presented below (please note that the values in the table are for illustrative purposes and not based on actual data). In Table 3.1, the dominant month per year for the station with ID 9 is depicted; however, similar analysis is also conducted for all the stations for all the years of analysis and for Minima values as well.

Table 3.1: Station ID 9: Dominant Month for Maxima Values (2001-2002):

Year	Max (mm/year)	Date of occurrence	Dominant Month (Max)
2001	0.5	05/02/2001	2
2002	0.7	05/12/2001	12

Having obtained the 'dominant months' for both maxima and minima values, a variety of statistical metrics and visualization plots (such as heatmaps and histograms) are employed to investigate potential changes in the months with the highest and lowest discharge (mm/year) across different timeframes. The statistical metrics used for this timing perspective are analyzed in detail in the subsequent sections of 3.4 and particularly in section 3.4.2. The listed metrics include:

- Statistical Entropy
- Concentration
- Kullback–Leibler divergence (KL Divergence)

3.3 Trend analysis

Having outlined the methodology for the time series analysis in the preceding sections, it is now crucial to delve into the examination of non-parametric methods employed for identifying trends in both yearly and monthly analyses (the first sub-research question). First, we provide comprehensive descriptions of the Sen's slope and Mann Kendall methods. Following that, we address the issue of autocorrelation, including the detection of autocorrelated data and proposed solutions to prevent potentially misleading trend analysis results. One such solution to tackle the aforementioned challenge involves implementing the Modified Mann Kendall method, which is a modification of the well-known Mann Kendall method designed specifically to address autocorrelation issues.

3.3.1 Sen's slope

Sen's slope (also known as Sen's estimator or Sen's slope estimator) (Sen, 1968) is a reliable nonparametric technique for determining the rate of change and the directions of trends in a dataset over time. The method is particularly useful to evaluate the trends of the hydrological or environmental data since the presence of outliers or non-normal distributions can result in misleading trends.

The median of the pairwise slope between all potential pairings of data points is used to generate the Sen's slope. The following steps describe the computation of the Sen's slope:

Step 1: Based on the corresponding time index, arrangement of the data points in ascending order.

Step 2: Calculation of the pairwise differences between all data points, resulting in a set of slopes.

Step 3: Calculation of the median of the slopes. In case the number of slopes is even, the average of the two middle values is used (Wilcox, 2022).

Step 4: Based on the 3.2 equation, the trend over time is calculated, regardless if this trend is increasing or decreasing. The magnitude of the slope indicates the rate of change.

$$\text{Sen's Slope} = \text{Median}\left(\frac{x_j - x_i}{t_j - t_i}\right) \tag{3.2}$$

3.3.2 Mann Kendall

Mann-Kendall test (Mann, 1945), (Kendall, 1975) is also a statistical method used to analyze trends and detect important changes in a dataset over time. According to World Meteorological Organization (WMO) the Mann Kendall is proposed as an effective method for hydro-meteorological trend assessment (Diress and Bedada, 2021).

The Mann-Kendall test calculates a statistic called S or *tau* value (also known as the Mann-Kendall statistic) to measure the strength and direction of the trend. The steps involved in performing the Mann-Kendall test are listed below:

Step 1: Based on the corresponding time index, arrangement of the data points in ascending order.

Step 2: Calculation of Mann Kendall statistic:

- Computation of the differences between all possible pairs of data points, x_j and x_i, where $j > i$.
- Determination of the sign of each difference.
- Sum them up to obtain the Mann-Kendall statistic:

$$S = \sum_{i=1}^{n-1} \sum_{j=i+1}^{n} \operatorname{sgn}(x_j - x_i) \tag{3.3}$$

where n represents the total number of data points and the $sgn(x_j - x_i)$ returns the sign of difference between the data points x_j and x_i.

Step 3: Calculation of the variance of the Mann-Kendall statistic using the equation 3.4, if there are not tied values in the dataset. While, in case of tied values the equation 3.5 should be used:

- If there is no ties in the dataset (Hamed, 2008):

$$\operatorname{Var}(S) = \frac{n(n-1)(2n+5)}{18} \tag{3.4}$$

- If there is ties in the dataset (Hamed, 2008):

$$\mathrm{Var}(S) = \frac{n(n-1)(2n+5) - \sum_{p=1}^{g} t_p(t_p-1)(2t_p+5)}{18} \tag{3.5}$$

At the equations 3.4 and 3.5, the variable "n" represents the total number of data points in the dataset. Additionally, the variable "tp" in the equation 3.5 denotes the number of tied groups within the dataset. Tied values refer to observations in the dataset that possess identical values. Specifically, in the context of the current MSc Thesis, tied values correspond to discharge amount measurements of which multiple observations having the same value.

Step 4: Calculation of the standard deviation (σ) of the Mann-Kendall statistic. Taking the square root of the variance: $\sigma = \sqrt{\mathrm{Var}(S)}$.

Step 5: Calculation of the standard normal test statistic (Z) using the equation 3.6:

$$Z = \frac{S}{\sigma} \tag{3.6}$$

Step 6: Calculation of the p-value. More precisely, the Z value obtained from the Mann-Kendall test is used to compute the p-value. If there is no trend in the data (according to the null hypothesis), this p-value reflects the probability of observing a Mann-Kendall statistic that is as extreme as, or even more extreme than, the observed value. In other words, it measures the likelihood that the observed trend or an even stronger trend might have arisen by chance alone, assuming that there isn't any underlying trend. We can determine whether to reject the null hypothesis (signifying a significant trend) or fail to reject it (signifying insufficient evidence to support a significant trend) by comparing the p-value to a selected significance level.

$$p\text{-value} = 2 \times [1 - \Phi(|Z|)] \tag{3.7}$$

Where:

- **p-value** is the probability value you're trying to calculate.
- **Z** is the Z-score, which is obtained as part of the Mann-Kendall test.

- $|\mathbf{Z}|$ is the absolute value of the Z-score.
- $\Phi(|Z|)$ represents the cumulative distribution function (CDF) of the standard normal distribution evaluated at the absolute value of the Z-score.

Step 7: Comparison of the pvalue with the chosen significance level (α). If the pvalue is less than α, reject the null hypothesis and conclude that there is a significant trend present in the dataset. For the current MSc Thesis, the $(\alpha) = 0.05$, which means that the stations with pvalue < 0.05 have trend while the stations with pvalue $>$ 0.05 the null hypothesis is accepted and the conclusion is that there is insufficient evidence to suggest a significant trend.

In the provided Figure 3.4, you can examine the case of Station ID 430601001 situated in France. The trend analysis of maximum yearly mean daily flow reveals a consistent upward trend spanning from 1970 to 2021.

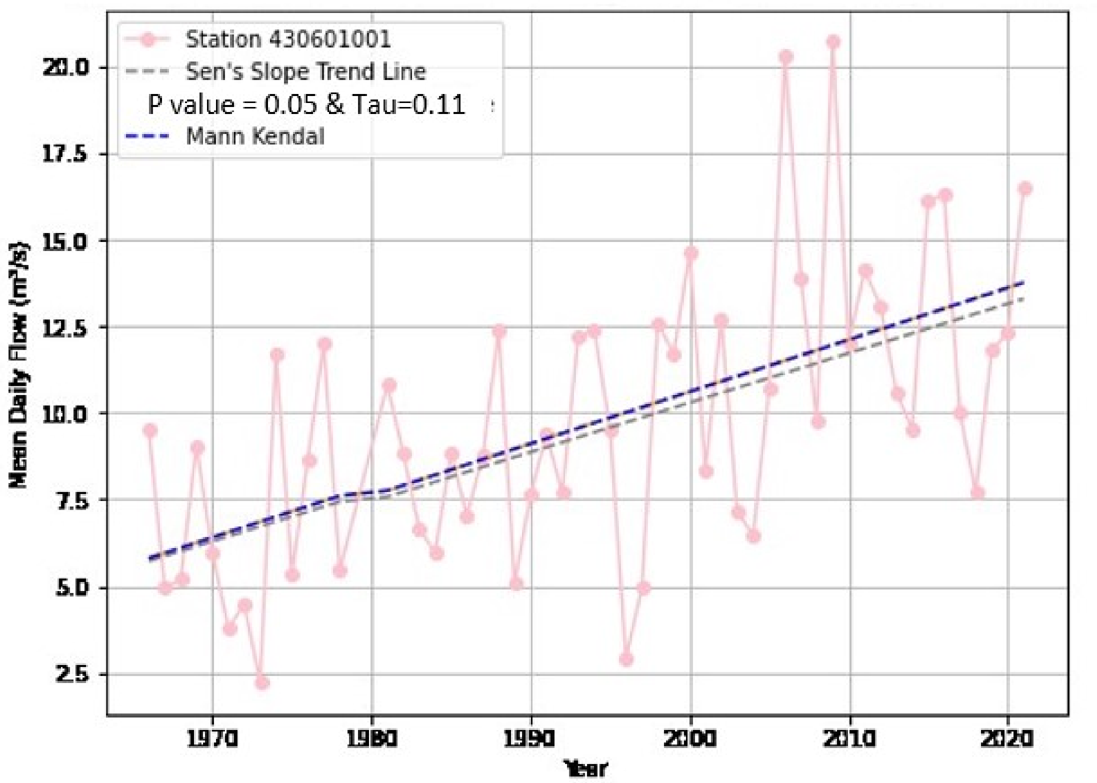

Figure 3.4: Trend Analysis of Station ID 430601001: The calculated Pvalue is less than 0.05, indicating a statistically significant trend over the years.

3.3.3 Autocorrelation issue

It is noteworthy that the Mann-Kendall test requires the time series to be independent (Hamed and Ramachandra Rao, 1998). If the independence assumption is violated alternative trend tests may be more appropriate. The presence of autocorrelation is very common in discharge flows because of seasonality. Moreover, autocorrelation can have a significant effect on the accurancy of the results and notional trends.

3.3.3.1 Definition & Types

Autocorrelation, also known as serial correlation, refers to the correlation between observations at different time lags. In discharge flows, if the current flow measurement is correlated with previous flow measurements, there is a degree of dependence between the observation (autocorrelation).

The identidication of the type of autocorrelation is crucial for the accurate data analysis. The different types of autocorrelation are listed below (Hamed and Ramachandra Rao, 1998):

- Positive autocorrelation - Values tend to be similar.
- Negative autocorrelation - Values tend to be dissimilar.
- No autocorrelation - Values are independent.

In the current MSc Thesis, almost 85% of the stations have autocorrelated values.

3.3.3.2 Tests for detection

Autocorrelation in time series data can be found using a variety of techniques and tests. Regarding the visual techniques, autocorrelation function (ACF) and partial autocorrelation function (PACF) graphs are used to detect the autocorrelation in a dataset (Okafor et al., 2017).

The correlation between observations of a variable at various lags can be seen using ACF plots. The correlation between observations is displayed whereas the effects of intermediate lags are eliminated in PACF plots, on the other hand. These diagrams can be used to determine the existence and the magnitude of autocorrelation.

A Python algorithm is used in the current MSc thesis to find autocorrelation in discharge flow data. The time series data is analyzed by the algorithm to check for autocorrelation, which is necessary for precise trend analysis. The code investigates the correlation between observations at different time lags (one year and one month time lag) and uses a variety of statistical libraries and tools.

Within the code, the discharge flow data is preprocessed and filtered based on the specified date range (i.e the mean daily flow is filtered in yearly and monthly level for one year and one month lag respectively). The autocorrelation function (ACF) is computed using the sm.tsa.stattools.acf() function from the statsmodels library. The resulting ACF plot provides insights into the correlation structure of the data.

To determine the significance of observed autocorrelation, the absolute values of the autocorrelation coefficients and p values are calculated. If any p value is below the threshold of 0.05, suggesting the presence of autocorrelation. For stations with autocorrelation, a modification of the original Mann Kendall is used and called Modified Mann Kendall (it is analysed in the subsequent section 3.3.4).

For instance, considering the Graph 3.5 below, which illustrates a station with ID 1642 located in the Netherlands. Here, the data displays autocorrelation since p-value is below 0.05 (above the significance level) and a correlation coefficient of approximately 0.79. Consequently, for this station, the implementation of the Modified Mann-Kendall test becomes imperative to address the autocorrelation issue.

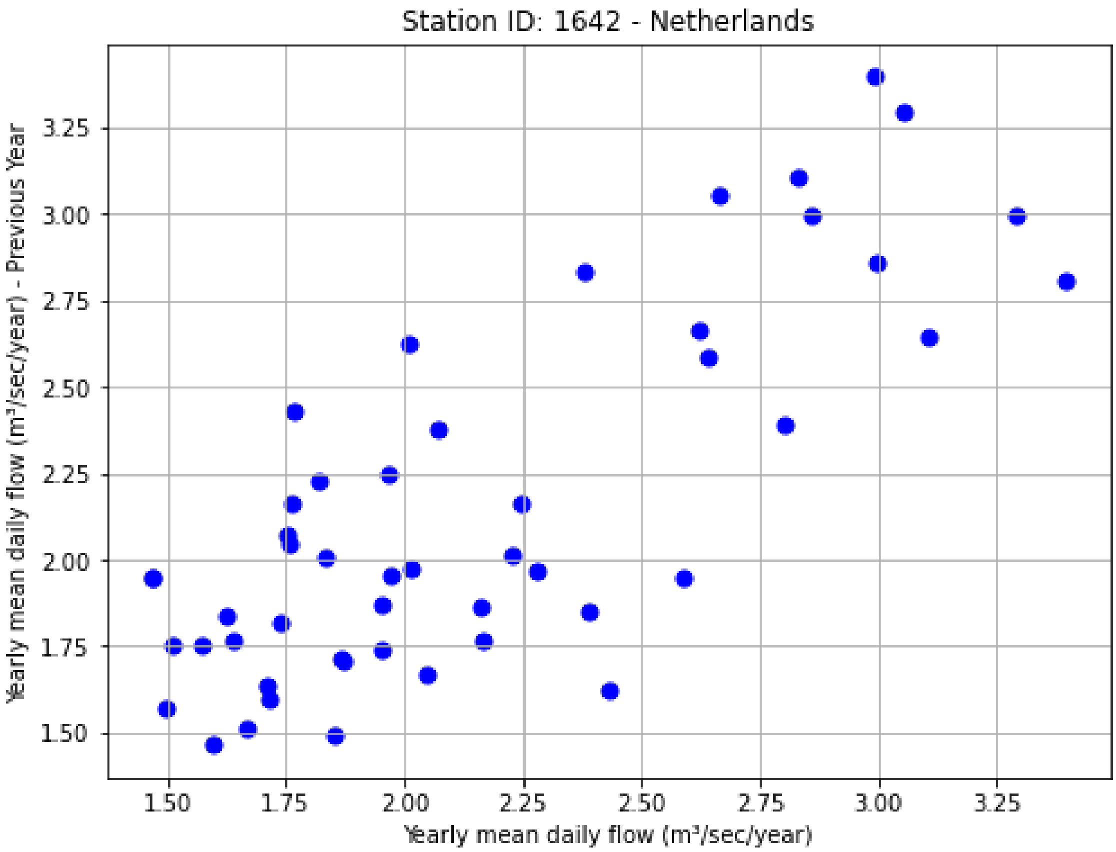

Figure 3.5: Autocorrelation Function Plot - Lag 1 year: High correlation coefficient = 0.79 & Pvalue < 0.05

3.3.4 Hamed-Rao Modification

As mentioned before, to address the issue of autocorrelation and avoid unreliable p-values, leading to incorrect conclusions concerning the presence or the absence of trends, a modified version of the Mann-Kendall test is developed. The Modified version, which is used is based on the study conducted by Hamed and Ramachandra Rao (1998).

Based on the Hamed-Rao Modification, the addressement of the autocorrelation issue is done with the correction of the variance of the trend statistic 3.4 or 3.5. If the data is autocorrelated the variance calculation is underestimated by the equations 3.4 or 3.5 (Okafor et al., 2017). To modify and correct the variance an adjustment factor (3.8) is used and improves the trend detection accuracy and the validity of the hypothesis testing.

First, the autocorrelation function (ACF) of the time series data is estimated. The autocorrelation coefficients provide insights into the temporal dependencies within the data. The adjustment factor is then calculated based on the estimated autocorrelation coefficients and is used to modify the variance of the test statistic (Hamed and Ramachandra Rao, 1998).

$$n_{ns} = 1 + \frac{n \cdot (n-1) \cdot (n-2)}{2} \cdot \mathrm{sni} \tag{3.8}$$

In the equation 3.8, the calculation of the number of non-serially independent values (ns) in the Hamed-Rao modification of the Mann-Kendall test. It takes into account the number of observations (n) and the sum of non-serially independent data (sni).

Second, the adjustment factor is used to calculate the corrected-modified variance as follows (Hamed and Ramachandra Rao, 1998):

$$\mathrm{var}_s^{'} = \mathrm{var}_s \cdot n_{\mathrm{ns}} \tag{3.9}$$

After adjusting the variance, the same steps (Steps 4 to 7) are followed as described in the Mann Kendall section 3.3.2.

3.4 Statistical analysis

3.4.1 Descriptive statistics

The area of statistics known as descriptive statistics is concerned with summarizing and describing a dataset's key features. In order to understand the central tendency, variability, distribution, and other pertinent features of the discharge volumes is provided by descriptive statistics' numerical and graphical measures.

In this MSc Thesis, measures of central tendency (such as mean, median, and mode) are used to represent a variable's typical value. Also, measures of variability (such as range and standard deviation) are used to evaluate how evenly distributed the data is, and measures of shape (such as skewness and kurtosis) are used to describe the distribution of the data.

Additionally, a variety of visualizations are created, including pie charts, histograms and Kernel Density estimate (KDE) plots. In contrast to pie charts, which are intended to show the distribution or features of categorical data, histograms are used to visually represent the distribution and characteristics of numerical variables. Finally, KDE plot is a similar with histogram. Nevertheless, instead of discrete bars, KDE uses a smooth, continuous curve to depict the likelihood of finding data points at different values or positions, whether it is in one dimension or more.

3.4.2 Entropy & Concentration

To address the second sub-research question and examine possible changes in timing of maximum and minimum discharge through the years; this study employs the concept of statistical entropy. Based on this concept, a new metric is derived, namely concentration, which is essentially the inverse of entropy. Concentration is used to make the potential changes in timing more comprehensible to the readers. The following paragraphs explain the terminology of entropy and concentration and then discuss how these metrics are applied in the present study.

3.4.2.1 Entropy: Terminology & Interpretation

Statistical entropy, also known as Shannon entropy (Torres-García et al., 2022), is a measure of the complexity, unpredictability, or regularity of a set of data across time. Entropy can be used to compare different time series or to detect possible variations or uncertainties among them.

As mentioned previously, statistical entropy is used in this study to examine whether the distribution of the months with the highest and lowest flow over the years is uniform or skewed.

To calculate the statistical entropy, the equation 3.10 is used. Regarding the interpretation of the Shannon entropy is a number between 0 to 1. If the entropy value is high, this means that the distribution is uniform and the maxima and minima discharge volumes vary a lot with respect to the month of occurrence through the years. The distributions resemble more normal distributions and the maximum and minimum discharge is observed in more than one specific month through the years. On the other hand, if the entropy has lower values, close to zero, this means that there is a dominant month in which the maximum and minimum discharge is observed through the years (McClean, 2003).

$$S = -k \sum_i P_i \log(P_i) \tag{3.10}$$

In equation 3.10, the variable "k" represents a constant that is used in the calculation of statistical entropy. It is called Boltzmann constant and correspond to the value of 1.38 $\times 10^{-6}$ erg/K.

3.4.2.2 Concentration: Terminology & Interpretation

However, since the study uses multiple maps, such as Figure 4.38, to depict the shift of timing, it is more convenient for the reader to introduce a reverse metric of statistical entropy, which is called concentration. Consequently, if the concentration is small (close to zero), this means that the distributions are uniform and more than one month can have the highest and lowest discharge of the year. Conversely, if the concentration is close to one, this means that there is a dominant month in which the maximum and minimum discharge of each year occurs.

Concentration is used to establish a proportional link between arrow length and the dominant month. Employing statistical entropy, longer arrows signify higher entropy values, signifying the absence of a single dominant month. To enhance clarity, we aimed for the opposite interpretation and found the metric of concentration in which longer arrows now indicate the dominant month, implying that this particular month frequently hosted peak or minimum discharge occurrences.

The statistical entropy and concentration metric can provide information about the distribution of the months with the maximum and minimum discharge over the years, but they cannot capture the potential shift of the month in which the highest and lowest flow occur over time. Therefore, the Kullback-Leibler (KL) divergence is used to compare the distributions with each other.

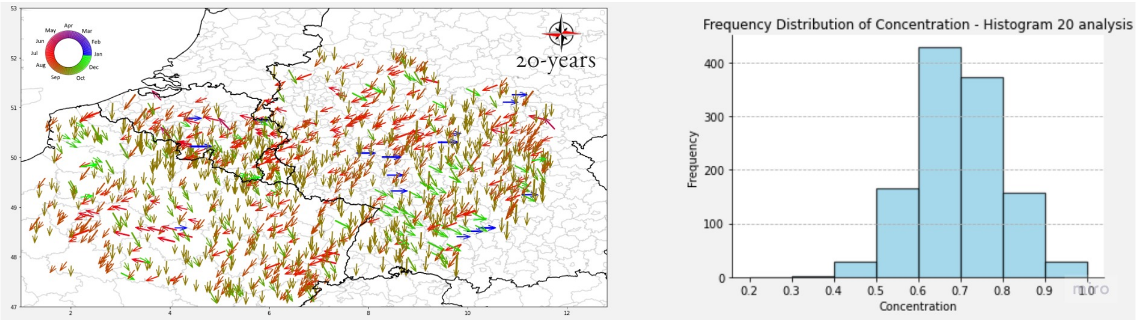

Figure 3.6: Concentration map for the 20 years of analysis (2001 - 2021) - Dominant month of the Minima discharges

3.4.3 Kullback–Leibler Divergence

Kullback–Leibler Divergence: Terminology The Kullback-Leibler (KL) divergence (Dhinakaran, 2023), also called relative entropy, is a concept from information theory and statistics that quantifies the discrepancy between two probability distributions. It gives a measure of how much one probability distribution deviates from another.

Given two discrete probability distributions P and Q, the KL divergence from P to Q is defined in the equation 3.11:

$$D_{\mathrm{KL}}(P\|Q) = \sum_i P(i) \log\left(\frac{P(i)}{Q(i)}\right) \tag{3.11}$$

In the formula 3.11, the sum is over all possible values of i. The KL divergence measures how different P is from Q.

3.4.3.1 Kullback–Leibler Divergence: Interpretation

As previously mentioned, the Kullback-Leibler (KL) divergence quantifies how different two probability distributions are (Wicklin, 2020). A larger KL divergence indicates greater dissimilarity, while a smaller one suggests more similarity. KL divergence can potentially become very large, especially with continuous distributions or when distributions have different ranges.

In our study, we're dealing with discrete probability distributions for months (January to December), resulting in 12 possible outcomes. For discrete distributions, the KL divergence is limited by the logarithm of the number of outcomes. In our case, with 12 possible outcomes (the months of the year), the KL divergence is constrained by the logarithm of 12, approximately 2.4849.

4 Results

The Results chapter encompasses two primary analyses: one centered on magnitude and the other on timing. The initial sub-research question concerning changes in magnitude is addressed, encompassing trends and statistical analyses of both yearly and monthly data. The results of the second sub-research question are derived from the timing analysis.

Concerning the structure of yearly analysis, the section begins with a helpful introduction which explains how the maps and the graphs were made and describes what exactly these maps and graphs depict. All of them concern the examination of magnitude changes. The analysis of the average yearly mean daily flow is initiated, presenting results for various time spans (20, 40, 60, and 80 years). Towards the conclusion of this section, pie charts, histograms and a KDE plot are included to facilitate a comparison of the average yearly results over the years. Subsequently, the analysis of the maximum yearly mean daily flow is conducted, with results provided for different time spans. The section concludes with a comparative analysis of these results across the years. The chapter culminates with an analysis of the minimum yearly mean daily flow, mirroring the structure of the previous analyses.

At the conclusion of each yearly analysis (average, maxima, and minima yearly mean daily flow), a scatter plot and a confusion matrix are employed to assess the magnitude changes for stations with data spanning 80 years. This provides insight into how these stations' magnitudes have evolved over the last 20 years of analysis.

Moving on to the monthly analysis, coverage includes the average monthly mean daily flow, maximum monthly mean daily flow, and minimum monthly mean daily flow analyses. For each of these, the months with the highest and lowest trends across different time spans and locations are found.

After addressing the magnitude perspective, attention is directed to the section titled "Changes in Timing." Within this section, a comprehensive analysis of extreme discharges is conducted, with a specific emphasis on identifying shifts in the month associated with maximum and minimum flow over the years. Additionally, a focal point of this section involves a comparative examination of the time spans of 1980-2000 and 2001-2021, aiming to gain insights into the temporal shifts occurring between these two 20-year periods.

4.1 Changes in magnitude

4.1.1 Yearly analysis

In our annual analysis, we present trend results through two distinct types of maps. The initial type utilizes the Digital Elevation Map (DEM), employing red to indicate stations with declining trends, blue for those with rising trends, and gray for stations exhibiting no discernible trend. This map serves a dual purpose, not only displaying station locations but also their respective elevations. These maps, specific to each time span (20, 40, 60, and 80), can be found in the Appendix 6, with a dedicated section titled "Changes in Magnitude" in A1.

The second map highlights stations with trends—red and brown for decreasing trends, and blue and light blue for increasing ones—alongside stations lacking any observable trends, depicted in gray. Additionally, it showcases the significance of these trends. As previously discussed in Chapter 3, when the p-value falls below 0.05, it signifies a statistically significant trend that did not emerge by chance. Moreover, trends with p-values smaller than 0.03 are considered even more significant. This vital information is also communicated in the second map through variations in color and circle size. Larger circles denote prominent trends, while smaller circles represent more modest ones.

Following these maps, KDE plot and histograms are made. To be more precise, in order to understand the differences between the time series of the different time frames, the KDE (Kernel Density Estimation) is calculated. By looking the KDE, the aim is the investigation of similar patterns and/or differences. The x-axis shows the discharge rate of change based on the Sen's slope analysis in mm/year normalized in respect with the catchment area. Moreover, the y-axis represents the density of the estimated probability distribution. Overall, KDE plot estimates how likely it is to find a data point with a specific rate of change value.

Moreover, for each yearly analysis, histogram are created which deoicts the results of the slopes of the discharge form different catchments to be comparable, normalization is done as it is described in the chapter of Methodology 3 and especially in Trend analysis section of 3.3.

Finally, it is also important to be informed about the percentage of stations that exhibit consistent trends across different time spans. For these reason, the pie charts which visually represent the distribution of matching stations were created.

The following set of pie charts (all of them are in the Appendix 6 in A1.1) has been created to visually represent the distribution of matching stations and, in particular, to illustrate the percentage of stations that exhibit consistent trends across different time spans. In these charts, matching stations are denoted by the pink color. For example, for the comparison of 20 and 80 years of analysis, the number of stations, which maintain having trends over an 80-year period and also exhibit trends in the most recent 20 years of analysis, are called as "matching stations".

The presence of blue and yellow colors in the charts serves to distinguish stations with trends unique to a single analysis period. For instance, in the comparison between 20-year and 80-year analyses, the yellow color represents the number of stations with trends exclusively over the 20-year span. Conversely, the blue color indicates the number of stations with trends solely within the 80-year analysis, which do not extend to the most recent 20 years. These pie charts provide valuable insights into the continuity and uniqueness of trends among machine stations, helping us understand which stations consistently maintain their patterns and which exhibit distinct trends during various time intervals. In the Results section, you will find pie charts comparing data from 20 and 40 years of analysis, highlighting matching stations.

4.1.1.1 Average yearly mean daily flow

- **20-Year Analysis:** First, for the period between the 2002 to 2021, from the 1186 stations the 221 have trend. From the stations with trend the 84% of them have decreasing trend and almost 16% have increasing trends. More specifically, the 963 stations they do not have trend while the 185 have decreasing trends and 35 have increasing trend. Concerning the location of the stations, as it is seen in the Maps A1.1 and 4.1 most of the stations do not have trend and they are located in the center of the case study area, on the other hand the stations with decreasing trends are located in the in the North - East part of the case study area with most of them to be in Germany, while the stations with increasing trends are located Western part of the case study area and especially in France. Regarding the connection between the elevation of the stations with decreasing trends, they are located in 194 - 581 m, while the stations with increasing trends are located in a lower elevation range which means until 194m.

Regarding the significance of trends based on p-values, our analysis reveals noteworthy insights. Examining the Map 4.1, covering a span of 20 years, we observe that the most substantial declining trends are concentrated in the North-Eastern sector of the case study area, near the borders of Germany, where p-values consistently fall below 0.03. A similar pattern emerges in the South-Eastern region of Germany, characterized by numerous stations with p-values < 0.03, all indicating declining trends. Meanwhile, in the northern reaches of the case study area encompassing Belgium and the border region between the Netherlands and Germany, a few stations also exhibit p-values < 0.03, though their numbers are relatively modest.

In contrast, when considering average values, stations displaying increasing trends are predominantly situated in the western portion of the case study area, particularly in North-Western France, which includes the vicinity of Paris. Notably, the number of stations showcasing increasing trends is substantially lower compared to those with declining trends. Moreover, the stations displaying increasing trends, while spread across the western sector, also feature some presence in the central part of the case study area. However, these trends are not as statistically significant in terms of p-values as the prominent declining trends observed elsewhere.

- **40-Year Analysis:** Second, concerning the range between 1982-2021, namely 40 years of analysis, the amount of stations which have available data for this time frame is 725 stations. From them, 481 they do not have trend, 242 stations have decreasing trend and only 2 stations have increasing trends, which have a increase of almost 15 mm/year and 2.6 mm/year. Regarding the location of the stations with decreasing trends are (as for 20 year-analysis) mainly located in the North - East part of the case study area and the elevation of these stations range between 194 to 581 m. All the aforementioned information can be seen in the DEM map in the Appendix A1.2 and Map 4.1 for the 40-years of analysis.

In the context of 40 years of analysis, the p-values reaffirm the prominence of declining trends in the North and North-Eastern sectors of the case study area. Notably, this time frame also reveals a significant number of stations exhibiting declining trends in the central region of the study area. In contrast, the count of stations showcasing increasing trends remains limited, with just two identified in the aforementioned areas. However, it is worth highlighting that these stations exhibit substantial and noteworthy increasing trends.

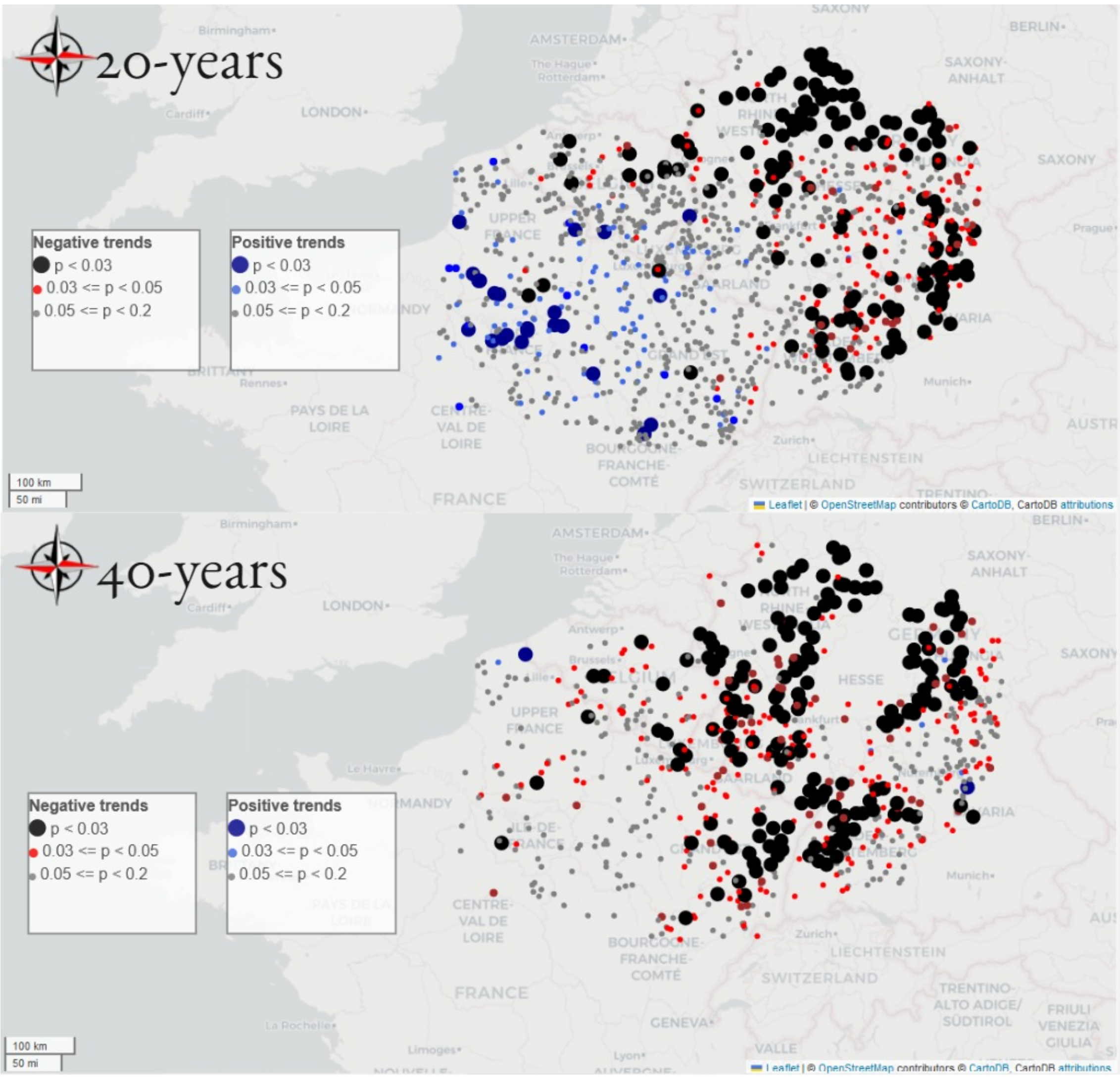

Figure 4.1: 2002-2021 & 1982-2021 Average mean daily flow - P values

- **60-Year Analysis:** About the 60 years average yearly mean daily flow (mainly from 1962-2021), the stations which have available data they are 266. From them, the stations with decreasing trend are 30 stations, the stations with increasing trend are two while the rest 234 they do not have any significant trend. The stations with decreasing trend are mainly located in the center, East and South part of the case study area, while the only two stations with increasing trends are located in the Eastern part of the case study. On the other hand, the stations without trend are located around the case study area, and especially in France and Germany where there are available data for 60 years of analysis, with France to have only one station with decreasing trend while Germany has all stations without, and with increasing and decreasing trends. In this analysis, the stations with decreasing trends are located in heights from 194-775m, while the only two stations with increasing trends are located in a height around 200 m (all the aforementioned information can be seen in the DEM map A1.3).

As depicted in Map 4.2 spanning 60 years, the station count is notably reduced. Despite this, the most significant trends are evident in the northern and central regions of Germany. Additionally, there are declining trends of lesser significance in the southern and northern parts of the same country. In contrast, a limited number of stations with increasing trends are situated in the eastern section of the case study area. Remarkably, these trends hold considerable importance, as they are associated with p-values < 0.03.

- **80-Year Analysis:** Concerning the 80 years of analysis is hard to conclude in clear patterns since only Germany and one station located in the Netherlands and another one located in North East part of France have available measurements during this time frame. More precisely, the total number of stations are 106, from them only 7 have increasing trend and 2 have decreasing trend. All the rest have no trend. The only two stations with decreasing trend are located in Germany in elevations close to 200m, and the stations with increasing trend are also located in Germany in heights from almost 200-400m (all the aforementioned information can be seen in the DEM map A1.4).

  Examining the 80-year analysis, in Figure 4.2, a distinct trend emerges in the p-values. Stations displaying increasing trends consistently exhibit p-values below the threshold of 0.03, predominantly concentrated in the southern regions near the country's center. In stark contrast, decreasing trends are notably concentrated in the central areas and exhibit similarly small p-values, all falling below 0.03.

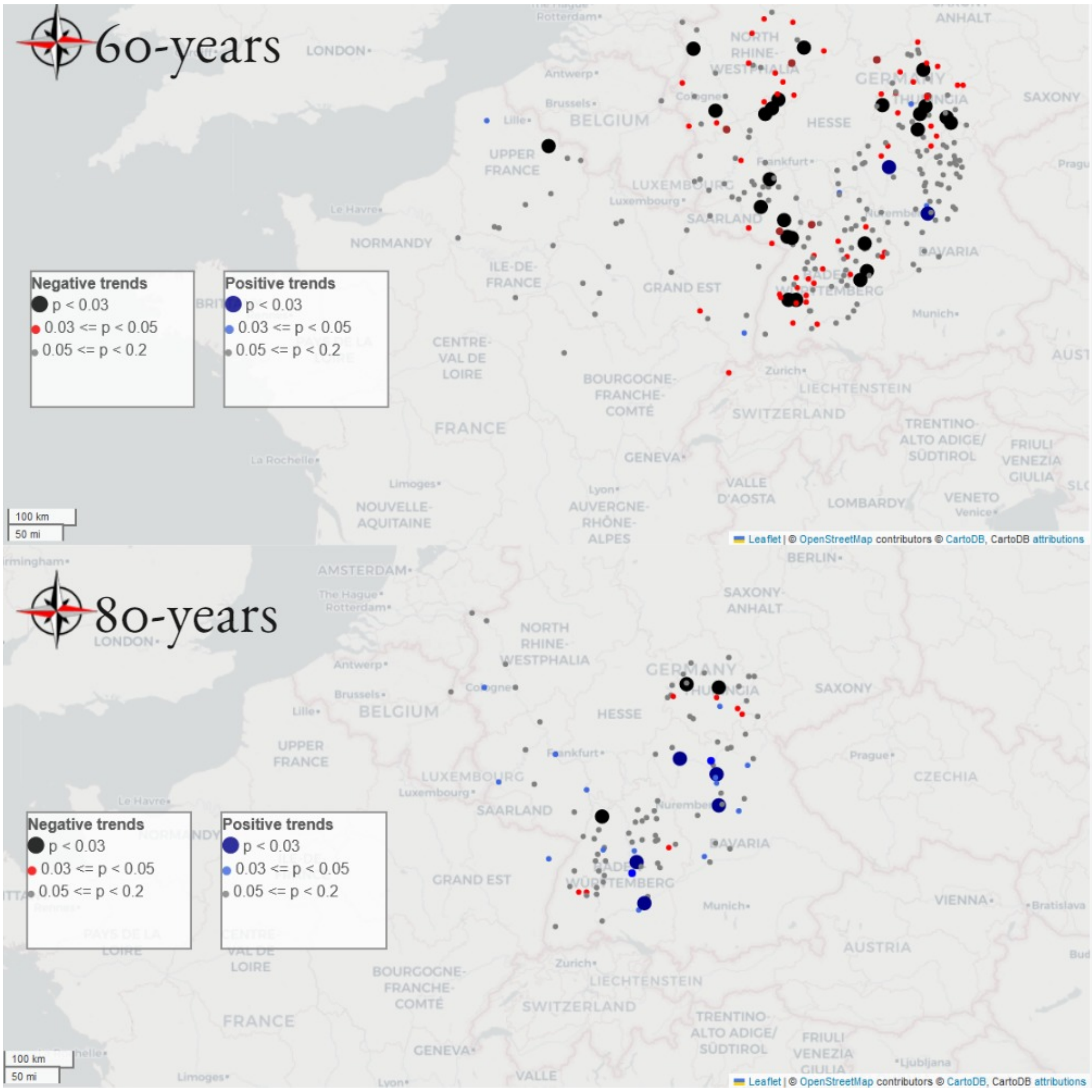

Figure 4.2: 1962-2021 & 1942-2021 Average mean daily flow - P values

- **Histogram of different time spans:** For the average values for all of the different time frames, the stations which show decreasing trends are more than the stations with the increasing trends. The one exception is the 80 years of analysis, where the number of increasing trends are almost the same with the number of decreasing ones. Also, the rate of changes shows a different pattern between the 80-yearly analysis and the 60-yearly analysis, since in the 80-yearly analysis the most negative trend of average mean daily flow is -2 mm/year, which is changed for the 60-yearly analysis when the most negative trend of the average mean daily flow is around -10 mm/year. Also, in 60-yearly analysis, almost none of the stations depict increasing trends. Regarding the 40 and 20 year of analysis, the rate of changes of 20 years of analysis is much more negative than the 40-yearly analysis. Specifically, the last 20 years, the number of stations with increasing trends are more and the most negative rate of change noticed the last 20 years is -100mm/year, while in 40-yearly analysis is the -30mm/year (see Figure 4.3).

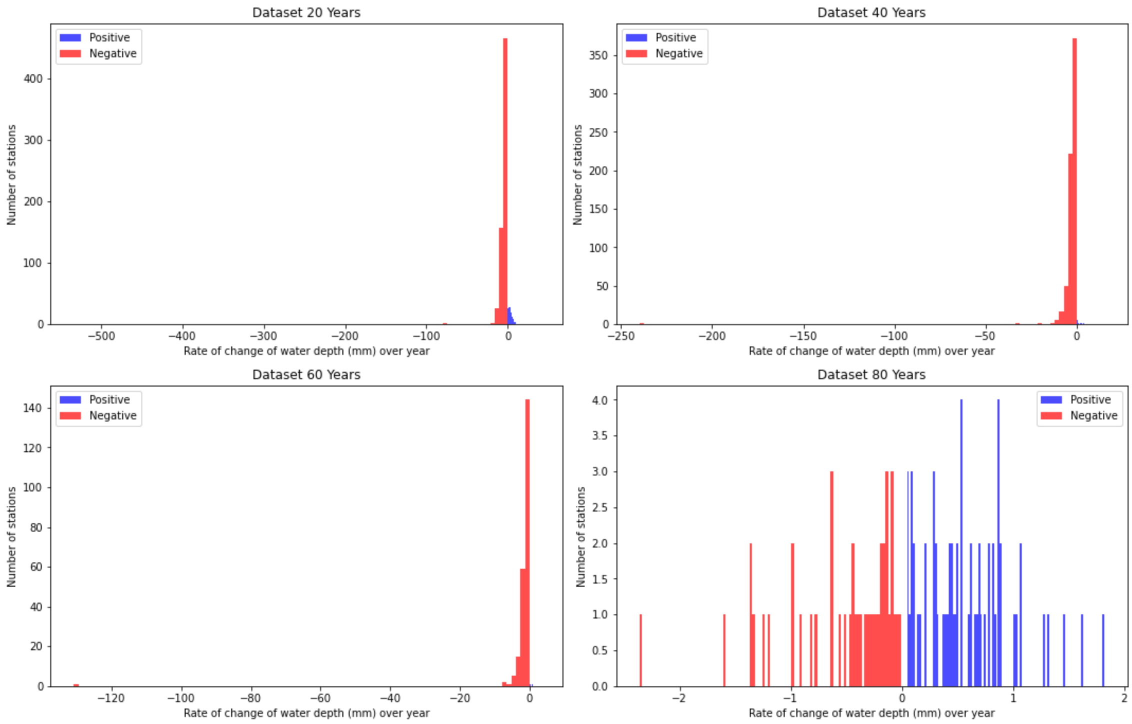

Figure 4.3: Histogram - Average mean daily flow - Rate of change

- **KDE plot of different time spans:** At the same time, a clear image to support all the aforementioned is also given in the Graph 4.4. Higher peaks, like the case of the time frame of 1942-2021 indicates that the change of discharge is around to zero,more densely concentrated, and the with mean value to be a little positive value, however the rest analyses (namely 1962-2021, 1982-2021) have in the KDE plot indicate regions where the data points have lower peaks represent regions where the data points are less concentrated. Furthermore, their mean values are negative. In the last 20 years of analyses (from 2002 - 2021), we can see another pattern, the values are much more less concentrated and in this analysis, there are also some positive trends but the decreasing trend are predominant in that time frame as well.

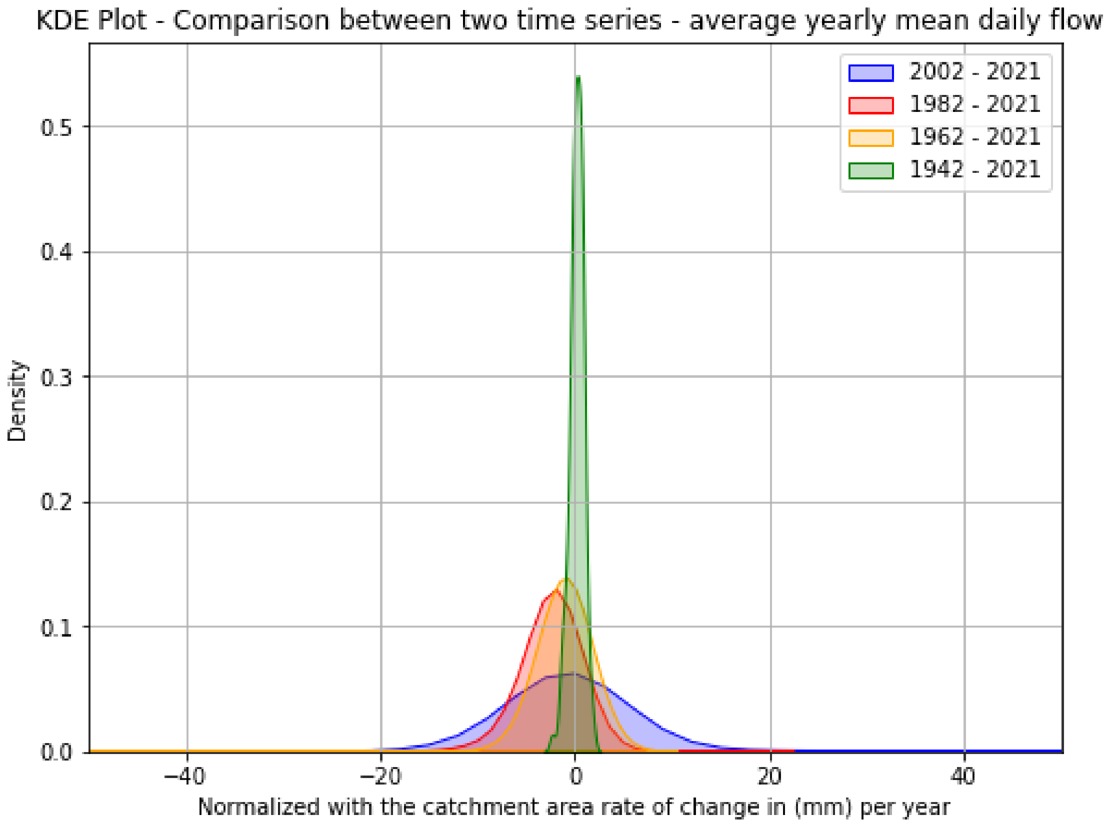

Figure 4.4: KDE Plot - Average mean daily flow - Rate of change: Comparison of the time series distribution

- **Pie charts of different time spans:** All pie charts are accessible in the Appendix 6; however, it is interesting to focus on the recent 20 years and compare them with the 40 years of analysis. As depicted in the Pie Chart 4.5, only 22% of the stations that were active during both the 40 and 20-year analysis periods have consistently maintained their trends. Remarkably, 42% of the stations displayed trends exclusively within the 40-year analysis, while nearly 38% exhibited trends only in the last two decades (from 2001 to 2021).

  Taking into account the introduction of new stations over the last 20 years, it becomes apparent that during the intermediate time period from 1982 to 2001, some stations displayed trends, but in the subsequent 20 years, these trends diminished or disappeared. This is supported why the last 20 years, even the number of stations is 1185, the percentage of the station with trends is smaller than the corresponding percentage of 40 years of analysis, when the number of installed stations is 725.

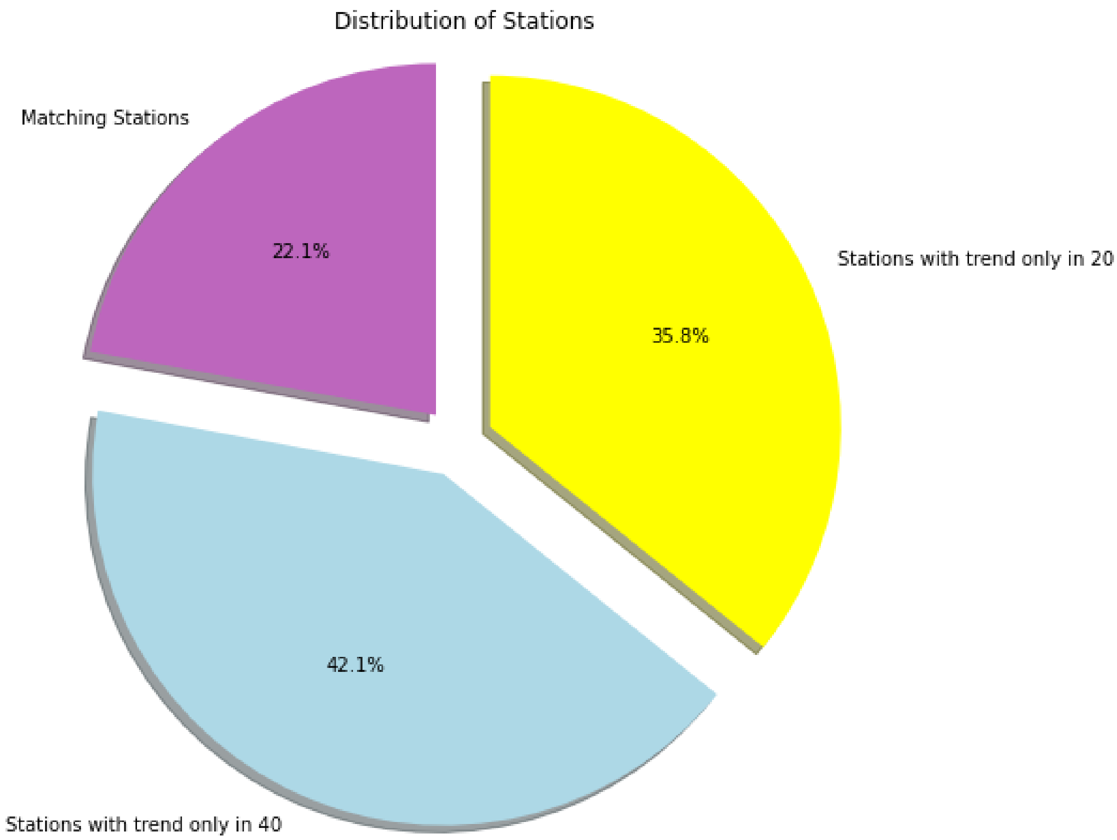

Figure 4.5: 2002-2021 & 1982-2021 Average mean daily flow - Matching stations.

- **Stations with 80 years of data: Discharge trends over the last 20 years:** In the Scatter Plot 4.6, most stations exhibit no trends for both the 80-year and last 20-year analysis periods. Notably, a significant number of stations show trends over the last 20 years (highlighted in pink on the scatter plot), while only four stations demonstrate trends for both analysis time spans. A closer examination using the P-values Confusion Matrix 4.7 reveals that just two stations maintained negative trends for both the 80-year and last 20-year periods, while two other stations exhibited positive trends for both time spans of analysis.

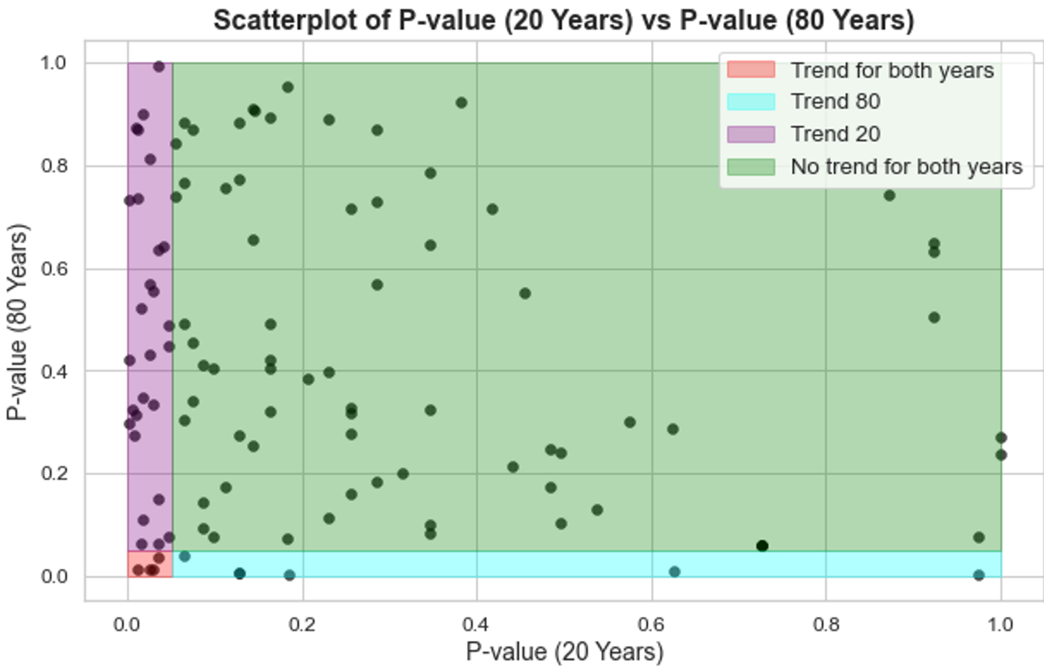

Figure 4.6: P-values Scatter Plot: Comparing the average discharge trends of stations from 1942 to 2021 with their corresponding trends from 2001 to 2021.

Figure 4.7: P-values Confusion Matrix: Comparing the average discharge trends of stations from 1942 to 2021 with their corresponding trends from 2001 to 2021.

4.1.1.2 Maximum yearly mean daily flow

- **20-Year Analysis:** First, for 20-yearly analysis the maximum values per year calculated. Based on the results from the 1186, the 1074 do not have any significant trends (p values > 0.05), while the 75 have decreasing trends and 37 have increasing trends. Concerning the location of the stations, the stations without any trend are located in the center and western part of the case study area with Belgium, Luxembourg and the main part of the North East part of France to have stations without trend in their yearly maxima. On the other hand, the stations with decreasing trends are located in the Eastern part of the area, and the increasing trend in the Western part of the case study area. Moreover, the stations with decreasing trends are located in heights range from 200 to almost 800m; however, the increasing trends are located in elevations until 200m (see Map A1.10).

  Regarding the p-values, a discernible pattern emerges when examining the maxima mean daily flows (see Figure 4.8). Stations displaying decreasing trends are predominantly situated in the North-Eastern portion of the case study area, coinciding with a concentration of stations featuring p-values smaller than 0.03. Conversely, stations with significant increasing trends (p-values < 0.03) are primarily found in the Western sector of the case study area, particularly in North France. This spatial distribution underscores the regional variability in flow trends and their statistical significance.

- **40-Year Analysis:** For the 40 maximum yearly analysis the 576 stations, out of them 134 have decreasing trend and 15 have increasing. Most of the the stations do not have any significant trend and are located around the whole case study area. On the other hand, the stations with decreasing trends are located mainly in Germany, and the less amount of stations with increasing trends are mainly located in North part of France. Concerning the elevation the decreasing trends of the maxima values are located in elevations range from 1 to almost 700 m, while the increasing trends are located in lower elevations from 10 to 200 m, apart from three stations, in Germany, which have increasing trends and are located in elevations between 400 to 750m approximately (see Map A1.11).

  Regarding p-values, the most significant decreasing trends are centrally located within the case study area. Additionally, p-values < 0.03 are prevalent along the northern, southern, and eastern borders. However, the increasing trends, depicted in blue, lack a distinct pattern. Notably, a cluster of stations near the northern border with Belgium exhibits increasing trends in their p-values (see Figure 4.8).

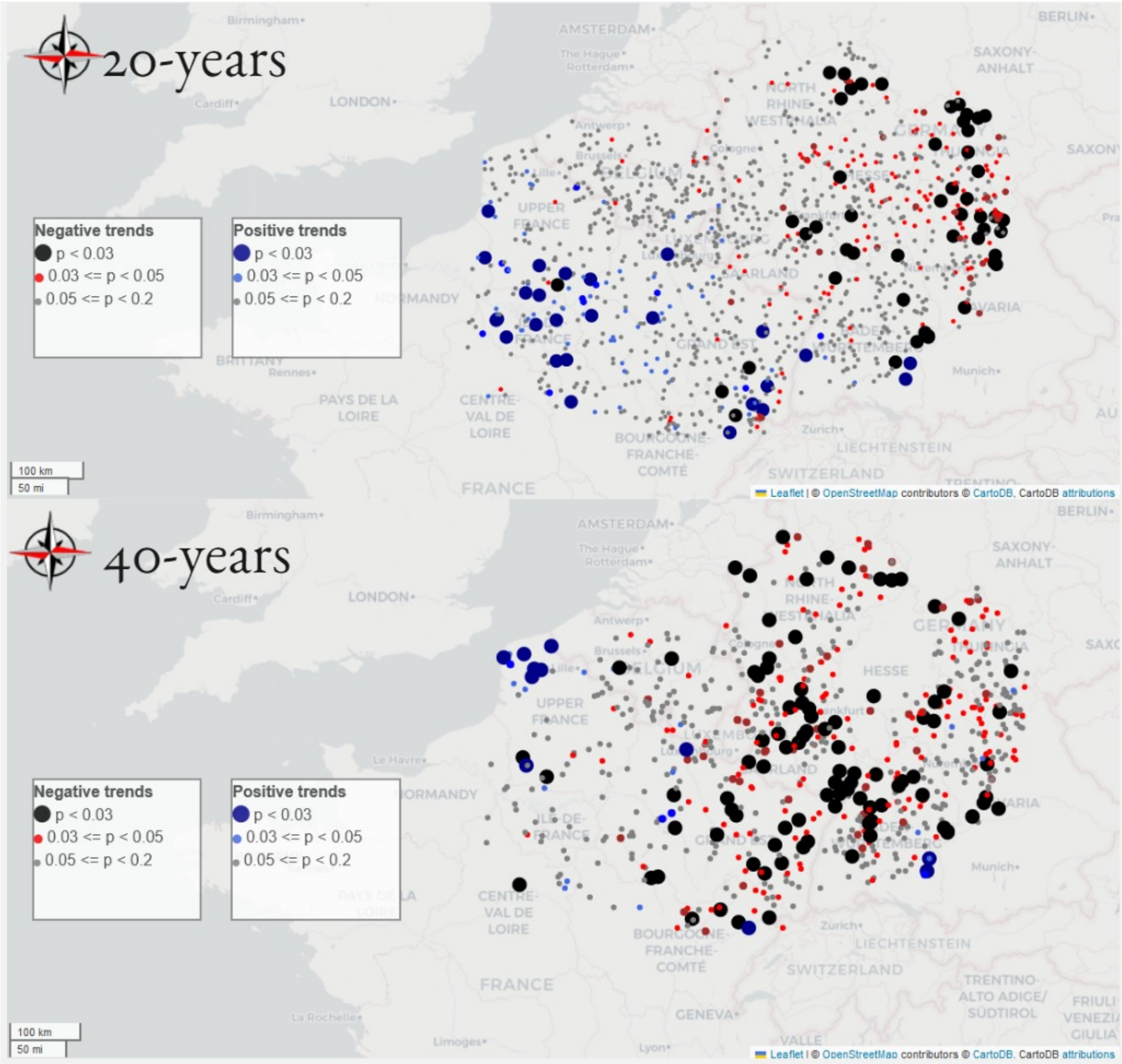

Figure 4.8: 2002-2021 & 1982-2021 Maximum mean daily flow - P values

- **60-Year Analysis:** About the 60 years maxima yearly mean daily flow (mainly from 1962-2021), the stations which have available data they are 266. Most of them they do not have any trend, especially 245 out of 266, do not have trend. While, the stations with decreasing trend are seven and with increasing are 14 stations. As can be seen in the corresponding Map A1.12, the less amount of decreasing stations are located only in Germany in elevations from 1 to 200m, while the stations with increasing trends are located both in France in elevations until around 200m, and in

Germany in higher elevations until almost 600m (see Map A1.12).

In the context of the 60-yearly analysis, a notable observation emerges: a substantial number of stations exhibit significant increasing trends (p-value < 0.03). These stations are predominantly situated in upper France and extend throughout the central to southern regions of the case study area (see Figure 4.9). This spatial distribution highlights the prevalence of substantial upward trends in these areas.

- **80-Year Analysis:** Concerning the 80 years of analysis is hard to conclude in clear patterns since only Germany and one station located in the Netherlands without have trend. From 106 stations only five of them have decreasing trends and are located in the South part of Germany in elevations from 400 to almost 600m. Moreover, there are five stations with increasing trends in the East part of Germany and are located in heights from almost 200 to 400 m. All the rest of stations as can be seen in the Map A1.13 do not have any trend.

  Understanding patterns in the 80-year analysis proves challenging as most stations do not exhibit discernible trends. Notably, significant increasing trends are concentrated in the central region of Germany, while significant decreasing trends (p-values $<$ 0.03) are observed in close proximity to Bavaria, Germany (see Figure 4.9).

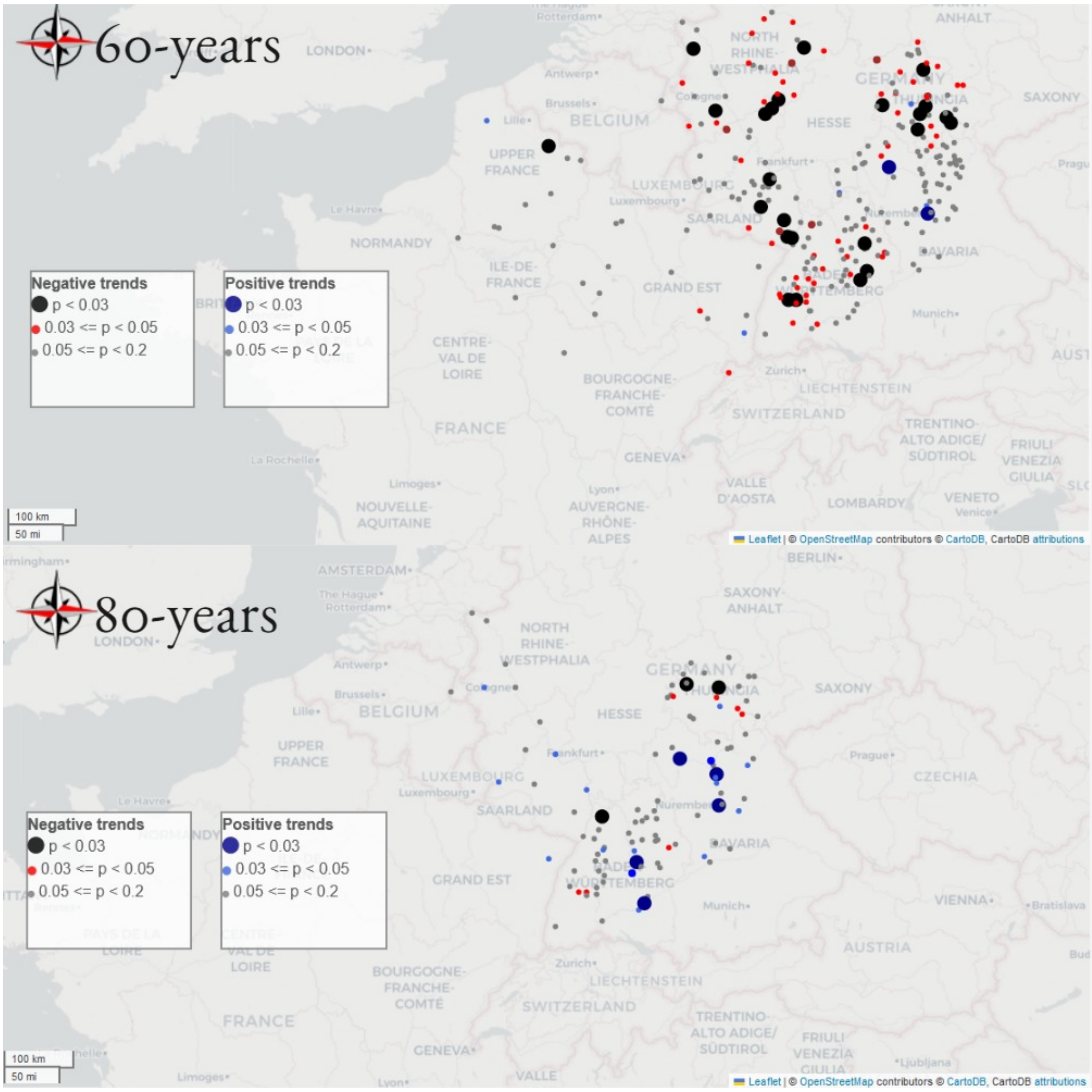

Figure 4.9: 1962-2021 & 1942-2021 Maximum mean daily flow - P values

- **Histogram of different time spans:** For the maxima values for all of the different time frames, the stations which show decreasing trends are more than the stations with the increasing trends. The one exception is the 80 years of analysis, where the number of increasing trends are almost the same with the number of decreasing. Also, the rate of changes shows a different pattern between the 80-yearly analysis and the 60-yearly analysis, since in the 80-yearly analysis the most negative trend of maximum mean daily flow is -45 mm/year, which is changed for the 60-yearly analysis when the most negative trend of the maximum mean daily flow is around -50 mm/year. Also, in 60-yearly analysis, more stations depict decreasing trends than increasing. Regarding the 40 and 20 year of analysis, the rate of changes of 20 years of analysis is much more negative than the 40-yearly analysis. Specifically, the last 20 years, the number of stations with increasing trends are more and the most negative rate of change noticed the last 20 years is -500mm/year, while in 40-yearly analysis is the -250mm/year (see Figure 4.10).

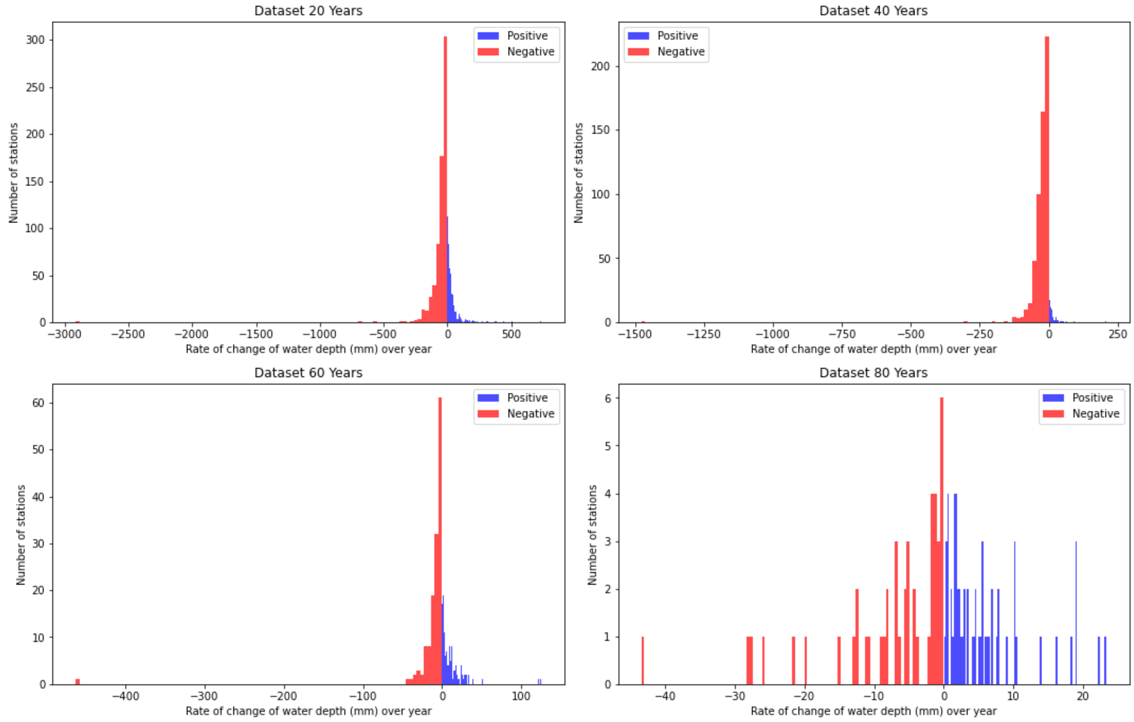

Figure 4.10: Histogram - Maximum mean daily flow - Rate of change

- **KDE plot of different time spans:** KDE plot 4.11 aids in understanding the patterns and time series variations of the yearly maxima mean daily flow. Over the 80-year analysis period, trends in the maxima values span from -50mm to +40mm per year, with nearly equal occurrences of decreasing and increasing trends. However, in the 60-year analysis, stations with decreasing trends become more prevalent compared to those with increasing trends. The rate of change is notably larger, ranging from -60mm to almost +50mm per year. Similarly, in the 40-year analysis, the trends range from -150mm to almost +75mm per year, with decreasing trends outweighing increasing trends. Over the last twenty years of analysis, the number of stations with increasing trends rises, and the rate of discharge change ranges from -400mm to +150mm per year.

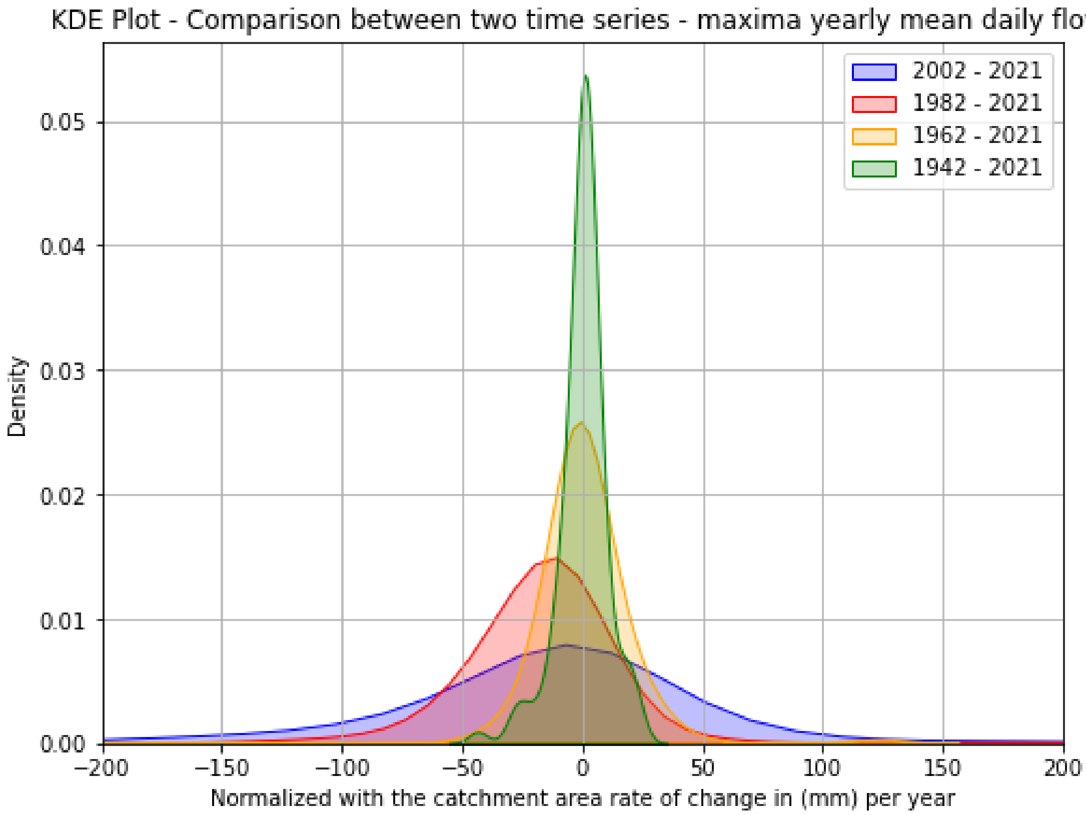

Figure 4.11: KDE Plot - Maximum mean daily flow - Rate of change: Comparison of the time series distribution

- **Pie charts of different time spans:** Regarding matching stations for maximum values, all associated pie charts can be found in the Appendix A1.1. Here, we focus on the 20 and 40 years of analysis, which collectively comprise 13% of stations exhibiting trends during both the 1982-2001 and 2001-2021 periods (see Pie Chart 4.12). Simultaneously, nearly 50% of stations exclusively display trends within the 40-year analysis, while roughly 36% exhibit trends exclusively in the 20-year analysis. Notably, this is significant because there are significantly more stations (1185) with data available for the last 20 years compared to those (725 stations) with data spanning 40 years. This observation suggests that, for the period from 1980-2000, some stations displayed trends that subsequently ceased during the last 20 years, specifically from 2001 to 2021.

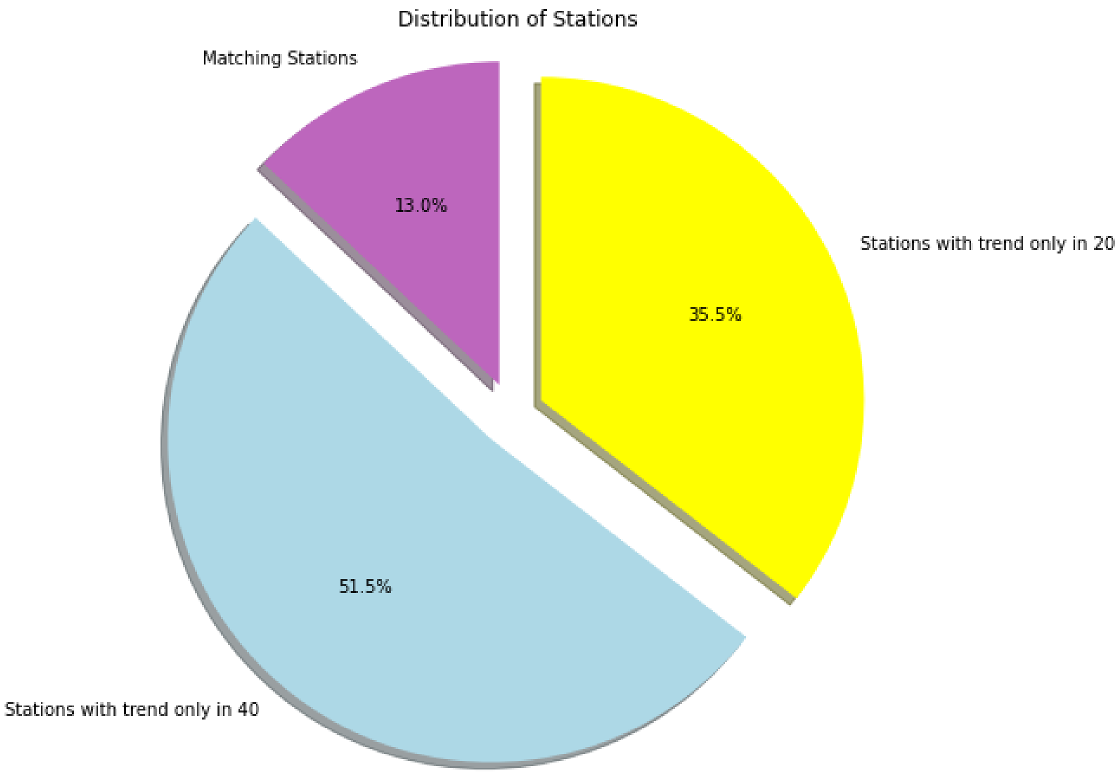

Figure 4.12: 2002-2021 & 1982-2021 Maximum mean daily flow - Matching stations.

- **Stations with 80 years of data: Discharge trends over the last 20 years:** In the scatter plot comparison (see Figure 4.13), most stations do not exhibit trends for either the 80-year or last 20-year analysis periods. Interestingly, ten stations display trends over the last 20 years, highlighted in pink on the scatter plot, while only three stations demonstrate trends for both analysis time spans. A more detailed examination using the P-values confusion matrix (see Figure 4.14) reveals that only three stations maintained negative trends for both the 80-year and last 20-year periods, with no other stations showing positive trends for both time spans of analysis.

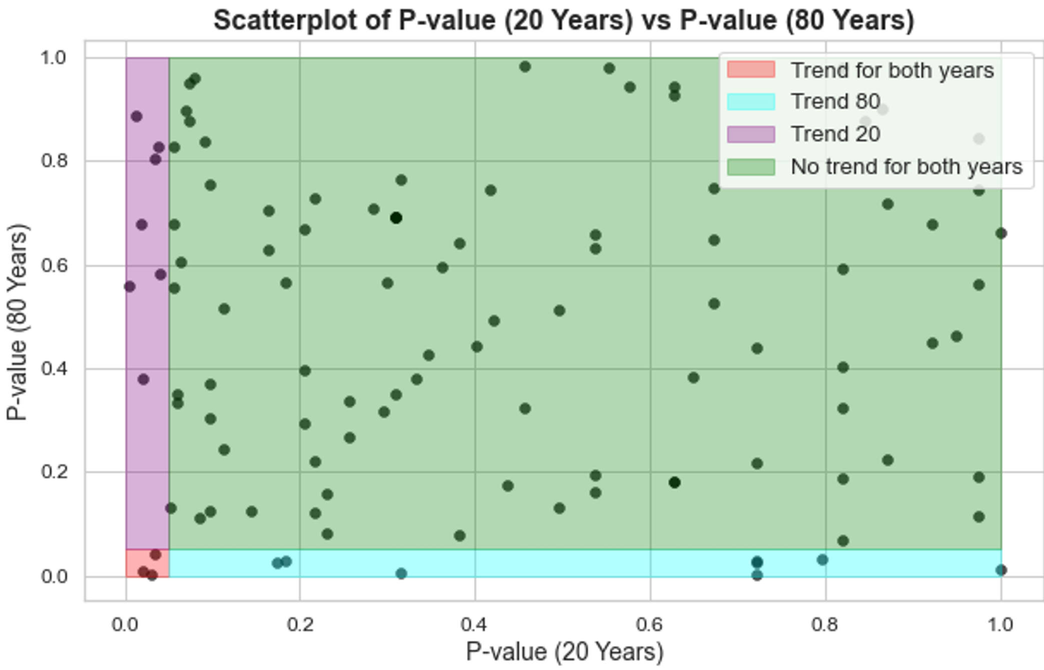

Figure 4.13: P-values Scatter Plot: Comparing the maximum discharge trends of stations from 1942 to 2021 with their corresponding trends from 2001 to 2021.

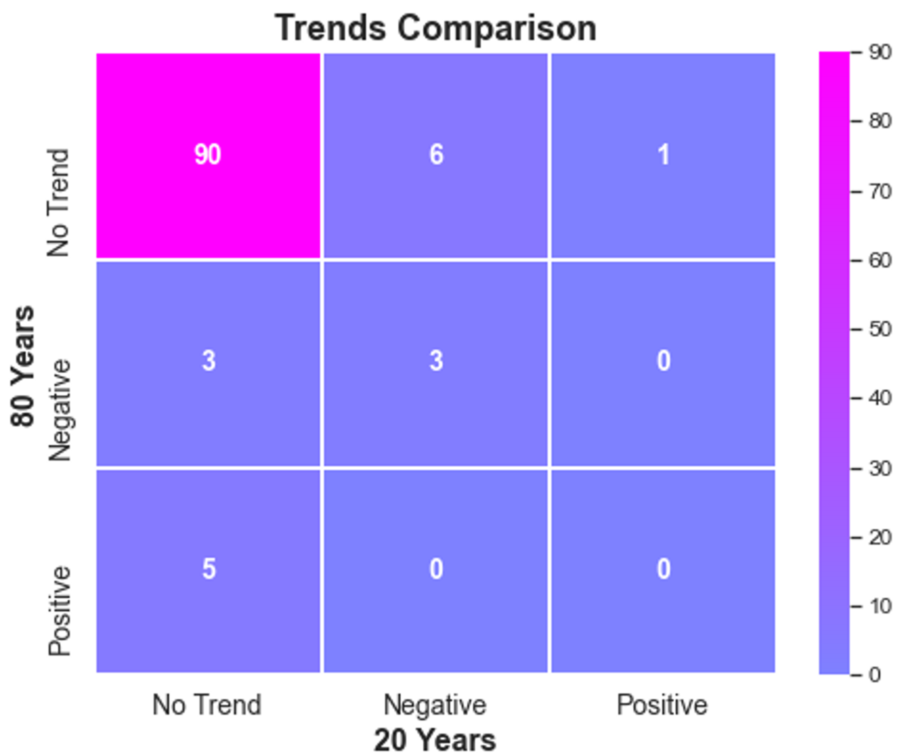

Figure 4.14: P-values Confusion Matrix: Comparing the maximum discharge trends of stations from 1942 to 2021 with their corresponding trends from 2001 to 2021.

4.1.1.3 Minimum yearly mean daily flow

- **20-Year Analysis:** The case study comprised a total of 1186 stations, with 880 of them showing no discernible trend in their data. Among the remaining stations, 23 exhibited a distinct increasing trend primarily concentrated in the western part of the study area, with elevations reaching almost 200 meters. Conversely, 283 stations displayed decreasing trends, which were distributed across the entire area, with fewer instances observed in the West-South region. These declining trend stations were situated at heights ranging from ground level up to approximately 800 meters. Regarding the p-values, a clear pattern emerges from the corresponding Map 4.15. The majority of stations exhibit decreasing trends, with significant trends (p-values < 0.03) dispersed across almost the entire case study area, excluding the Western region. In the West, although some stations display significant decreasing trends, their prevalence is lower compared to the rest of the case study area. However, when examining minima mean daily flow, the locations of stations with decreasing trends are less distinct. While some are discernible in North France, there is also a presence of such stations in the South and Eastern parts, indicating a more dispersed distribution of decreasing trends in this context.

- **40-Year Analysis:** For the 40 years of analysis, the minima values have 213 stations which depict decreasing trend, 18 with increasing trend and all the rest out of the 725 total number of stations, they do not have any trend. The stations with decreasing trends are located in the center of the case study area and in the West and South part of Germany in elevations range from 200 to 800m. On the other hand, the less amount of the increasing trends do not show any specific pattern, but they are mainly located in the edges of the case study area in heights range from 10 to almost 400m.

  Regarding p-values, a distinct pattern emerges: significant decreasing trends with p-values < 0.03 primarily cluster in the central area of the case study. Additionally, notable decreasing trends are observed in the southern and eastern borders of the case study area. Significant increasing trends, as depicted in the Map 4.15, are prevalent in France, with some stations displaying p-values > 0.03. Furthermore, increasing trends are noted in the northern region and the eastern part of the case study area.

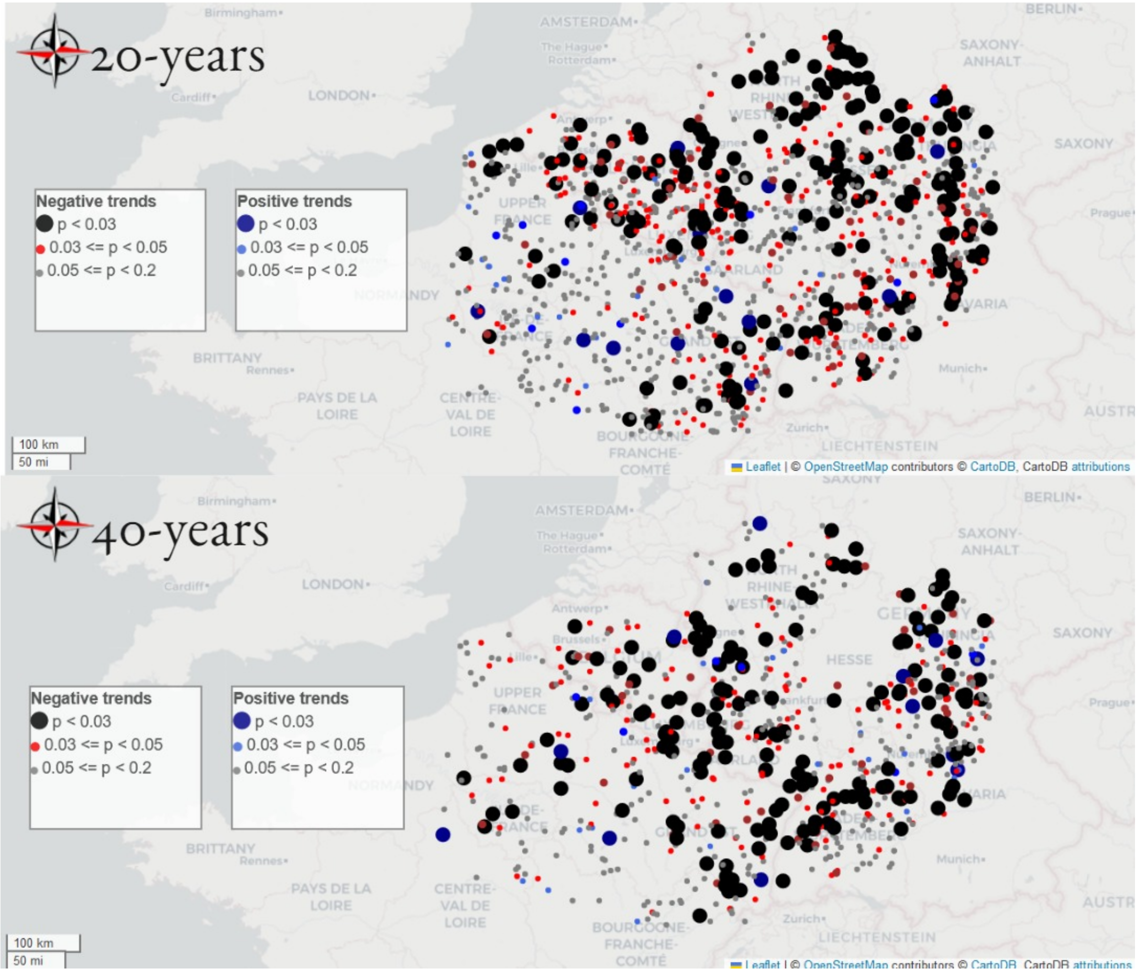

Figure 4.15: 2002-2021 & 1982-2021 Minimum mean daily flow - P values

- **60-Year Analysis:** For the 60 years of analysis, namely from 1962-2021, 266 available stations that they have data. From them, 43 stations have decreasing trend, 16 they have decreasing and the rest (namely 207) do not have any significant trend. Based on corresponding the map, the less stations with decreasing trend are located in South-East part of the case study area, while also the stations with increasing trend are located in the Eastern part of the case study area. Concerning the stations without trend, they are located in the centre and Eastern part as well as the small amount of stations with increasing trends. About the connection between the trend and the elevation, the stations with increasing trends are located in heights between 194-388 while the decreasing trends are also located and in higher elevations (194-581m).

Regarding p-values, Map 4.16, stations with significant decreasing trends are primarily found in the central area of the case study, as well as in the southern and some in the north-eastern regions. In these same areas, there are additional stations with decreasing trends, albeit with p-values ranging from 0.03 to 0.05. On the other hand, increasing trends are predominantly concentrated in the eastern part of the case study area, and most of these trends are statistically significant (p-values $<$ 0.05).

- **80-Year Analysis:** In the yearly analysis of the minima value, from 106 stations with available data only 5 have decreasing trends, 25 have increasing trend and all the rest have no significant pvalues $>$ 0.05, so they do not have trends. It is had to result in patterns, however, the stations with decreasing trends are located at the bottom of the mountains in Germany, in elevations almost 200 m. On the other hand, the stations with increasing trends are located predominantly in lower elevations until 200m.

As previously noted, there is a prevalence of increasing trends compared to stations displaying decreasing trends. In Map 4.16, it becomes evident that these trends are not only on the rise but also highly significant, with p-values consistently lower than 0.03.

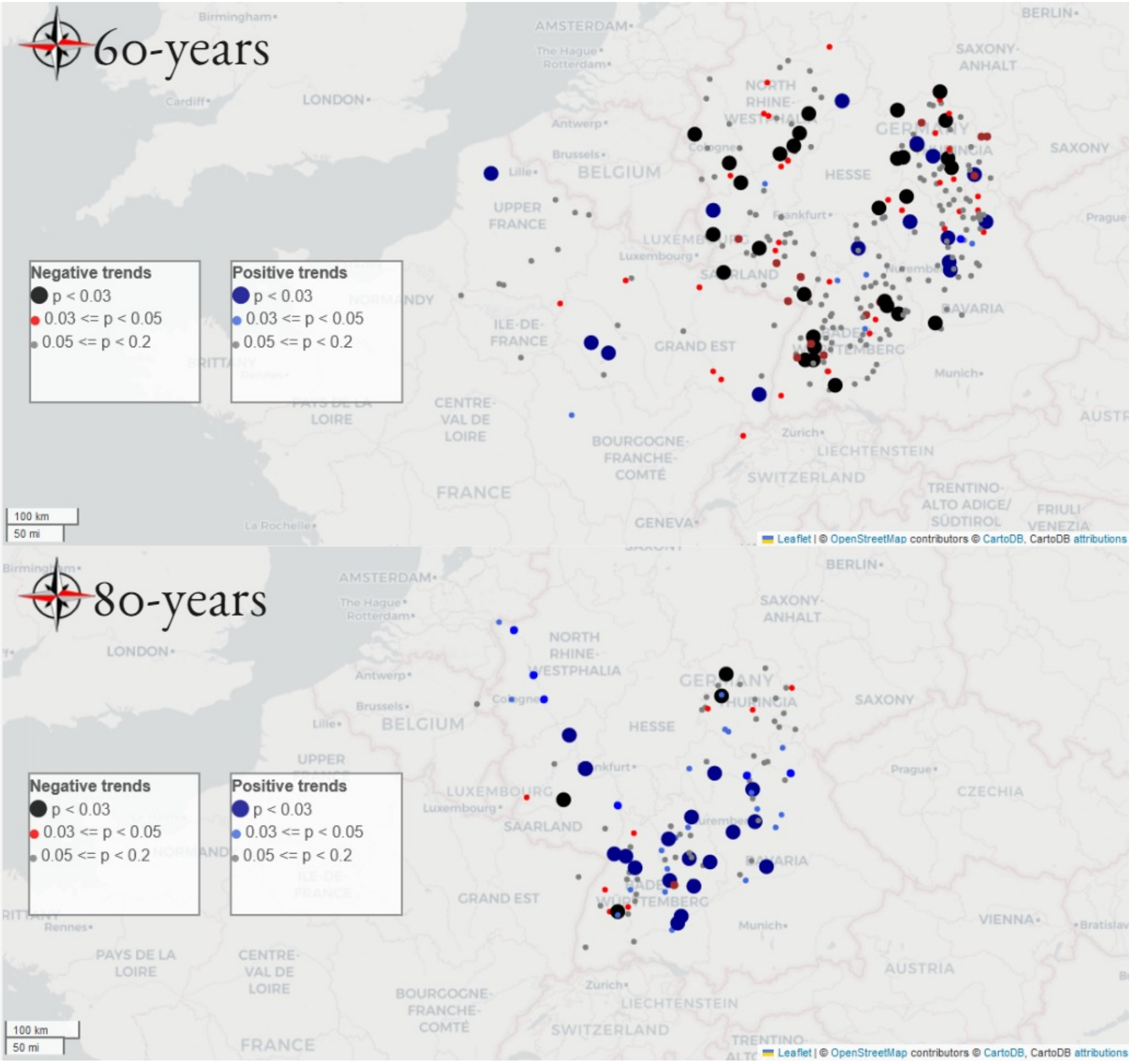

Figure 4.16: 1962-2021 & 1942-2021 Minimum mean daily flow - P values

- **Histogram of different time spans:** The minima analysis, as shown in the Histogram 4.17, reveals that over the 80-year analysis period, the proportions of stations with increasing trends are more than the number of stations decreasing trends in their minima values. However, this pattern shifts in the 60, 40, and 20 years of analysis, with a notable decrease in the number of stations displaying increasing trends. Remarkably, the most negative trend observed over 80 years is -1 mm/year, and this trend has evolved over time. In the most recent 20 years, it matches the most negative trend observed, which stands at -20 mm/year for the minima mean daily flows.

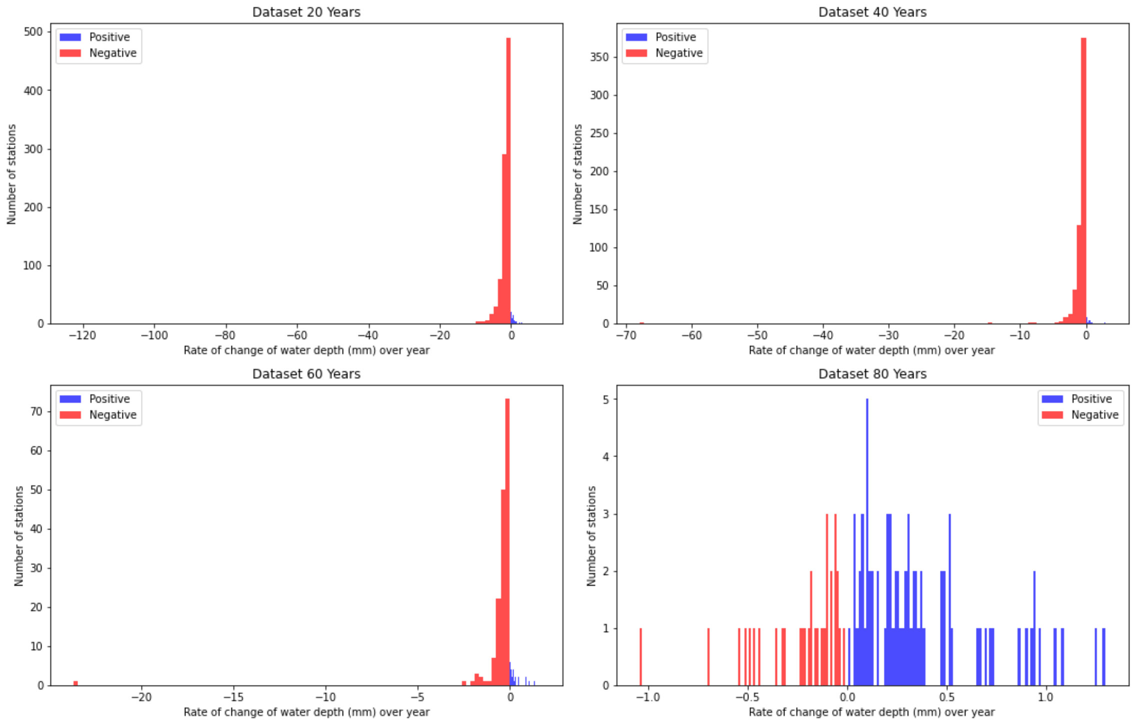

Figure 4.17: Histogram - Minimum mean daily flow - Rate of change

- **KDE plot of different time spans:** At the same time, the KDE plot 4.18 also supports the same results with histogram. Specifically, the rate of change for 80-years of analysis is close to zero, ranging from -2mm to +1.5mm per year. In the 60 and 40-year analyses, there is a higher occurrence of stations with decreasing trends compared to those with increasing trends. The Sen's slope ranges from -5mm to +2.5mm per year for the 60-year analysis and -7.5mm to +5mm per year for the 40-year analysis. Lastly, in the most recent 20-year analysis (2002-2021), the number of stations with increasing trends slightly increases, along with the rate of change, ranging from -10mm to +7.5mm per year.

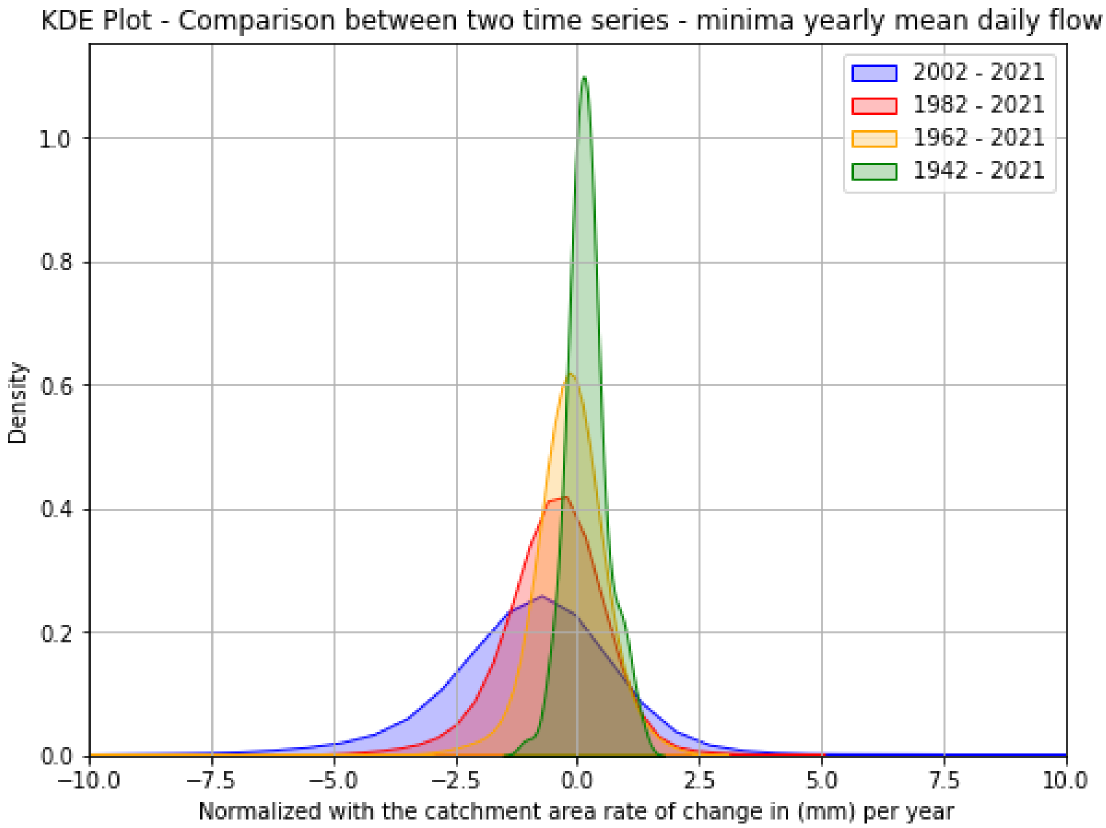

Figure 4.18: KDE Plot - Minimum mean daily flow - Rate of change: Comparison of the time series distribution

- **Pie charts of different time spans:** Regarding matching stations, when comparing the 20-year and 40-year analysis, it's evident that stations with matching trends account for approximately 21%. However, the dynamics shift when examining minima values, where stations exhibiting trends solely in the last 20 years (2001-2021) make up nearly 50% of the total. Remarkably, almost 30% of the 725 stations with available data spanning from 1980 to 2021 display trends. This suggests the addition of new stations with trends in the last 20 years, which were absent during the intermediate period from 1980 to 2000 (see Pie Chart 4.19).

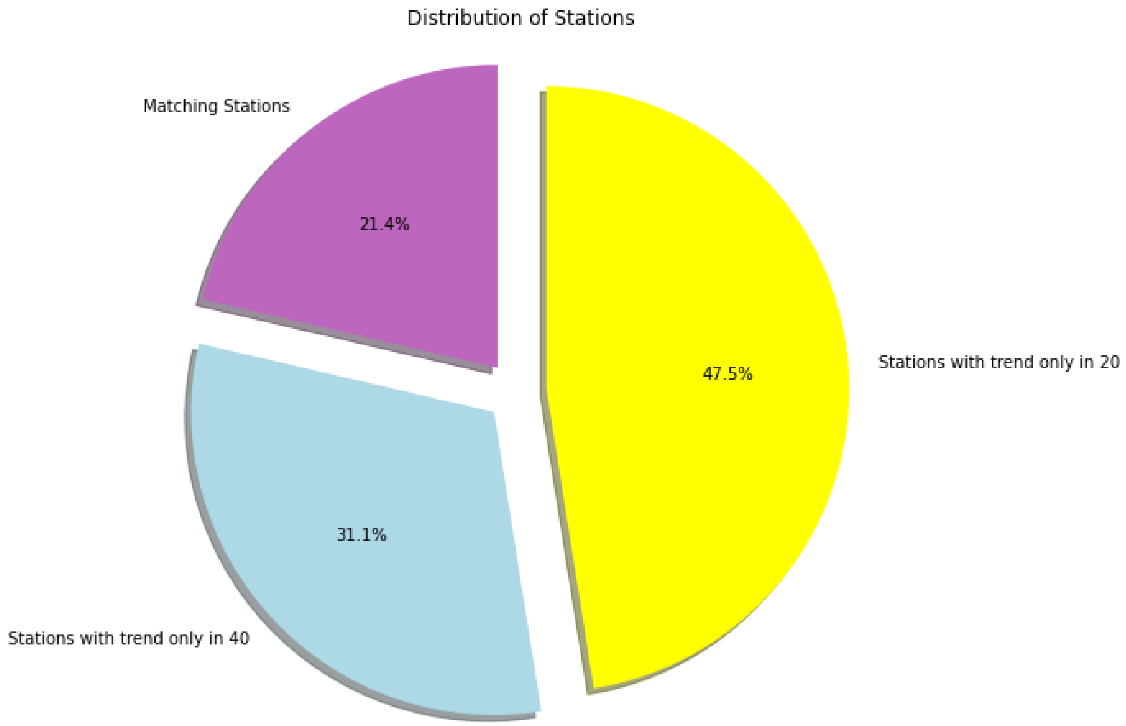

Figure 4.19: 2002-2021 & 1982-2021 Minimum mean daily flow - Matching stations.

- **Stations with 80 years of data: Discharge trends over the last 20 years:** In the scatter plot comparison (see Figure 4.20), the majority of stations do not exhibit trends for either the 80-year or last 20-year analysis periods. Remarkably, 22 stations display trends over the last 20 years, highlighted in pink on the scatter plot. However, a distinct pattern emerges: only four stations demonstrated increasing trends over 80 years, but these trends shifted to decreases in the last 20 years. This transformation is evident in the P-values confusion matrix (see Figure 4.21).

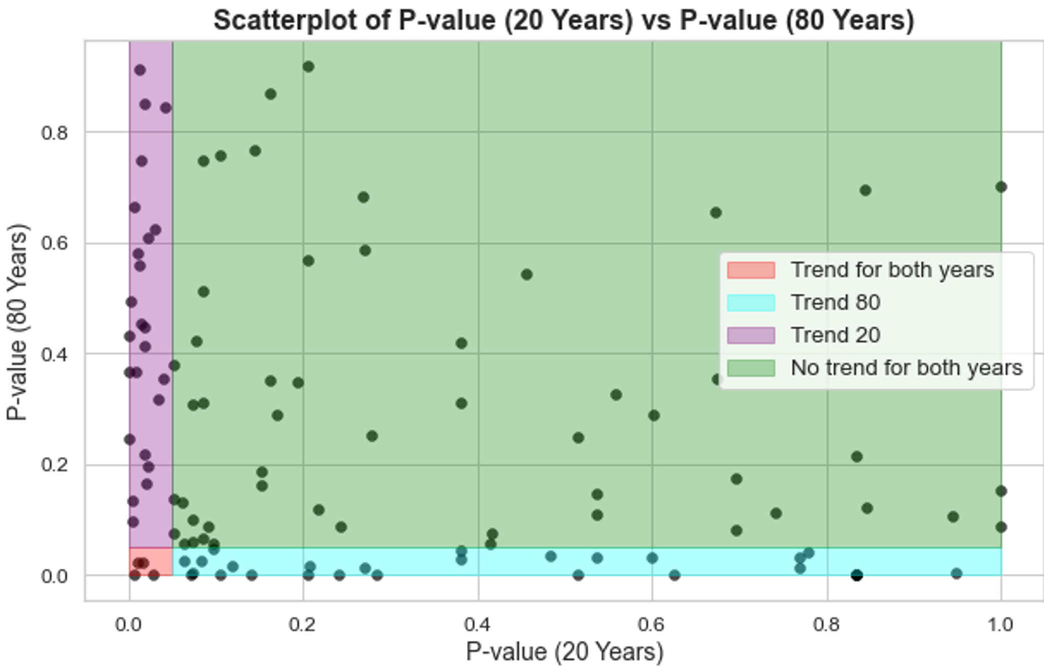

Figure 4.20: P-values Scatter Plot: Comparing the minimum discharge trends of stations from 1942 to 2021 with their corresponding trends from 2001 to 2021.

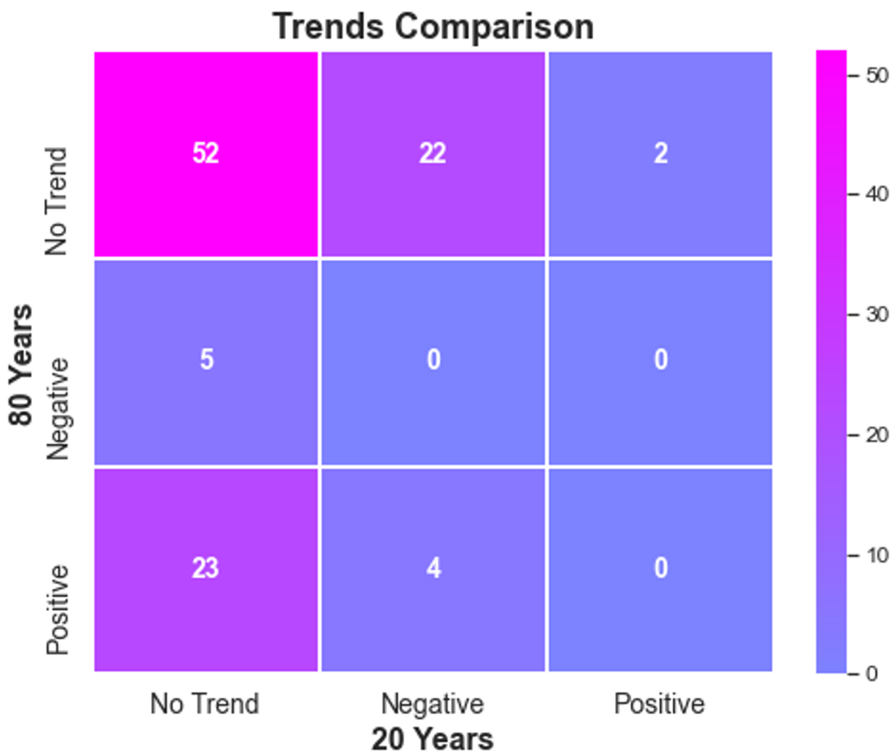

Figure 4.21: P-values Confusion Matrix: Comparing the minimum discharge trends of stations from 1942 to 2021 with their corresponding trends from 2001 to 2021.

4.1.2 Monthly analysis

4.1.2.1 Average monthly mean daily flow

In the context of Average Monthly Analysis, the results vividly illustrate the trends in average monthly discharge (in mm/month/year) for each station, as comprehensively discussed in the methodology chapter (Chapter 3).

To begin, Bar Charts were generated for different time spans 4.22, providing a clear depiction of the average contribution of each month. These bar charts offer insights into the average values for each month within specific time spans. For instance, the value of 0.01 mm/month/year for January over a 20-year analysis is computed by aggregating all January trends across the 20 years and dividing by 20, extending the same concept to other months.

Following the methodology outlined in the preceding section, stations were systematically categorized based on their geographical proximity using K-means clustering. Within each station group, we identified the most prevalent months for both the highest and lowest trends. Figure A1.29 in the Appendix effectively presents this information. The figure's distinct subplots are associated with varying observation time spans, ranging from 20 to 80 years. Each unique color corresponds to a different month, and each data point represents an individual station. The x-axis (Longitude) corresponds to the southern part of the case study area, while the y-axis depicts the Latitude in the eastern part of the area. The z-axis represents Sen's slope in mm/month. Further explanatory guidance on interpreting cardinal directions (North, East, West, and South) can be found in the Appendix 6, especially in A1.2, which includes an illustrative image. Throughout this chapter, the results arising from different time spans are commented upon based on the findings displayed in Figure A1.29. To maintain the chapter's flow and conciseness, we focus on the months with the most positive and negative trends for the 20-year period, as depicted in Figures 4.23 and 4.24.

Consequently, the interpretation of both bar charts and cluster plots yielded the following results. The bar charts provide insights into the range of average values for each month on average, while the cluster plots offer information about the geographical locations of the stations exhibiting the highest and lowest trends. This linkage between month and station group location provides valuable insights into the spatial distribution of hydrological trends within the study area.

Monthly average contribution over different time spans - Bar charts 4.22:

- **20 - Year Analysis:** Based on the results arose by clustering, of the 20 years under analysis, December emerges as the month of highest significance, boasting a substantial contribution of nearly 0.04 mm/month. Following closely, February and January exhibit notable average contributions of approximately 0.02 mm/month and 0.01 mm/month, respectively.

  Turning to months with negative contributions, May, April, and August assume positions of relatively diminished influence, ranked from the least negative to the most negative contribution. These three months collectively represent the period of lowest impact, a pattern also evident in the accompanying graph (refer to the provided graph). Particularly, May demonstrates a negative contribution of around -0.01 mm/month.

- **40 - Year Analysis:** In the context of 40 years of analysis, February takes the lead in positive contributions, while April demonstrates the lowest contribution, registering figures of 0.005 mm/month and -0.015 mm/month, respectively. Moreover, December displays almost negligible involvement in the discharge increment.

  Conversely, subsequent to April, both May and June emerge as months of diminished contribution, each hovering at around -0.005 mm/month. Generally, it's discernible that from April to July, a prevailing trend of negative discharge unfolds. It's noteworthy, however, that January also exhibits negative discharge trends, albeit of a lesser magnitude, falling below -0.005 mm/month.

- **60 - Year Analysis:** In the 60-year analysis, January shows high positive trends (0 - 0.005 mm/month/year). February and March follow with lower positive trends (around 0.03 and 0.01, respectively). December exhibits near-zero positive trends. Most months have negative trends. April has the most negative trends (up to -0.01 mm/month/year), while May and June follow with -0.05 and -0.03 mm/month/year. July, August, September, October, and December show negative trends ranging from -0.03 mm/month/year to near-zero.

- **80 - Year Analysis:** In 80 years, January and December exhibit the highest trends, registering 0.03 and 0.025 mm/month/year, respectively. Positive trends also emerge in February and March, hovering around 0.02 mm/month/year. Conversely, May, October, and November show positive trends but remain below 0.001 mm/month/year. April records the most negative trend, reaching -0.002 mm/month/year. Meanwhile, June, July, August, and September display negative trends within the range of 0 to -0.001 mm/month/year.

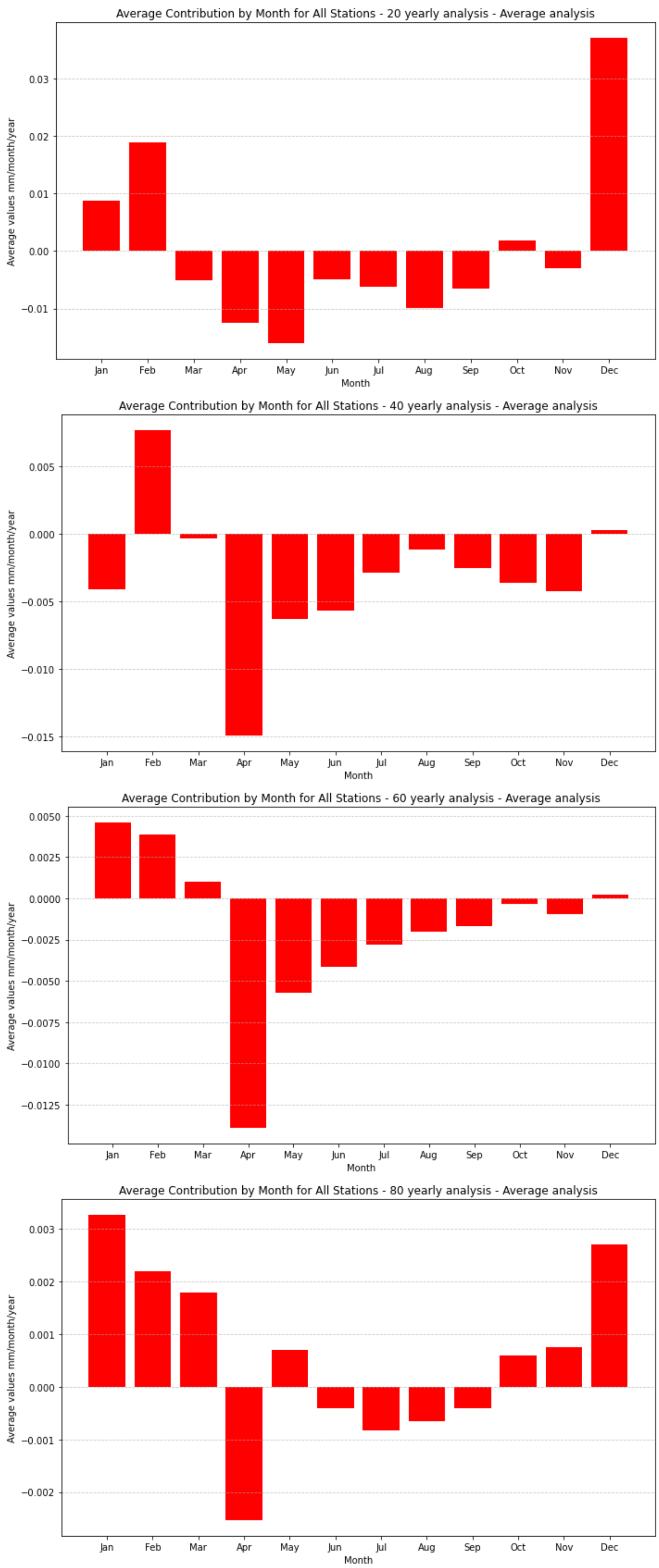

Figure 4.22: Bar charts of the average trend of each month for Average analysis

Geographical Correlation of Months with Most Positive and Negative Trends among Station Groups:

- **20 - Year Analysis (see Figures 4.23, 4.24):** Moreover, the analysis delved into further detail by partitioning the study area into distinct groups of stations using K-means clustering, a machine learning tool. Within this context, the 20-year analysis of positive contributions (see Figure 4.23) revealed consistent patterns that highlight the spatial variability across the study area. December consistently emerged as the dominant month across the entire case study area, indicating its significance in shaping positive contribution trends. However, a notable distinction emerged in the East region, where February took precedence as the dominant month of positive contribution.

  In the realm of negative contributions (see Figure 4.24) within the 20-year analysis, the distribution of months with negative discharges showcased intriguing spatial variability. March surfaced as the dominant month for negative contributions in both the Central and North-East parts of the study area. In the North-West region, August emerged as the month with the most significant negative contributions, emphasizing its pivotal role in shaping unfavorable discharge trends. Similarly, in the Central and North-West areas, May took center stage as the dominant month for negative contributions. Notably, the West region exhibited considerable diversity among station groups, with April, September, and February emerging as the dominant months in various clusters. These refined analyses illuminated the intricate spatial intricacies of discharge trends, contributing a layer of complexity that enriches our understanding of the broader temporal patterns observed.

- **40 - Year Analysis - Figure A1.29:** Shifting our focus to the 40-year analysis, the location factor continues to hold sway over discharge trends. Mirroring the 20-year analysis, December remained the unequivocal dominant month of positive contribution throughout the case study area. However, a shift was observed in the North-West region, where February claimed dominance in terms of positive contributions.

  Examining negative contributions over 40 years, a singular pattern emerged as April consistently appeared as the dominant month across the entire case study area. This underscores the enduring influence of April in shaping negative discharge trends. This trend persisted regardless of the spatial divisions within the study area.

- **60 - Year Analysis - Figure A1.29:** The 60-year analysis revealed higher variability in months with positive trends. January dominated the central area, while in North the dominant month is February. August emerged as the dominant month in the South-West. The North-East has also a group with August as the dominant month. There is an exception of a group located in East, where February stood out as the dominant month. April consistently appeared as the month with the most negative trends across all station groups.
- **80 - Year Analysis - Figure A1.29:** In the 80-year analysis, spatial variations in months with the highest contributions were evident. January dominated in multiple North, Center, and North-West groups. In the North-Eastern region, there exists a cluster of stations where March stands out as the predominant month for positive trends. Meanwhile, a central group favored May as the dominant month with the highest trends. In the North-West, two groups favored February and October, and the Center of case study area featured March as the dominant month. Concerning the most negative trends, April mainly presented them across the entire study area, except for one cluster of stations located in the North-West, where January showed the most negative trends.

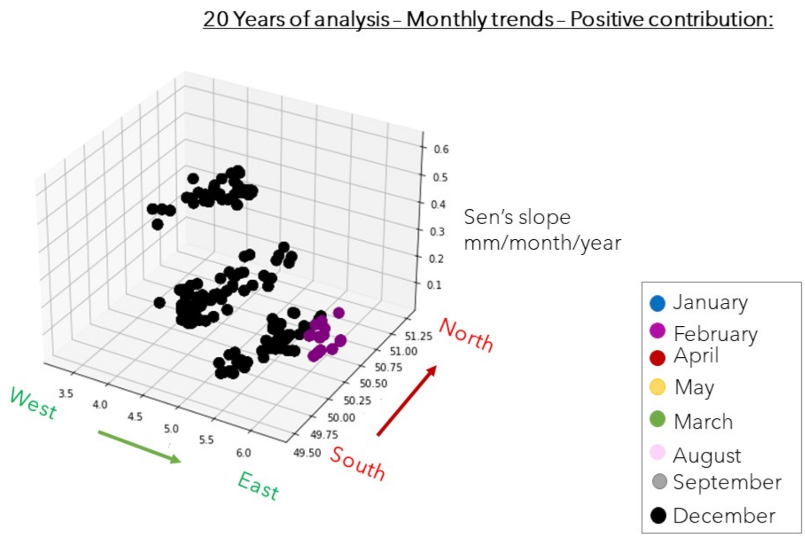

Figure 4.23: Cluster plot: Average monthly positive trends over a 20-year analysis period for station groups.

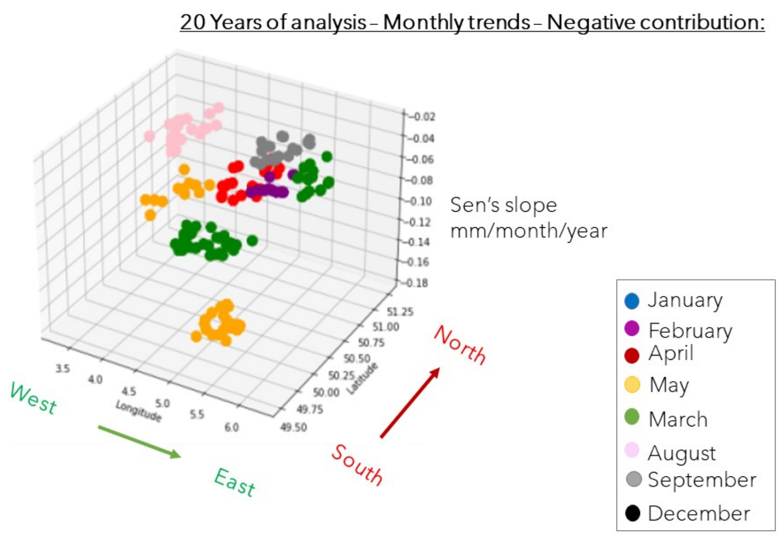

Figure 4.24: Cluster plot: Average monthly negative trends over a 20-year analysis period for station groups.

4.1.2.2 Maximum monthly mean daily flow

As previously described and discussed in the preceding section covering Average Monthly Results, two distinct types of plots were employed: bar charts and cluster plots, tailored for various time spans.

In the Maxima Analysis, the bar charts succinctly convey the average trends of maximum values for each month. For instance, in the case of January, the histogram depicts the average trend value of January's maximum values. This process is reiterated for all other months.

Additionally, the cluster plots visually represent the identification of the months exhibiting the most positive and most negative trends within specific station groups.

Monthly average contribution over different time spans - Bar charts 4.25:

- **20 - Year Analysis:** Within the realm of the 20-year analysis, December stands as the month with the highest average trend, reaching 0.04 mm/month/year. February ensues with an average of 0.02 mm/month/year, while January holds an average of 0.0.1 mm/month/year. In terms of negative contributions on average, May exhibits the lowest trends with almost -0.02 mm/month on average, followed by April and August with almost -0.02 mm/month/year on average.
- **40 - Year Analysis:** Over a 40-year analysis period, February consistently exhibits the highest trends, averaging around 0.02 mm/month/year. In comparison, December closely follows with an average of nearly 0.01 mm/month/year. Conversely, the remaining months display negative trends, with April registering the most pronounced negative trend, notably averaging -0.03 mm/month/year.
- **60 - Year Analysis:** In this time frame, January, February, March, and December exhibit positive trends, while the remaining months show negative values. Specifically, January averages around 0.005 mm/month/year, while February, March, and December display lower positive trends, with December approaching negligible trends near zero. Conversely, a greater number of months demonstrate negative trends. April, for instance, averages a trend of -0.0125 mm/month/year. Meanwhile, from May to November, the trends are notably lower, averaging -0.0052 mm/month/year.
- **80 - Year Analysis:** Over 80 years of analysis, positive trends appear in the following months: January, December, February, March, May, October, and November. Conversely, the remaining months exhibit negative trends. Notably, January boasts the highest positive trend, averaging 0.0033 mm/month/year, closely followed by December at nearly 0.003 mm/month/year on average. The rest of

the months displaying positive trends range from 0 to 0.002 mm/month/year on average. On the flip side, April registers as the month with the most pronounced negative trends, averaging -0.002 mm/month/year. In contrast, June, July, August, September, and October exhibit trends ranging from 0 to -0.001 mm/month/year on average.

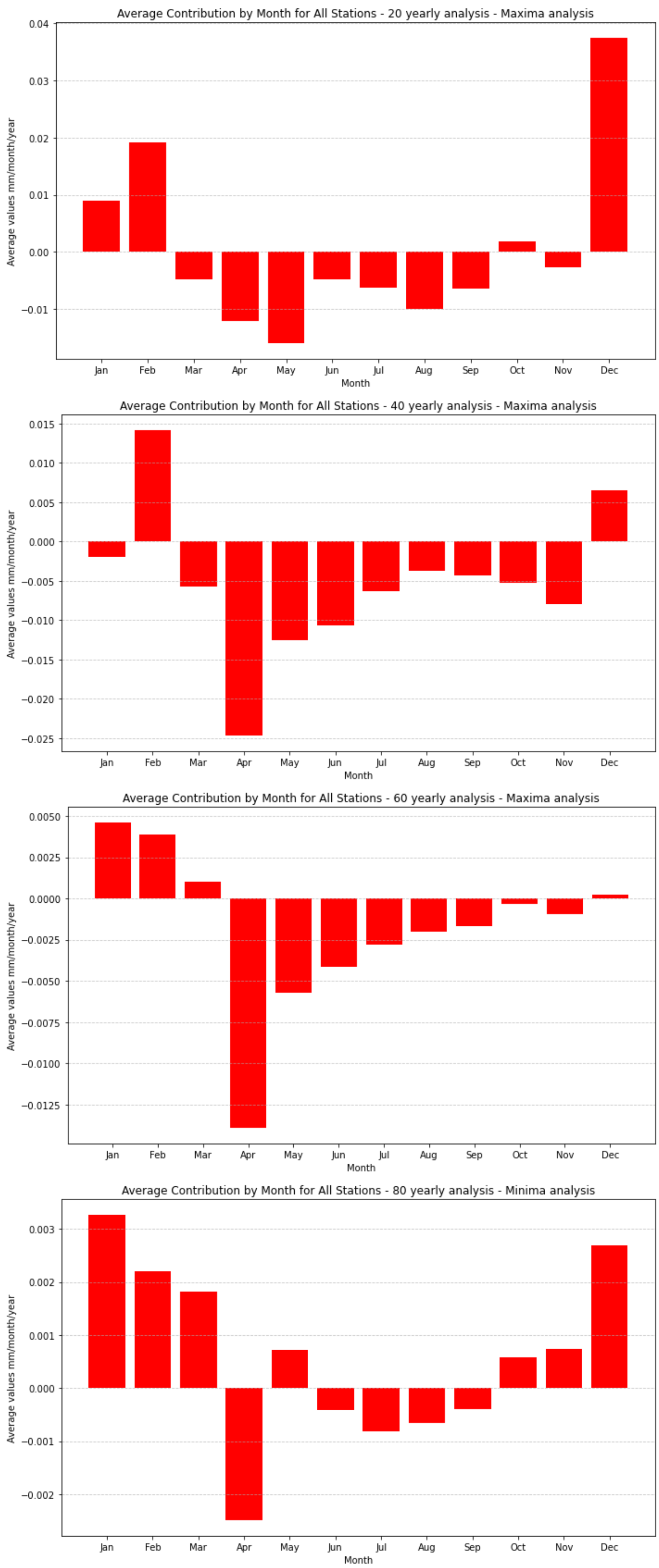

Figure 4.25: Barch charts of the average trend of each month for Maxima analysis

Geographical Correlation of Months with Most Positive and Negative Trends among Station Groups:

- **20 - Year Analysis (see Figures 4.26, 4.27):** In the context of positive contributions, Figure 4.26, across the 20-year analysis, December maintains its dominance across the entire case study area. Additionally, a subset of stations in close proximity to the center of the case study area exhibits dual dominant months, with both December and February holding significance. In the East, February emerges as the dominant month for positive contributions.

  For negative contributions, Figure 4.27 within the 20-year analysis, a diverse pattern unfolds across different areas. In the North-West, August emerges as the dominant month with the most negative contributions. The central and North-West regions depict May as the dominant month in terms of negative trends. Notably, the central area features March as the dominant month with the lowest negative contribution. Meanwhile, in the North region, February assumes the role of the dominant month with the lowest contribution in the negative range.

- **40 - Year Analysis - Figure A1.30:** Shifting to the 40-year analysis, the location factor continues to influence discharge trends. Similar to the 20-year analysis, February emerges as the dominant month of positive contribution across the entire case study area. However, a change occurs in the North region, where December takes precedence in terms of positive contributions.

  Examining negative contributions over 40 years, a consistent trend arises with April serving as the dominant month across the entire case study area. This trend underscores the sustained impact of April on shaping unfavorable discharge trends, irrespective of spatial divisions within the study area.

- **60 - Year Analysis - Figure A1.30:** In the context of 60 years of analysis, January consistently emerges as the prevailing month for positive trends among stations, particularly within the central region of the study area. Additionally, February holds dominance in the North, East, and a group located in West portions of the case study area. Conversely, across all groups within the study area, April consistently stands out as the month most frequently associated with negative trends.

- **80 - Year Analysis - FigureA1.30:** In the comprehensive 80-year analysis, January emerged as the predominant month in multiple groups located in the North, Central, and North-West regions. In North-East part, there is also a group of stations with March as dominant month of positive trends. In contrast, a central cluster exhibited a preference for May as the leading month with the highest trends. In the North-West, two distinct groups favored February and October, while the central area of the case study featured March as the prevailing month. In terms of the most adverse trends, April was the primary contributor across the entire study area, except for one cluster of stations situated in the North-West, where January exhibited the most negative trends.

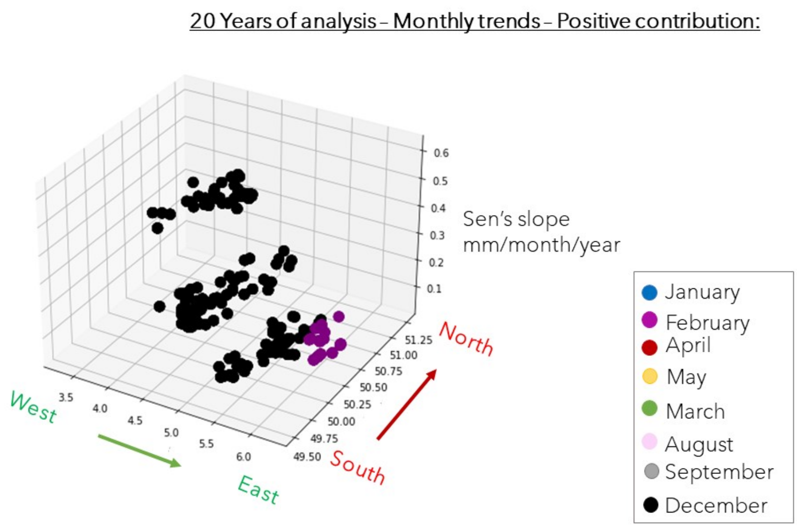

Figure 4.26: Cluster plot: Maximum monthly positive trends over a 20-year analysis period for station groups.

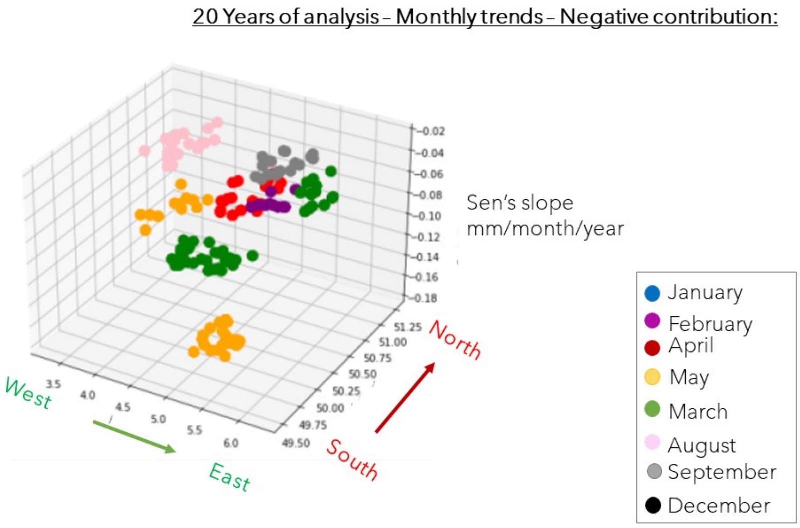

Figure 4.27: Cluster plot: Maximum monthly negative trends over a 20-year analysis period for station groups.

4.1.2.3 Minimum monthly mean daily flow

Also, regarding the Minimum analysis, bar charts and cluster plots, tailored for various time spans were made.

In the Minimum Analysis, the bar charts succinctly convey the average trends of minimum values for each month. Additionally, the cluster plots visually represent the identification of the months exhibiting the most positive and most negative trends within specific station groups.

Monthly average contribution over different time spans - Bar charts 4.28:

- **20 - Year Analysis:** In relation to the average contribution of months during low-flow conditions, December leads with the most positive average contribution, reflecting a discharge trend of approximately 0.45 mm/month/year. Similarly, January portrays average values of minima flows at 0.4 mm/month/year, while February also demonstrates a positive contribution, measuring 0.35 mm/month/year. Outside the realm of December, January, and February, all other months exhibit negative contributions, with May representing the most significant negative influence at nearly -0.2 mm/month. April and August follow suit with average negative contributions of almost -0.1 mm/month/year.

- **40 - Year Analysis:** Turning to the 40-year analysis of minima, solely February and January exhibit positive contributions, recording averages of approximately 0.2 and 0.1 mm/month/year, respectively. The remaining months display negative contributions, with April presenting the most noteworthy negative impact, reaching an approximate value of -0.45 mm/month/year.
- **60 - Year Analysis:** Over a 60-year analysis period, February and January exhibit positive trends, registering averages of 0.2 mm/month/year and 0.1 mm/month/year, respectively. Conversely, the remaining months manifest negative trends. Notably, April stands out with the highest average trends at 0.43 mm/month/year, closely trailed by May and June at approximately -0.2 mm/month/year each. The remaining months demonstrate trends spanning from 0 to -0.15 mm/month/year.
- **80 - Year Analysis:** Regarding this specific timeframe, January exhibits the most substantial positive trends, averaging at -0.005 mm/month/year. Following closely are February, March, and December, each with trends up to -0.003 mm/month/year. In contrast, April emerges with the most pronounced negative trends, averaging at -0.013 mm/month/year. May and June are also affected by these minimum flows, portraying negative trends averaging around -0.005 mm/month/year. The remaining months likewise demonstrate negative trends, albeit with variations ranging from 0 to -0.003 mm/month/year.

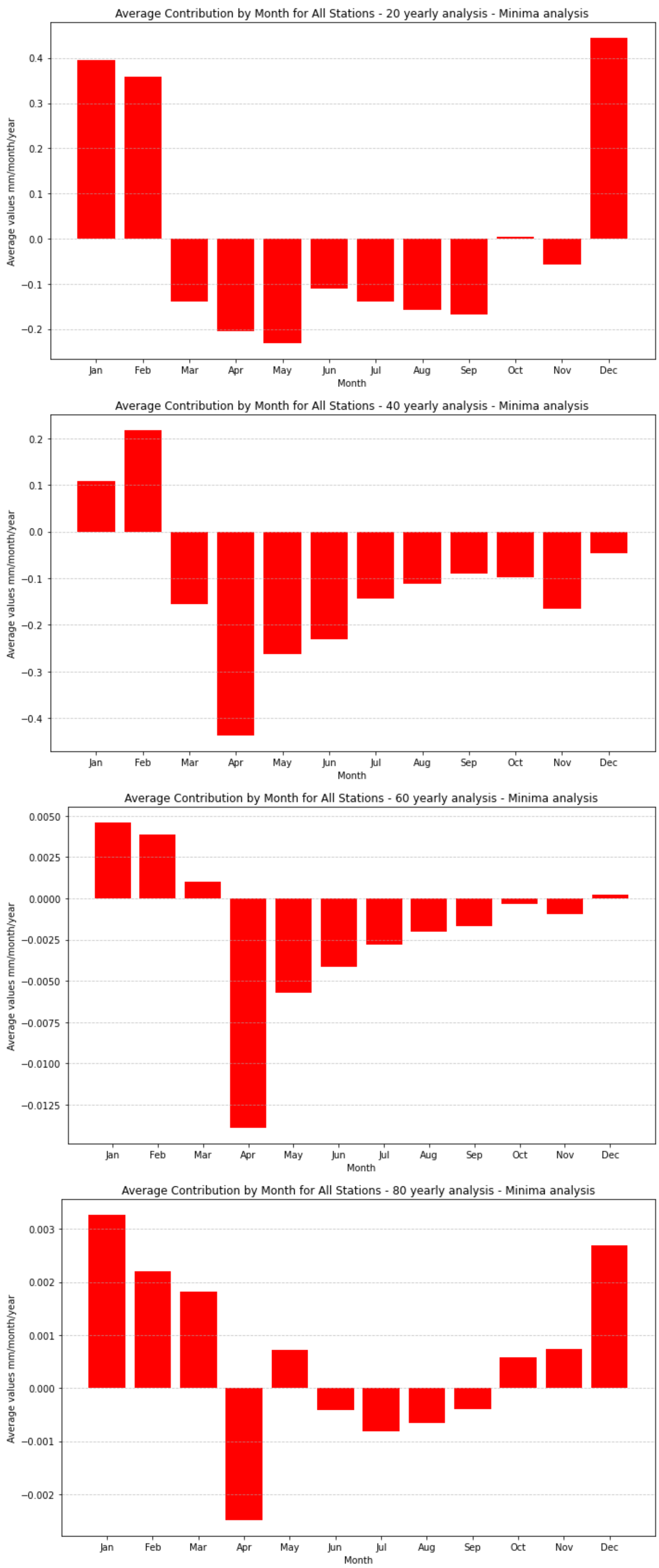

Figure 4.28: Bar charts of the average trend of each month for Minima analysis

Geographical Correlation of Months with Most Positive and Negative Trends among Station Groups:

- **20 - Year Analysis (see Figures 4.29, 4.30):** Understanding the spatial distribution of months with the highest and most negative discharge trends is imperative. Among positive contributions, Figure 4.29, across the 20-year analysis, January emerges as the dominant month, exerting its influence across the entire case study area. Additionally, December commands dominance in the North-West and Center regions, indicating its role in shaping favorable discharge patterns. In the South-East group of stations, February emerges as the dominant month of positive contribution.

  In the context of negative contributions, Figure 4.30, within the 20-year analysis, spatial variability comes to the fore. In the North and Center parts, March emerges as the dominant month with significant negative influence. The North reveals distinct patterns with groups characterized by dominance of August (North-West), January, March and April in terms of negative contributions. September, April and January are dominant in the center of the case study area.

- **40 - Year Analysis - Figure A1.31:** Transitioning to the 40-year analysis, February maintains dominance in terms of positive contributions across the entire case study area. However, a change occurs in the North-West region where December claims precedence.

  Examining negative contributions over 40 years, a recurring pattern emerges as April retains dominance across almost the entirety of the case study area. Notably, in the North-West, March also asserts its dominance, indicative of its role in shaping extended periods of negative discharge.

- **60 - Year Analysis - Figure A1.31:** In the context of the 60-year analysis, January emerges as the predominant month for the central and Eastern regions of the case study area. Furthermore, August takes the lead as the dominant month for two station groups situated in the Western and Eastern portions of the case study area. Additionally, February claims dominance within groups located in the Northern and Eastern sectors of the case study area. Conversely, when considering negative trends, April emerges as the prevailing month with negative trends spanning across the entire case study area.

- **80 - Year Analysis - Figure A1.31:** In our comprehensive 80-year analysis, we found that January emerged as the predominant month for positive trends in multiple clusters situated in the North, Central, and North-West regions. Additionally, in the North-Eastern part, there's a specific group of stations where March takes the lead in terms of positive trends. Conversely, a central cluster displayed a strong inclination towards May as the month with the highest trends. In the North-West region, we observed two distinct groups favoring February and October, while in the central area of the case study, March held sway as the prevailing month. When it comes to the most adverse trends, April took the lead across the entire study area, except for one cluster of stations located in the North-West, where January displayed the most negative trends.

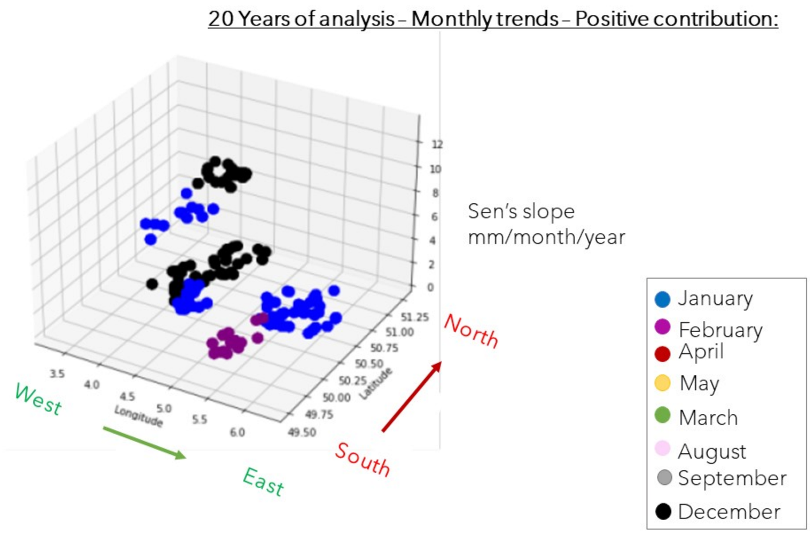

Figure 4.29: Cluster plot: Minimum monthly positive trends over a 20-year analysis period for station groups.

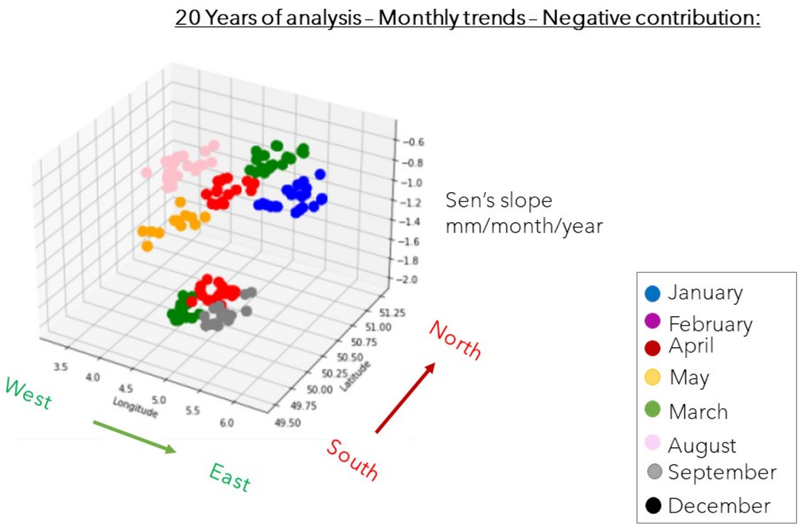

Figure 4.30: Cluster plot: Minimum monthly negative trends over a 20-year analysis period for station groups.

4.2 Changes in timing

To comprehend potential timing alterations, it's vital to pinpoint the dominant month. Specifically, this pertains to the month when the maximum and minimum mean daily flow occur each year. Unlike the previous monthly analysis which assessed individual months to gauge magnitude shifts, this section investigates whether the occurrence months of maxima and minima have changed over time.

This chapter presents maps illustrating the dominant month for each station. Two different metrics are used in this chapter:

1. Statistical entropy & Concentration
2. KL Divergence

As previously elucidated in the Chapter 3, maximum entropy yields a uniform time series distribution, indicating equal probability for all events. Conversely, skewed or concentrated distributions imply reduced entropy. However, this study employs a bespoke concentration metric, inversely related to entropy, establishing an analogical link between arrow length and concentration value. Thicker and longer arrows denote higher concentration rates, while thinner, shorter ones signify lower concentrations. Each arrow corresponds to a station, with color and direction representing the dominant month—the one occurring most frequently in the dataset. Larger arrows indicate a clear dominance of one month, while smaller arrows suggest proximity in values among multiple months, indicating greater variability.

Furthermore, there is a histogram provided alongside the concentration map, offering a visual representation of how the concentration values are distributed. When the concentration value is 0, it implies that multiple months exhibit discharge values close to the maximum, reflecting a high level of variability. Conversely, concentrations nearing 1 indicate that a single month consistently witnesses the maximum discharge throughout the years.

The KL Divergence metric is used to compare time series and uncover variations. It's visually represented with maps featuring arrows corresponding to station locations. There are 1185 stations in total. The color and direction of the arrows on the map provide valuable information about the time series data. They represent the specific month in which the maximum or minimum discharge occurs most frequently, based on both 20 and 40 years of analysis. Moreover, their length signifies the significance of changes between time series. In simpler terms, shorter arrows mean no significant month-to-month shifts, while longer arrows indicate substantial changes in the data. Nevertheless, stations with data for only the last 20 years are compared against themselves, explaining why Luxembourg's arrows are very short and with a vertical direction due to no changes when comparing the same time series.

The timing analysis encompasses two primary periods: the 20-year analysis (2001-2021) and the 40-year analysis (1982-2021). However, following the outcomes of KL divergence, which compared these two time series, the need to explore the time frames of 1980-2000 and 2001-2021 became apparent. It's worth noting that the analysis was also conducted for 60 and 80 years. Nonetheless, due to data limitations, distinct patterns and potential variations remained elusive.

4.2.1 Maxima analysis

4.2.1.1 Concentration maps & Dominant month

In 20 and 40 years of analysis, Figures 4.38 and 4.32, the stations show a clear dominant month for 20 years of analysis, which is January for the North, Central and West part of the case study area. lso the concentration has high values -most of the stations have concentration more than 0.7- which means that January is the month with high values most of the years. On the other hand, for France the dominant month varies more and apart from January, there are also other months which depict the highest values and these months are March (the purple color) in the center of France, December (light green color) mostly in the eastern part of France and few stations showed located in the western part of the country, June as the dominant month.

Regarding the 40-year analysis, it possesses a more limited dataset in comparison to the 20-year analysis. However, the overarching trend indicates a consistent dominant month over the span of 40 years. The primary distinction between these two analyses is notable in the western part of the case study area, where an increased number of stations recorded their maximum discharges in March—a shift that contrasts with the findings from the 20-year analysis.

Examining the frequency distribution of the stations, a significant majority exhibit high concentrations falling within the range of 0.8 to 0.9. This suggests a lack of substantial variability in the months characterized by high discharge levels throughout the years.

It's worth noting that for the 60 and 80 years of analysis, corresponding concentration maps were also prepared, accessible in the Appendix 6 and especially in Section A2. However, due to data availability, drawing definitive conclusions about variations and patterns would not be prudent.

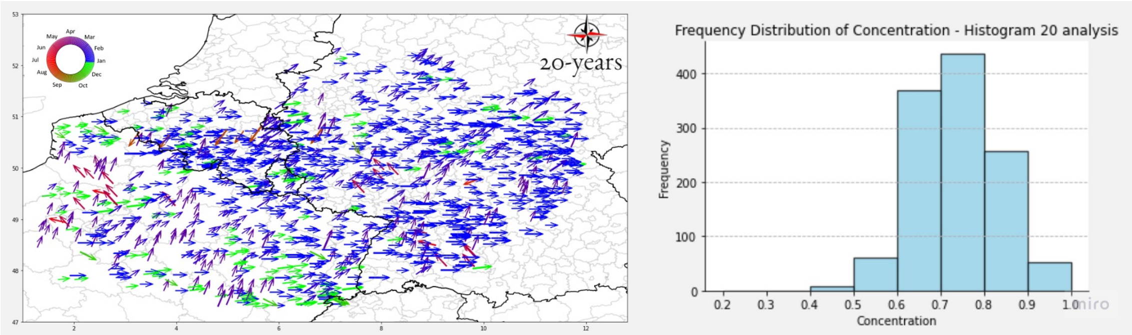

Figure 4.31: Concentration map for the 20 years of analysis (2001 - 2021) - Dominant month of the Maxima discharges

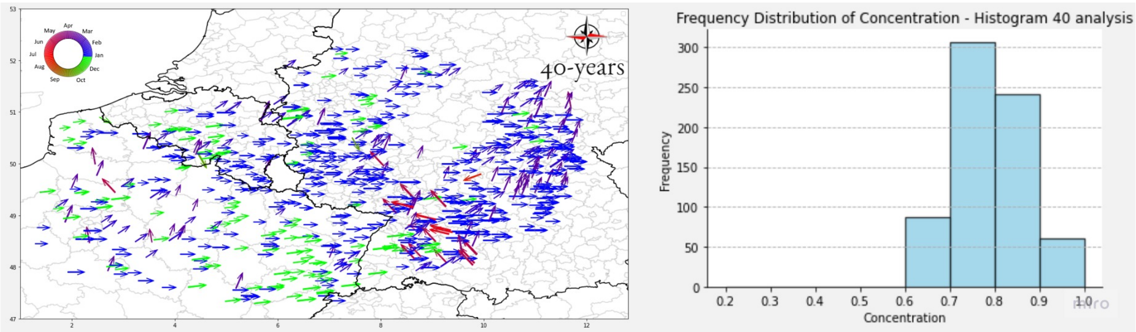

Figure 4.32: Concentration map for the 40 years of analysis (1982 - 2021) - Dominant month of the Maxima discharges

4.2.1.2 KL Divergence maps & Temporal changes

After examining the dominant month per station over the years, it's crucial to compare the 20-year and 40-year time series analyses to draw meaningful conclusions.

As depicted on the map 4.33, it is observed that January (indicated by the blue color) emerges as the dominant month, particularly in the central and eastern regions of the case study area. However, there are instances where December (shown in green) also takes precedence in the same area, without a discernible pattern. In the eastern border regions, March (in purple) exhibits dominance. Notably, in the southern part of the case study area, a few stations display summery months (in red) as dominant in both the 20-year and 40-year time series. Moving to the western and central areas, there are fewer instances of summery months being dominant. In the northern part of France, December (green) appears as the month with the highest flow.

Shifting the focus to the arrow lengths, which denote changes, it can be inferred from the corresponding histogram of the KL divergence frequency distribution that relatively short arrows are observed at most stations (see Figure 4.33). This suggests that the time series are not subject to significant variations from one another. However, it should be emphasized that a discernible shift or change is still observed, necessitating further examination, particularly within the context of the 40-year analysis and specific time periods, such as 1980-2000 and 2001-2021.

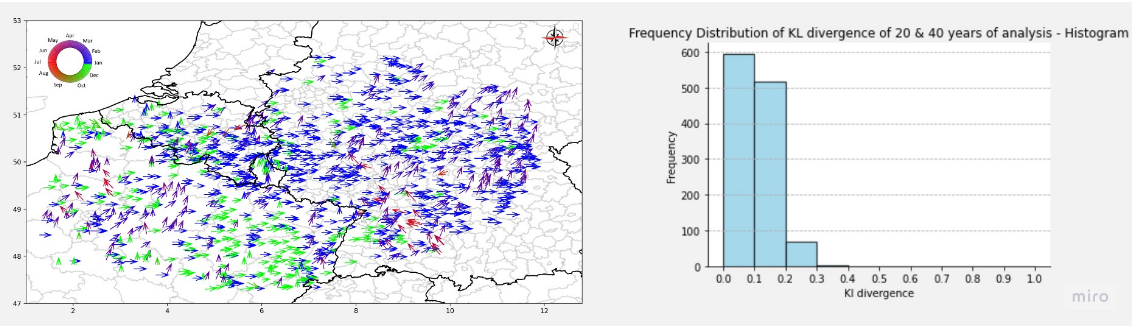

Figure 4.33: KL Divergence map - Comparison of 20 & 40 years of analysis - Frequency distribution of the KL Divergence values - Maxima analysis

4.2.1.3 1980 - 2000 & 2001 - 2021 Analyses - Temporal changes

After calculating the KL divergence between the 20-year and 40-year analysis periods, it became apparent that further investigation was necessary. This investigation focused on the time intervals of 1980-2000 and 2001-2021 to explore the shift in the months with the highest flow over the years. While we had already created a concentration map for the 2001-2021 period, we also generated a concentration map for the 1980-2000 period, which is accessible in the Appendix A2. This map served as our starting point to determine if there was a shift in the dominant month for maximum flow between these two 20-year periods.

As evident from the histogram below Figure 4.34, the majority of stations experienced a one-month shift (over 400 stations). It's essential to clarify that a one-month shift corresponds to a 30-day change. Following that, nearly 300 stations showed no change, and a negligible number of stations (close to zero) exhibited a six-month shift in dominant months.

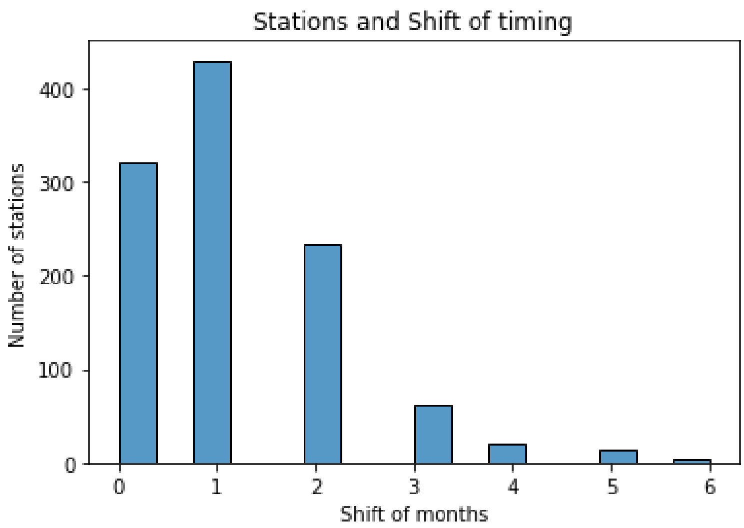

Figure 4.34: Histogram shift of months of stations between 1980-2000 & 2001-2021 - Maxima analysis

Additionally, in the corresponding Bar Chart 4.37, blue bars represent the most dominant month during the 2001-2021 period, while red bars correspond to the 1980-2000 period. Notably, almost 700 stations had January as the dominant month in the last 20 years, which differed from the previous 20 years when December held that position for maximum flows. Moreover, during the 2000-2021 period, there was minimal variability since most stations exhibited January dominance. In contrast, during the previous 20 years, December, January, February, and March all played significant roles and were dominant in multiple stations.

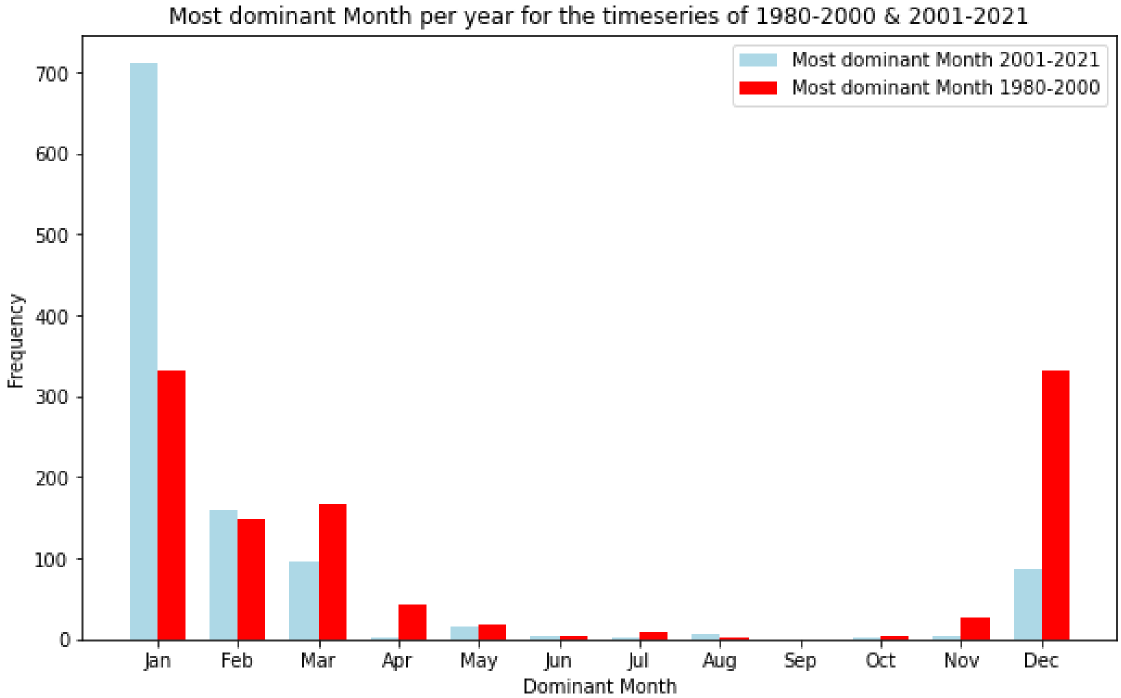

Figure 4.35: Bar chart for comparison of dominant months between 1980-2000 & 2001-2021 - Maxima analysis

Simultaneously, in Map 4.36, the variation in the month of peak flow for each station over the years is illustrated. The sequential color gradient, ranging from light blue small circles to big blue circles, represents whether stations maintain the same peak flow month over the years (small circle - light blue) or experience a six-month shift in the occurrence of high flows (big circle - dark blue).

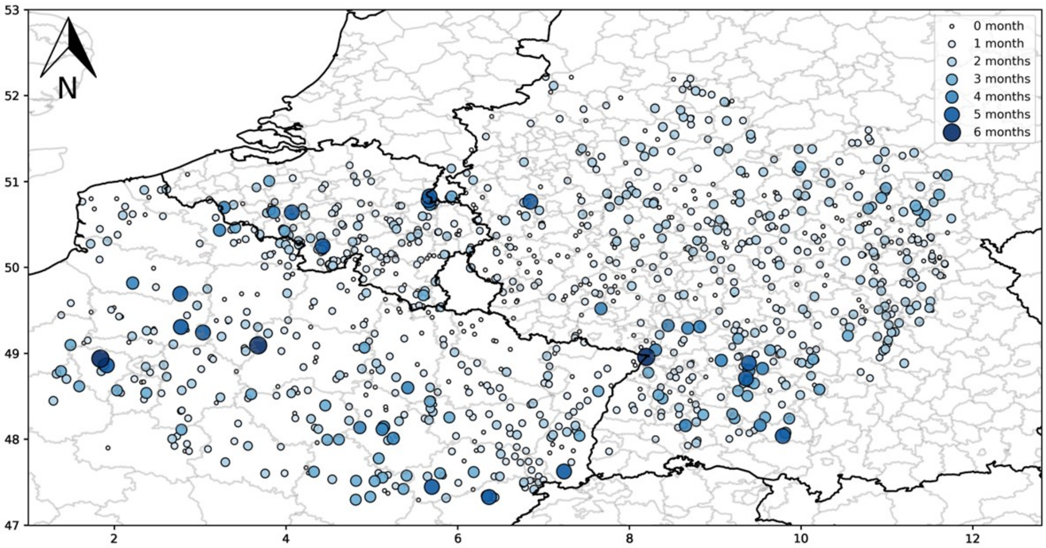

Figure 4.36: Shift in peak flow timing for all stations between 1980-2000 & 2001-2021

To delve deeper into understanding these changes, specifically the months in which shifts occurred, we created the following heatmap. On the x-axis, you can see the time period from 2001-2021, represented by the months from January (1) to December (12). On the y-axis, someone finds the time period from 1980-2000, also represented by the corresponding months. Each box within the heatmap represents the number of stations with a dominant month corresponding to the x-axis (2001-2021) and the y-axis (1980-2000). Notably, 232 stations did not change their dominant month, as they had January as the dominant month during both periods. Additionally, a shift from December (1980-2000) to January (2001-2021) was observed in 200 stations. The heatmap captures all possible changes in dominant months between these two distinct time periods.

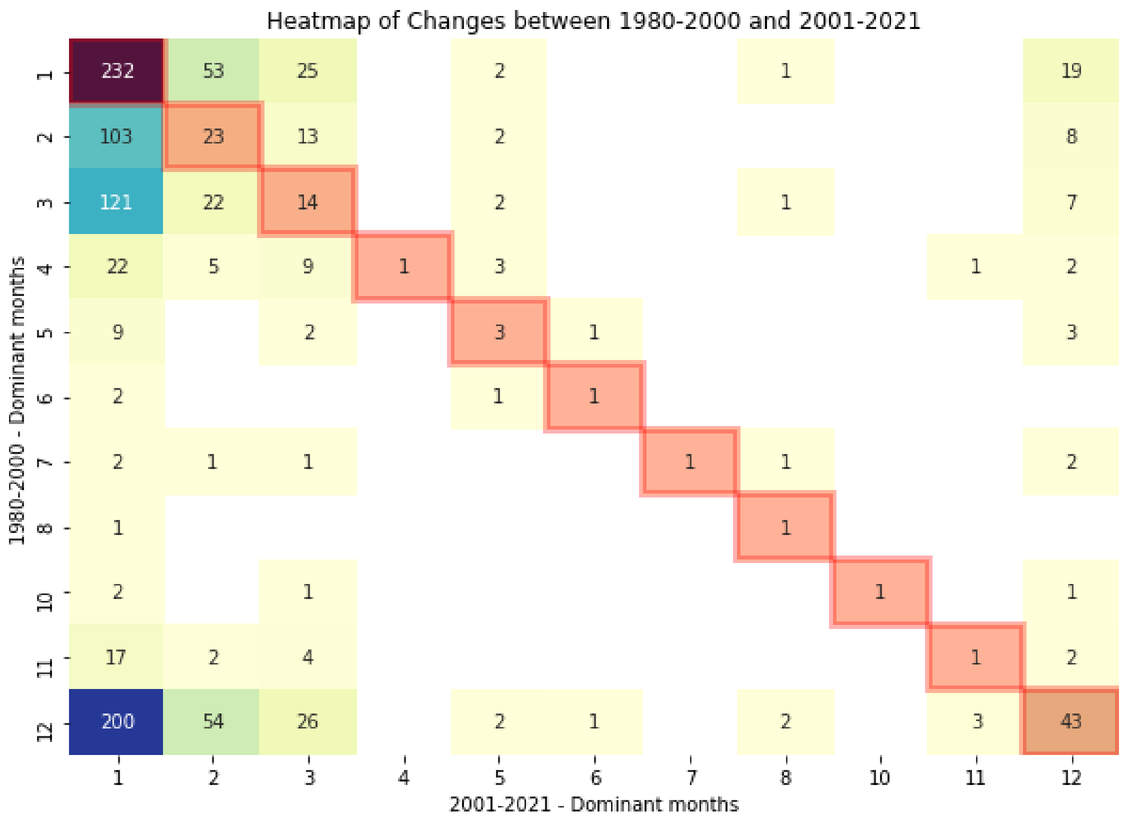

Figure 4.37: Heat-map to visualize all the month shifts from 1980-2000 & 2001-2021 - Maxima analysis

Furthermore, in the Table 4.2 was created to highlight the first four changes that involved a significant number of stations shifting from one dominant month to another (some with multiple month shifts). The corresponding numbers indicate how many of the 1185 stations experienced these changes, providing an overall perspective.

Table 4.1: Distribution of Stations with Dominant Month Shifts (1980-2000 to 2001-2021) - Maxima Analysis:

Shift of Dominant Month (1980-2000 to 2001-2021)	Number of Stations
Jan - Jan	232
Dec - Jan	200
Feb - Jan	103
Mar - Jan	121

4.2.2 Minima analysis

4.2.2.1 Concentration maps & Dominant month

Over the course of a 20-year analysis, as depicted in Figure 4.38, a clear dominant month emerges consistently across the entire study area: September, represented by a mustard-colored hue. Notably, this dominance lacks specific discernible patterns in terms of geographical distribution. Additionally, August, marked in red, emerges as the second most dominant month. However, its prevalence doesn't follow a distinct pattern either; it is predominantly found in the central and eastern regions, diminishing in occurrence towards the western part of the study area. Examining the arrow lengths, which can also be observed in the corresponding histogram, it becomes apparent that the majority of arrows (over 400 stations) fall within the 0.6-0.7 bin range. This indicates that most stations exhibit arrows with medium to significant lengths. Consequently, this suggests that one particular month is consistently dominant, and there is not a substantial increase in variability within the dataset.

In the context of a 40-year analysis, the data illustrates that August (red) and September (mustard) continue to dominate the entire study area, maintaining a similar geographical distribution pattern as in the 20-year analysis. December (light green) emerges as the next most dominant month, primarily concentrated in the eastern part of the study area. Moreover, within this 40-year timeframe, October (darker green, with a distinct arrow direction) also shows prominence, particularly in the northeastern and central regions.

The arrow length distribution, as reflected in the corresponding histogram, indicates that a significant portion of stations (more than 250) falls within the 0.6-0.7 bin range. This reaffirms the consistent dominance of a single month, with limited variability in the dataset.

It's important to note that for the 60 and 80-year analyses, concentration maps were also generated, accessible in the Appendix 6 and under section A2 in the Minima analysis. However, due to limitations in data availability, drawing definitive conclusions regarding variations and patterns would be cautious and less conclusive.

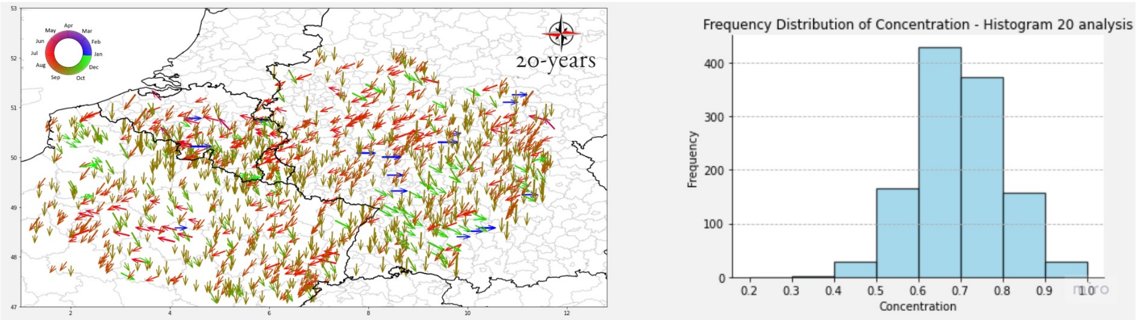

Figure 4.38: Concentration map for the 20 years of analysis (2001 - 2021) - Dominant month of the Minima discharges

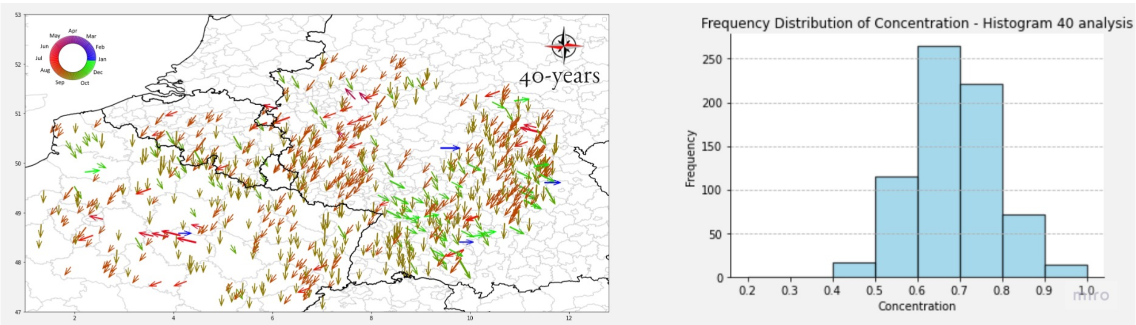

Figure 4.39: Concentration map for the 40 years of analysis (1982 - 2021) - Dominant month of the Minima discharges

4.2.2.2 KL Divergence maps & Temporal changes

Having examined the dominant month per station across multiple years, it becomes imperative to conduct a comparative analysis between the 20-year and 40-year time series. In Figure 4.40, we can identify the dominant month, which consistently emerges as the most prevalent across both the 20-year and 40-year analyses.

Turning our attention to Figure 4.40, a clear observation emerges: September, indicated by the mustard color, is a predominant presence throughout the vast majority of the case study area. This suggests that September consistently appears as the month with the minimum flow in both the 20-year and 40-year time series, with the exception of a portion in central Germany, near Luxembourg and the Netherlands.

Conversely, the red colors corresponding to August dominate the landscape, except for the aforementioned region in central Germany. This indicates that August frequently emerges as the dominant month in both time series, with its influence extending across the entire case study area, albeit without discernible patterns. In the southeastern part of the area, some stations display light green and darker green hues, representing December and October, respectively. These months also exhibit dominance in the west-northern regions of France and along the borders between France and Belgium.

Shifting our focus to arrow lengths, which symbolize changes, we can deduce from the corresponding KL divergence frequency distribution histogram in Figure 4.40 that most stations feature relatively short arrows. Nearly 700 stations exhibit no significant change. However, among the remaining stations, a trend emerges, with a concentration primarily in the 0.1-0.2 bin range, followed by lesser representation in the 0.2-0.3 bin, and a minimal number in the 0.3-0.4 bin. This suggests the possibility of at least a one-month shift in timing, prompting further investigation into the time periods between 1980-2000 and 2001-2021.

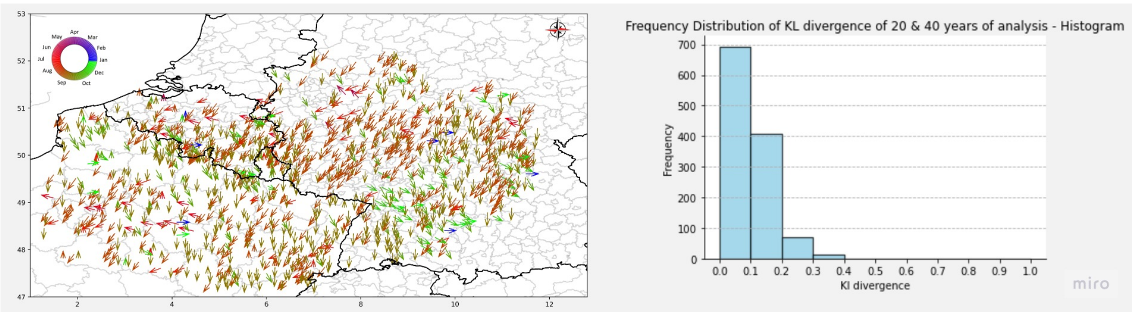

Figure 4.40: KL Divergence map - Comparison of 20 & 40 years of analysis - Frequency distribution of the KL Divergence values - Minima analysis

4.2.2.3 1980-2000 & 2001-2021 Analyses - Temporal changes

As previously mentioned, our focus post the KL divergence analysis between 20 and 40 years of data is squarely on the time intervals of 1980-2000 and 2001-2021, aimed at uncovering shifts in the months with the highest flow over the years. We've already created concentration maps for both these periods, accessible in the Appendix A2, which serve as our starting point for determining any alterations in the dominant month for maximum flow across these two distinct 20-year periods.

An examination of the histogram below (4.41) reveals significant insights. A substantial majority of stations (over 500) experienced a one-month shift, equating to a 30-day change. It's important to clarify that this shift signifies a noticeable transition in dominant months. Following that, nearly 400 stations exhibited no discernible change, while a minuscule number (close to zero) displayed a rather substantial six-month shift in dominant months.

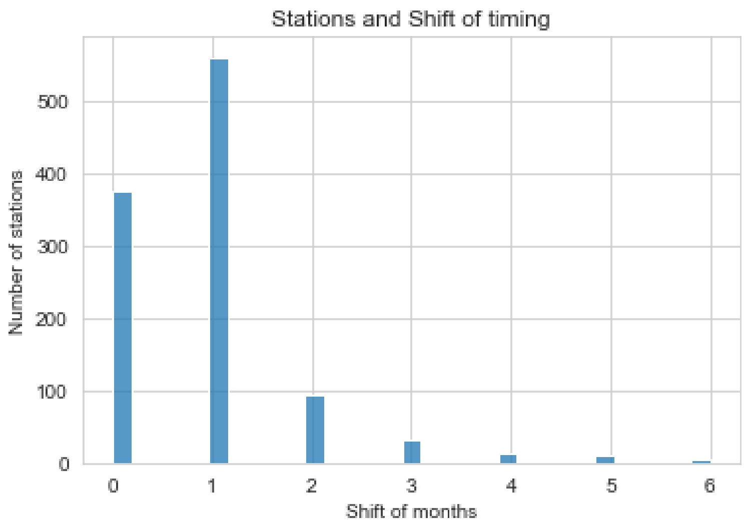

Figure 4.41: Histogram shift of months of stations between 1980-2000 & 2001-2021 - Minima analysis

In the corresponding Bar Chart (4.42), the blue bars represent the most dominant month during the 2001-2021 period, while the red bars correspond to the 1980-2000 period. Notably, for the 1980-2000 period, almost 600 stations had August as the dominant month, which changed in the subsequent 20 years (2001-2021) when September emerged as the predominant month, associated with the majority of instances of minimum flow across most stations. Moreover, during the 1980-2000 timeframe, there was minimal variability in the dominant flow months, with August dominating most stations. This situation changed drastically in the last 20 years of analysis, with more than one month featuring as the period of minimum flow for a significant number of stations.

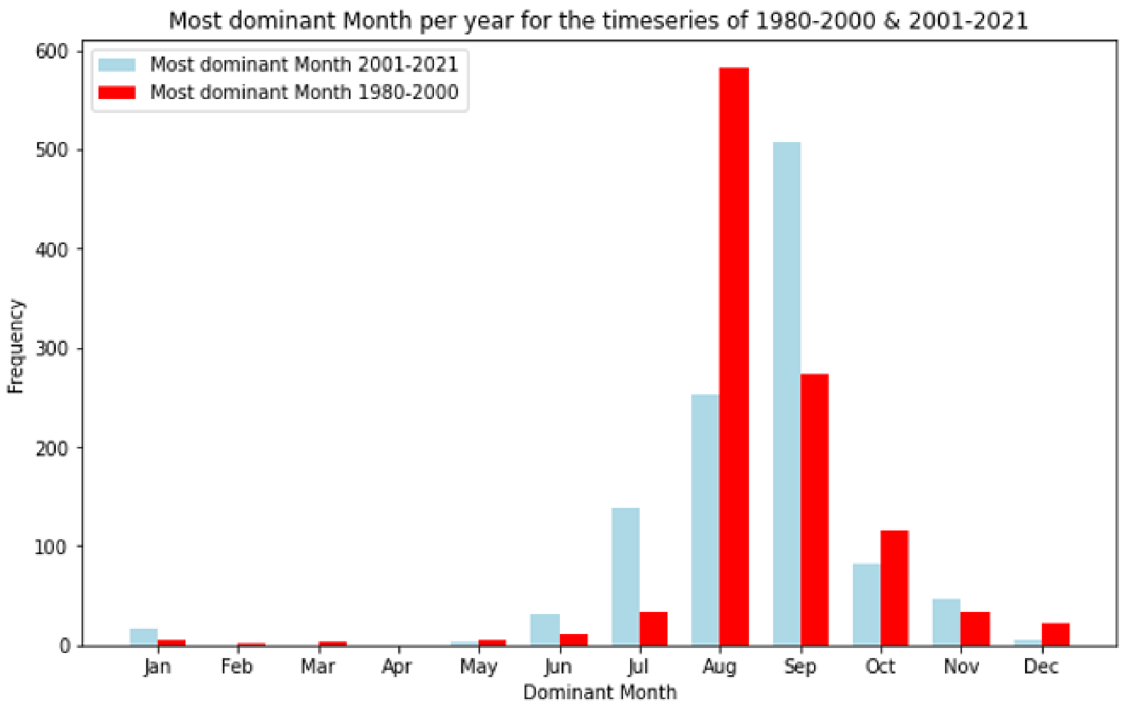

Figure 4.42: Bar chart for comparison of dominant months between 1980-2000 & 2001-2021 - Minima analysis

Simultaneously, in Map 4.43, the variation in the month of low flow for each station over the years is illustrated. The sequential color gradient, ranging from light blue small circles to big blue circles, represents whether stations maintain the same low flow month over the years (small circle - light blue) or experience a six-month shift in the occurrence of minima flows (big circle - dark blue).

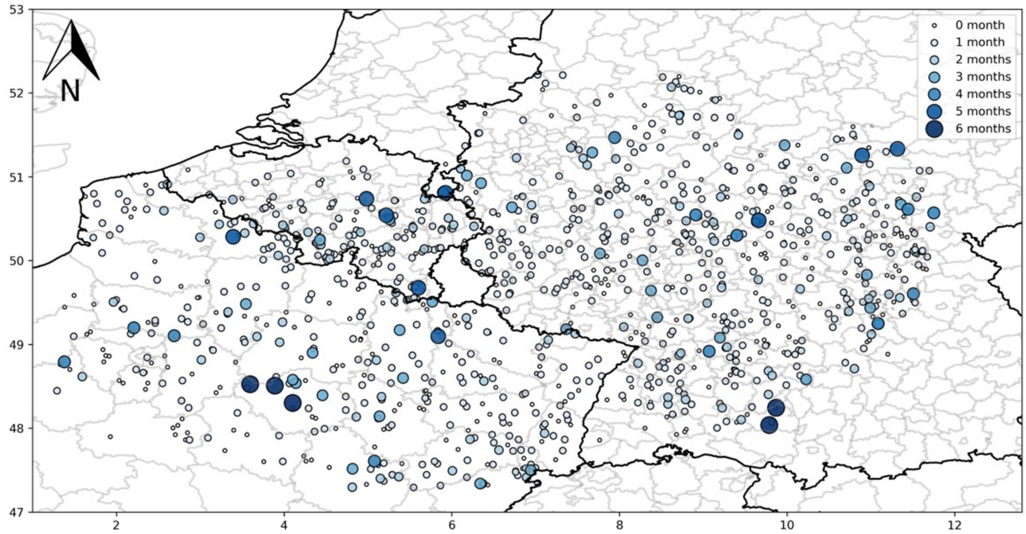

Figure 4.43: Shift in low flow timing for all stations between 1980-2000 & 2001-2021

To gain a deeper understanding of these changes, particularly the months in which shifts occurred, we created the following heatmap. The x-axis represents the time period from 2001-2021, with months from January (1) to December (12), while the y-axis corresponds to the 1980-2000 period, also represented by the corresponding months. Each cell within the heatmap indicates the number of stations with a dominant month corresponding to the x-axis (2001-2021) and the y-axis (1980-2000). Notably, 271 stations underwent a shift in their dominant month, transitioning from August before 2000 to September after 2001. Conversely, no change was observed for 173 stations, which maintained August as their dominant month throughout both time periods. The heatmap encapsulates all possible variations in dominant months between these two distinct time spans.

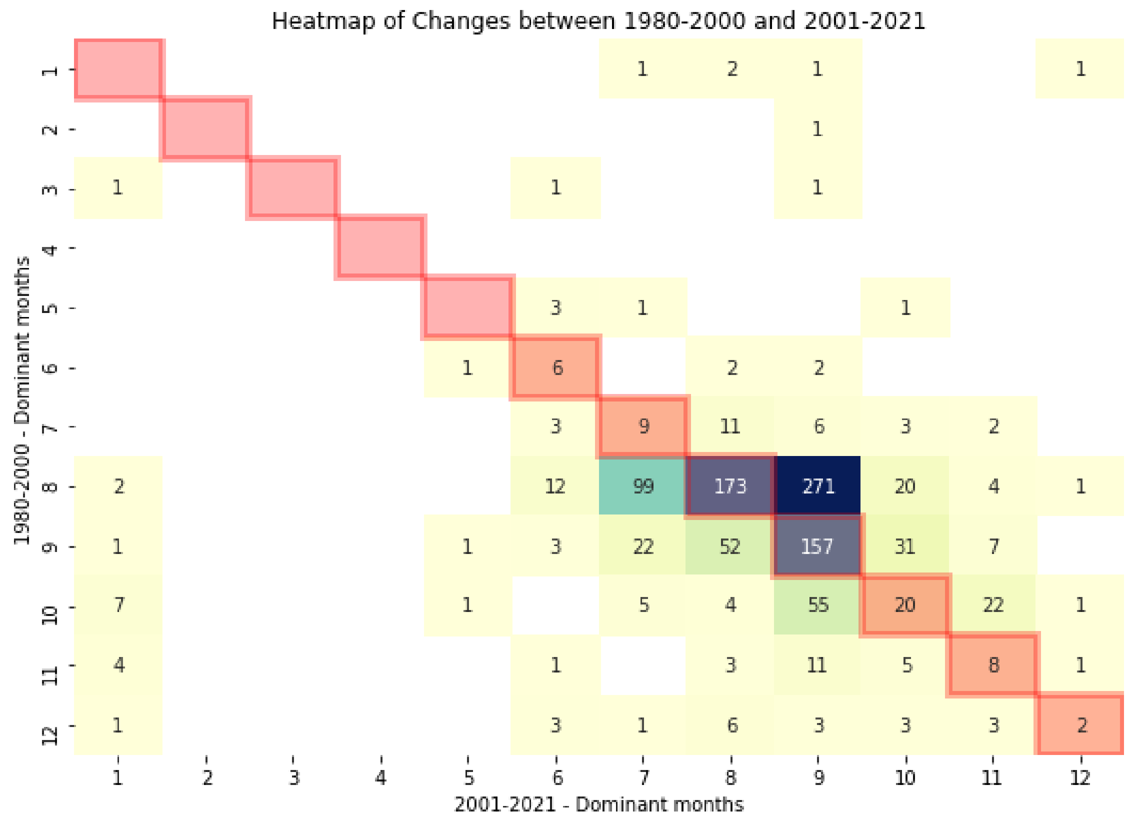

Figure 4.44: Heat-map to visualize all the month shifts from 1980-2000 & 2001-2021 - Minima analysis

Furthermore, in Table (4.2), the first four changes involve a substantial number of stations transitioning from one dominant month to another, with some experiencing multiple month shifts. The corresponding numbers provide an overview of how many of the 1185 stations experienced these significant changes, offering a holistic perspective.

Table 4.2: Distribution of Stations with Dominant Month Shifts (1980-2000 to 2001-2021) - Minima Analysis:

Shift of Dominant Month (1980-2000 to 2001-2021)	Number of Stations
Aug - Sep	271
Aug - Aug	173
Sep - Sep	157
Aug - Jun	99

5 Discussion

In this Master's Thesis, a comprehensive analysis of discharge flows in specific European catchments has been undertaken, with the primary objective of investigating potential changes in both magnitude and timing. Initially, the examination of magnitude shifts involved the application of trend analysis to annual and monthly data, utilizing Sen's slope and Mann-Kendall methods. Subsequently, in pursuit of alterations in timing, an investigation into the months exhibiting the highest and lowest discharge values was conducted. Employing a range of statistical and visualization techniques, this study delineated the temporal changes in months associated with maximum and minimum flow across the years.

In terms of the chapter's structure, it comprises three distinct sections. The initial section is focused on interpreting the results, encompassing a summary of the findings from each analysis, including the Yearly, Monthly (Magnitude perspective), and Timing perspective. It's important to note that this summary Table 5.1 reflects the analyses conducted for 20 and 40 years, since the availability of data in these time periods were adequate in order to results in patterns. Moreover, this section aims to provide a holistic interpretation. Moving forward, the subsequent part addresses the research's limitations, providing valuable insights into the boundaries of the study.

5.1 Changes in Magnitude

5.1.1 Yearly analysis

In summary, the majority of the stations exhibit a lack of trends. Nevertheless, notable patterns and consistent behaviors emerge across all three analyses, encompassing average, maximum, and minimum discharges. It is worth noting that the prevalence of decreasing trends surpasses that of increasing trends. These negative trends are predominantly concentrated in the Eastern and Central regions of the case study area, while relatively fewer increasing trends are observed in the Western part, specifically in North France, as also mentioned in Table 5.1.

Table 5.1: Summary Table of Trends Analysis - Yearly Analysis:

Years of Analysis	Type of Analysis	Decreasing Trends	Increasing Trends	Location of Decreasing Trends	Location of Increasing Trends
20	Average	185	35	North-East part of case study area	Western part
20	Maxima	75	37	Eastern part of case study area	Western part
20	Minima	283	23	East – Central part of case study area	North France
40	Average	242	2	North - East	-
40	Maxima	134	15	Germany	North France
40	Minima	213	18	Eastern part of case study area	East part of case study area

5.1.2 Monthly analysis

Regarding the monthly analysis, the Table below 5.2 presents an overview of the average contributions of the months, whether they exhibit positive or negative trends, across all the analyses. It is important to highlight that in the 40-year analysis, there are only two months considered, unlike the three months in the corresponding 20-year analysis. This adjustment is due to the fact that February distinctly emerges as the month with the most positive trends over the 40-year period, in contrast to the 20-year analysis where the prevalence of positive trends varies among February, December, and January across stations.

Table 5.2: Comparison of Prominent Months and Contributions in Different Analysis Types:

Years of Analysis	Analysis Type	Prominent Months	Average Contribution (mm/month)
20 years	Average	December	~0.04
		February	~0.02
		May	~-0.01
	Maxima	December	0.04
		February	~0.02
		May	~-0.01
	Minima	December	0.4
		January	0.35
		May	-0.20
40 years	Average	February	~0.01
		April	~-0.015
	Maxima	February	0.15
		April	~-0.025
	Minima	February	0.2
		April	-0.45

5.2 Changes in Timing

In the summary Table of the timing perspective 5.3, the analysis spans over different timeframes: 20 years (2001-2021), 40 years (1982-2021), and the decade from 1980 to 2000. This analysis encompasses both maxima and minima values. Within the Table 5.3, the month that frequently corresponds to the highest and lowest values among the majority of stations grouped into North, South, East, and West regions is identified. This exploration aims to unveil potential patterns and connections between these prominent months and geographical locations.

Table 5.3: Dominant Month for Maximum and Minimum Values in Each Region:

Years of Analysis	Type of Analysis	North	South	West	East	Center
20	Maxima	Jan, Dec	Jan, Dec	Dec, Feb	Jan	Jan, Dec
	Minima	Aug	Aug, Sep	Aug, Sep	Aug, Sep	Aug, Sep
40	Maxima	Jan, Dec	Jan, Dec, Aug	Jan, Dec, Mar	Jan, Dec	Jan, Dec
	Minima	Aug, Sep, Oct	Aug, Sep, Oct	Aug, Sep, Oct	Aug, Sep, Oct	Aug, Sep
1980 - 2000	Maxima	Jan, Dec, Mar	Jan, Dec	Jan, Dec, May	Jan, Dec, Mar	Jan, Dec
	Minima	Aug, Sep, Oct	Aug, Sep	Aug, Sep, Jul	Aug, Sep, Oct	Aug, Sep

5.3 Interpretation of the results

The summary tables mentioned earlier (Tables 5.1, 5.2 and 5.3) were generated through a visual examination of the maps presented in the Results chapter 4. In particular, it is worth noting that discerning clear and definitive patterns from the maps proved to be a challenging task in many instances. Nonetheless, below, we present the most significant findings, highlighting their consistency with the literature review and their interconnections across all analyses:

- **Yearly analysis** When examining the trend analysis of average, maximum, and minimum annual discharges, a notable decline in magnitude becomes evident in the eastern and central regions of the study area, particularly within the last two decades of analysis. This decline raises concerns about potential water scarcity in these regions. This finding is aligned with the results of the studies conducted by Al-Qubati et al. (2023), Villarini et al. (2011). The most possible reasons behind the decreasing trends of peaks and average discharge are both the decreasing SPEI (Standardized Precipitation Evaporation and transpiration Index) values in Germany, but also the land use changes since the expansion of agricultural activities and dams' construction have changed the water flow and decreased the discharge trends over the years.

However, a slightly different pattern emerges when analyzing peak flows over a 60-year period (1960-2021). While decreasing trends are observed in the central part of the case study area, stations in the eastern part of Germany, which had shown declining trends in the last 20 years, now exhibit increasing trends when viewed over the longer 60-year span. This pattern is also evident in Map [2] (See Figure 5.1) and aligns with findings from the research conducted by Petrow and Merz (2009) (Map [1] in Figure 5.1). Specifically, both the aforementioned study and this MSc Thesis, covering overlapping time periods of 1960-2010 (the scope of the study) and 1960-2021 (the 60-year time span of this MSc Thesis), indicate increasing trends in the eastern part of Germany (See the corresponding blue rectangle depicting Germany in Figure 5.1). These trends are particularly significant, represented by large blue circles, with additional moderate trends in the same geographical area indicated by smaller blue circles. Additionally, there is agreement in findings regarding the decreasing trends in the borders of Belgium and Germany (See the red rectangle in Figure 5.1).

Concerning the western part, specifically North France, presents a contrasting pattern characterized by a consistent increase in annual water discharge across average, maximum, and minimum flows. This unique hydrological behavior hints at a localized phenomenon meriting further scrutiny. This observation harmonizes with the research of Ward et al. (2008) and Ward et al. (2011), both of which reinforce the notion of a pronounced discharge increase in the region. It is worth noting the convergence with the findings of Blöschl et al. (2019) once more, where a rise in peak flows in Northwest France from 1960 to 2010 is depicted in Figure 5.1. This finding aligns with the trends observed in this MSc Thesis over the 60-year time frame, and these patterns have persisted for the past two decades. A plausible explanation, as also supported by Ward et al. (2011), is the presence of coniferous forests in the area, which leads to an elevated mean discharge and an increased frequency of floods. This phenomenon can be attributed to the needle leaves of the trees, which reduce transpiration by the plants. Combined with the projections for higher precipitation rates in the area (Terray and Boé, 2013), this can lead to water accumulation on the surface.

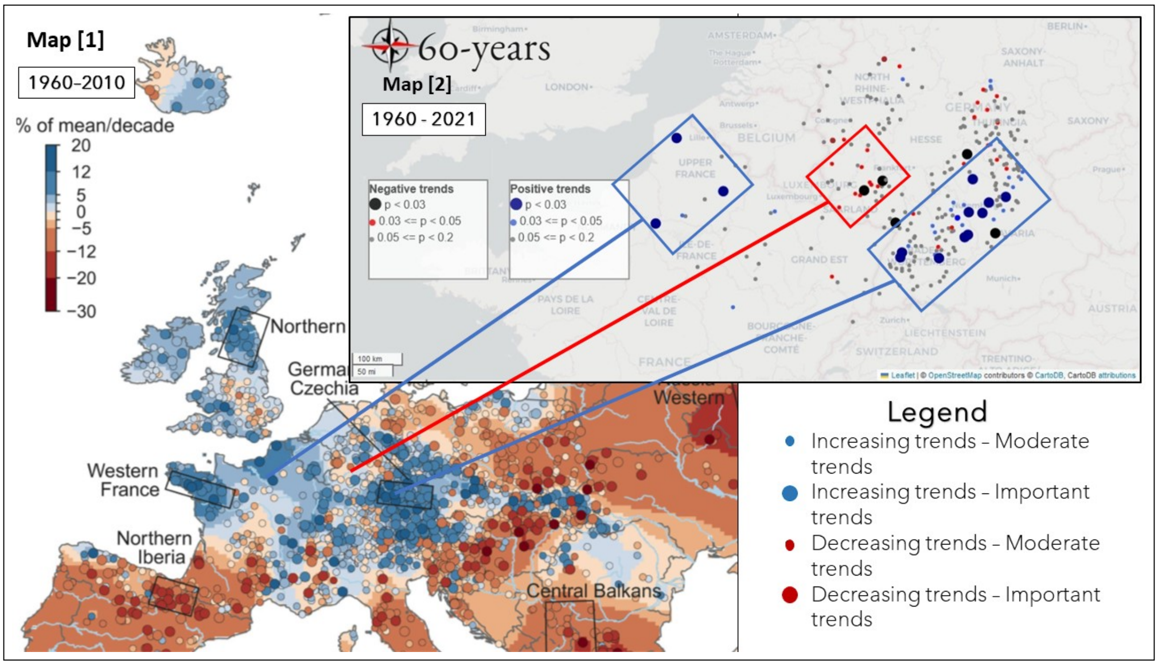

Figure 5.1: Alignment of trend analysis with research findings from Blöschl et al. (2019). Map [1], illustrating peak flow trends across the European continent, is sourced from Blöschl et al. (2019). Map [2], a zoom-in view featuring stations over a 60-year period, is an outcome of the present MSc Thesis for a specific case study area.

- **Monthly analysis** Focusing on each month, it becomes evident that during winter, such as December and February, there is generally an increase in water flow, albeit not substantial. These increasing trends are prominent in the North-Western region, aligning with the annual trend analysis. Thus, from a combination of the findings from yearly and monthly analyses, we can result in that December and February are mainly the months which contribute more to the increasing trends in the area.

  On the other hand, during spring, particularly in April and May, there is a slight decrease in water flow. However, this decline is generally not significant for most analyses, except when considering the minimum discharges. The decreasing monthly trends are mainly met in the Central-Eastern part of the case study area, a finding which is consistent with the results arose by yearly trend analysis. Hence, we can also support that the decreasing yearly trends noticed, may also arose by the negative trends of discharge during spring months.

  Moreover, it's noteworthy that the results of the monthly analysis in this MSc Thesis align with the findings of the Copernicus Climate Change Service. Specifically, their monthly analysis of monthly average river discharge anomalies (m^3/sec) reveals that in February 2021, river discharge exceeded the regional average across much of Europe, with southeastern areas even surpassing the maximum discharge of the reference period from 1991 to 2020. February notably stands out with the largest above-average discharge, while April records the most significant below-average river discharge. These findings substantiate our results, indicating a consistent increasing monthly trend during the winter months and decreasing trends during the spring months over the years (Copernicus EMS/ECMWF., 2021).

- **Timing perspective - Maximum Discharges** Regarding timing shifts, historically, peak water flows in our case study area typically occurred in the winter months: January, February, and December. This pattern held consistently over a 40-year and 20-year analysis period. However, when we scrutinized two specific decades – 1980 to 2000 and 2001 to 2021 – a noteworthy change emerged. In the most recent 20 years, January has replaced December as the dominant month for peak water flows.

  This shift has potential implications for snowmelt dynamics. January's colder temperatures influence snow accumulation. If maximum discharge previously occurred in December but has shifted to January in the last two decades, it could signify delayed snow shaping. Consequently, this alteration might affect the timing of snowmelt in the future. A similar interpretation is also supported by a study conducted by Blöschl et al. (2019), where they concluded that delayed winter snow lead to postponed winter floods.

  Furthermore, in our examination of maximum monthly flow patterns over the past two decades, we noticed that both February and December displayed increasing trends. However, in contrast, January's increasing trend in peak flows was negligible during this same period.

  Considering the aforementioned finding from monthly analysis, our conclusion is that up until 2021, January remained the month with the highest water flows at most stations; while, the rising trends observed in December and February were insufficient to surpass January's dominance as the month with the maximum water flows.

- **Timing perspective - Minimum Discharges** Additionally, with regards to the timing of minimum discharge levels, historically, August and September predominantly recorded the lowest water flows across the majority of monitoring stations. However, an intriguing shift in this temporal pattern becomes evident when we examine the most recent two decades, spanning from 2000 to 2021. During this period, a transition occurred, as stations increasingly registered their minimum discharges in September instead of August.

  This temporal shift is not only an isolated observation but is further substantiated by our monthly analysis of minimum discharge trends. Specifically, when examining the plots featuring station data, it becomes apparent that on average,September consistently exhibits more pronounced negative trends in comparison to August (See Figure 5.2). This compelling correlation reinforces the conclusion that the timing of minimum discharges has indeed shifted in the last two decades; with September being the month of occurrence the minimum discharge most of the times the last 20 years of analysis. This finding aligns with the insights from the literature review, as highlighted in Copernicus EMS/ECMWF. (2021). Their data supports the notion that, in Northwestern and Northeastern Europe, September has experienced decreasing trends, whereas August has shown increasing trends. This contrast was even observed in 2021, with September having lower discharge than the average river discharge for the reference period from 1990 to 2020, while August demonstrated slightly higher discharge than the average discharge for that same reference period.

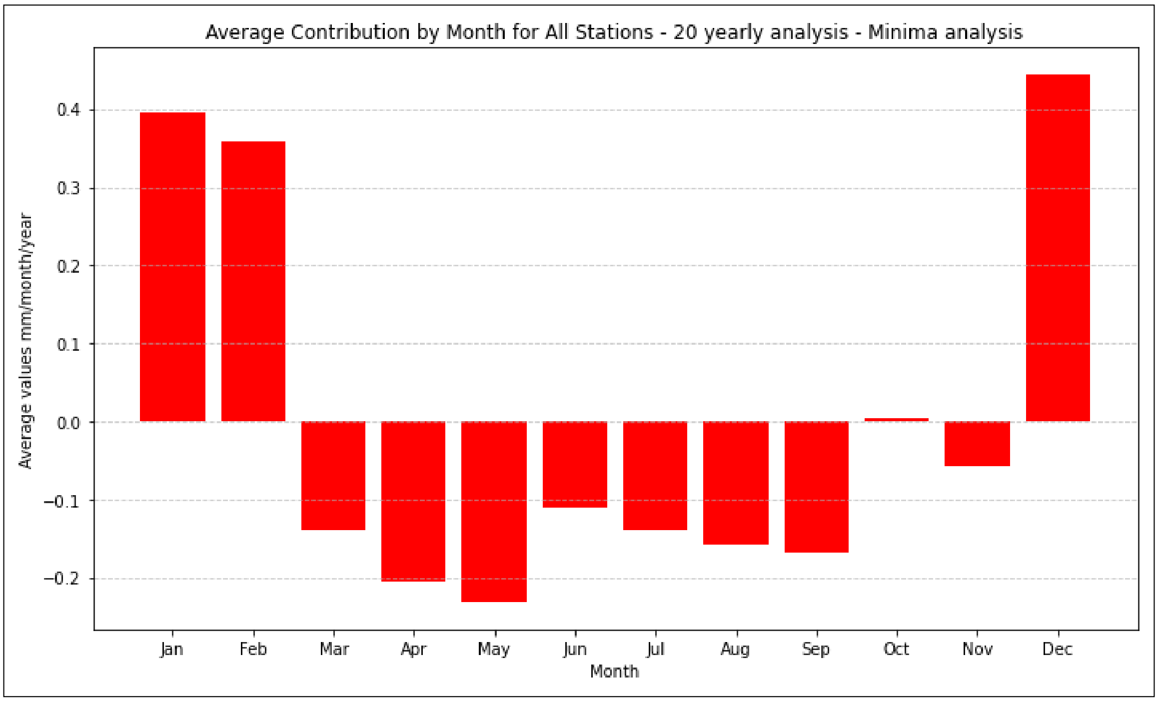

Figure 5.2: Average Monthly Contribution Bar Chart from Monthly Minimum Discharge Analysis. The chart illustrates that, on average, the trend in August is nearly -0.1 mm per month per year. On the other hand, during September, the average trend in monthly minimum discharge is slightly more negative.

One plausible explanation for this phenomenon may be a lag effect on discharge volumes. This suggests that elevated temperatures in August can cause increased evaporation and transpiration from the land, which subsequently reduces soil moisture. This, in turn, leads to lower water levels and flow rates in rivers and streams during September. In simple terms, the impact of August's heat on water levels and flow is only fully felt a month later in September.

5.4 Limitations of the study

The primary challenge encountered during this study revolved around data limitations and certain analytical hurdles that emerged during the research process.

One notable limitation was related to the available data. For the 60 and 80-year analysis periods, the stations with measurement data were predominantly located in Germany. This geographical concentration limited our ability to extrapolate patterns and variations across the entire case study area with a high degree of confidence. Additionally, the inherent variability in the data posed a significant challenge. Some stations had data spanning different time periods, rendering direct comparisons difficult. This variability, especially in analyses exploring possible temporal changes, made it challenging to draw definitive conclusions.

Another significant challenge we encountered was the absence of shapefile files for catchment areas. Our response to this limitation involved the creation of Digital Elevation Maps for the region. However, complications emerged during the watershed delineation process. We managed to overcome these obstacles, thanks to the assistance of automated processing tools and custom codes. Nevertheless, due to the considerable number of monitoring stations, we had to adopt a 90-meter resolution, which raises concerns about the representativeness of some basin outlines due to the potentially lower accuracy.

6 Conclusion

In the current chapter, the answers of the research question and the subquestions are clearly stated. In the end of the chapter, there are some recommendations for future research endeavors in order to be able to contribute to a more comprehensive and nuanced understanding of water discharge trends in North and Central Europe.

6.1 Answers to research question

To remind the research question and the subquestions are below:

Are there any historical changes in the discharge patterns in specific European catchments?

Sub-questions:

- Are there any trends in magnitude (increasing or decreasing) of the runoff (average, maximum and minimum) of the examined catchments based on the given dataset? Which month contributes more to changes?

  Answer In the context of the analysis of annual discharge magnitude, certain discernible trends were identified, with the majority of them exhibiting a decreasing pattern. It is noteworthy, however, there was a consistency of the trends across the case study area through the years. This observation finds robust support in the extensive analysis spanning at least the last 80 years, revealing the enduring stability of the hydrological behavior of the stations within the case study area.

  Regarding the monthly trend analysis, while notable changes were identified, the overall hydrological system exhibited a remarkable degree of stability. To delve deeper into specifics, it became evident that the winter months played a prominent role in driving increases in discharge, while the spring months had a more pronounced influence in decreasing discharge within the case study area. However, it is important to note that some decreasing trends observed in September led to a notable shift in the timing of when minimum discharge levels occur.

- Are there any changes in the timing of the runoff of the examined catchments (change of the month when the maximum and minimum flow happens during the year)?

Answer The analysis of discharge timing witnessed more clear changes. In the case of maximum flows, a significant shift was noted, with 56% of the stations experiencing alterations in the month when their maximum flows occurred between the periods of 1980-2000 and 2001-2021. The primary alteration witnessed was the transition from December to January as the main month for maximum flows. Similarly, in the context of minimum flows, notable adjustments were observed, with 59% of the stations undergoing changes in the month when their minimum flows were recorded over the same time intervals. The predominant shift was from August to September as the primary month for minimum flows. These shifts in timing underscore the dynamic nature of discharge patterns in the studied catchments.

6.2 Recommendations for future research

In light of our findings, there are several avenues for future research that can provide deeper insights into water discharge trends in the case study area.

Firstly, the interpretation of our finding are mainly arose by the examination of the time spans of 20 (2001-2021) and 40 (1980-2021) years of analysis for both yearly and monthly analyses. However, the data we used exhibited high variability, making it essential to perform more granular examinations. It is recommended to conduct separate analyses for the time periods of 1980-2000 and 2001-2021, respectively. This approach would allow researchers to identify potential patterns and trends within these sub-periods and facilitate comparisons, thus providing a more nuanced perspective on how discharge patterns have evolved over time.

In our monthly analysis, we clustered stations solely based on their geographic location. To enhance our understanding of discharge trends, it would be worthwhile to consider additional parameters when clustering stations. For instance, incorporating data on the elevations of catchment areas could help establish connections between elevation and the observed decreasing or increasing trends in discharge. This multi-dimensional clustering approach may reveal valuable insights into the influence of topography on hydrological patterns.

Examining the potential shifts in timing when determining the dominant month for low flow events, as explained in the Chapter 3. The approach used involves counting occurrences of these events within specific time spans from 20 to 80 years. In some cases, this approach may reveal results where there is a noticeable difference between the first and second dominant months (i.e. the shift is significant), while it may reveal some other cases which this difference is small.

For instance, when examining Station ID: 10461002 over the past two decades, it was found that low flow events occurred most frequently in August, totaling seven years out of 20, while June saw five occurrences out of 20. This leads us to the conclusion that August should be designated as the dominant month for low flow events during this period. Nevertheless, August (i.e. the dominant month) has only two-year difference with the second dominant month (i.e. June) as can be seen in Figure 6.1.

To gain a deeper understanding the timing shifts, it is advisable to create histograms that depict the distribution of differences in the occurrence between the first two most dominant months at each station (i.e., frequency distributions of flows). For example, if approximately 80% of the stations exhibit minor differences, such as a two-year gap, this could indicate that the timing shift lacks statistical significance. This information holds value in evaluating the timing shifts.

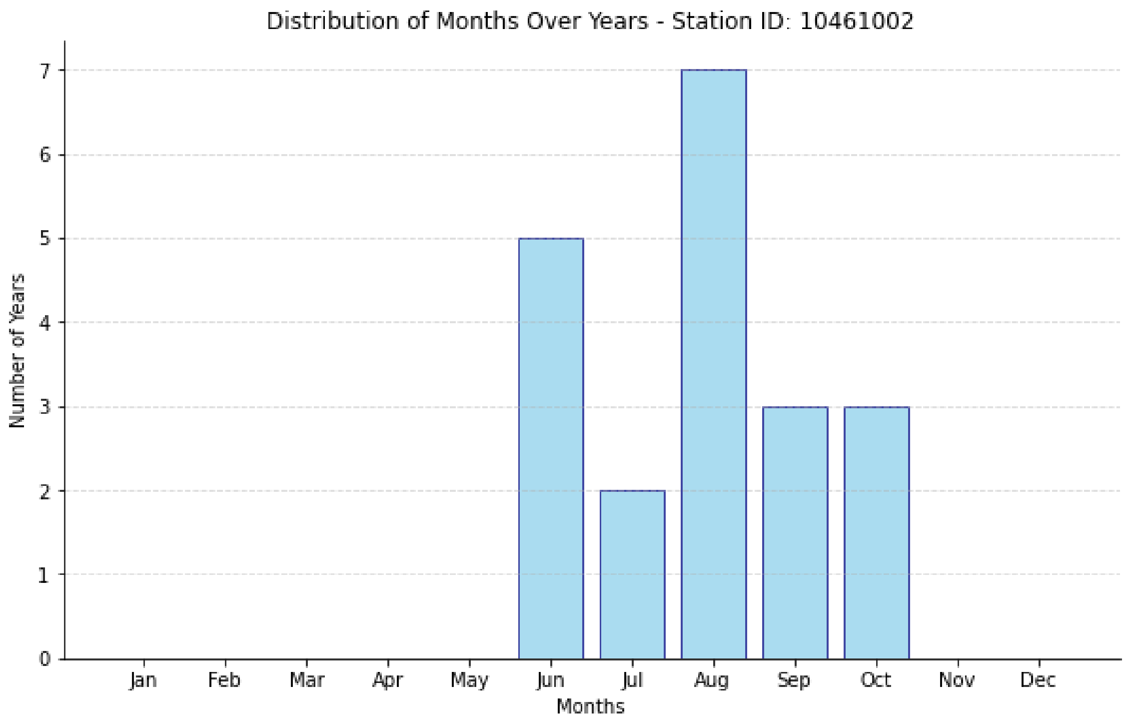

Figure 6.1: Station ID 10461002: Distribution Frequency of Minimum Flow Months Over a 20-Year Period. August recorded the lowest flow in seven out of 20 years, while June was the minimum flow month in five out of 20 years.

Moreover, to gain a more comprehensive understanding of the drivers behind the observed discharge trends, it is essential to integrate climate-related data. Acquiring information on temperature and precipitation for the catchment areas under study would enable researchers to investigate potential links between climatic variables and hydrological patterns. This data integration could shed light on whether changing climate conditions are contributing to the observed shifts in water discharge, providing critical information for both researchers and policymakers.

By pursuing these recommendations, future research endeavors can contribute to a more comprehensive and nuanced understanding of water discharge trends in specific European catchments. This, in turn, will aid in the development of informed strategies for water resource management and environmental preservation in the region.

References

A. Al-Qubati, L. Zhang, and K. Pyarali. Climatic drought impacts on key ecosystem services of a low mountain region in germany. *Environmental Monitoring and Assessment*, 195:800, 2023. doi: 10.1007/s10661-023-11397-1. URL https://doi.org/10.1007/s10661-023-11397-1.

Belgian Federal Public Service for Public Health, Food Chain Safety and Environment. Waterinfo belgium, n.d. URL https://www.waterinfo.be/. Accessed on 26 September, 2023.

M. Bertola, A. Viglione, D. Lun, J. Hall, and G. Blöschl. Flood trends in europe: are changes in small and big floods different? *Hydrology and Earth System Sciences*, 24(4): 1805–1822, 2020.

G. Blöschl, J. Hall, J. Parajka, R. Perdigao, B. Merz, B. Arheimer, G. Aronica, A. Bilibashi, O. Bonacci, M. Borga, I. Čanjevac, A. Castellarin, G. B. Chirico, P. Claps, K. Fiala, N. Frolova, G. Liudmyla, A. Gül, J. Hannaford, and Nenad. Changing climate shifts timing of european floods. *Science*, 357:588–590, 08 2017. doi: 10.1126/science.aan2506.

G. Blöschl, J. Hall, A. Viglione, R. A. P. Perdigão, J. Parajka, B. Merz, D. Lun, B. Arheimer, G. T. Aronica, A. Bilibashi, M. Boháč, O. Bonacci, M. Borga, I. Čanjevac, A. Castellarin, G. B. Chirico, P. Claps, N. Frolova, D. Ganora, L. Gorbachova, A. Gül, J. Hannaford, S. Harrigan, M. Kireeva, A. Kiss, T. R. Kjeldsen, S. Kohnová, J. J. Koskela, O. Ledvinka, N. Macdonald, M. Mavrova-Guirguinova, L. Mediero, R. Merz, P. Molnar, A. Montanari, C. Murphy, M. Osuch, V. Ovcharuk, I. Radevski, J. L. Salinas, E. Sauquet, M. Šraj, J. Szolgay, E. Volpi, D. Wilson, K. Zaimi, and N. Živković. Changing climate both increases and decreases european river floods. *Nature*, 573(7772): 108—111, September 2019. ISSN 0028-0836. doi: 10.1038/s41586-019-1495-6. URL http://mural.maynoothuniversity.ie/13850/1/CM_changing.pdf.

A. Bring, J. Thorslund, L. Rosén, and et al. Effects on groundwater storage of restoring, constructing or draining wetlands in temperate and boreal climates: a systematic review. *Environmental Evidence*, 11(38), 2022. doi: 10.1186/s13750-022-00289-5. URL https://doi.org/10.1186/s13750-022-00289-5.

A. Bronstert, D. Niehoff, and G. Bürger. Effects of climate and land-use change on storm runoff generation: present knowledge and modelling capabilities. *Hydrological Processes*, 16(2):509–529, 2002. doi: 10.1002/hyp.326.

S. Connors, S. Berger, C. Péan, G. Bala, N. Caud, D. Chen, T. Edwards, S. Fuzzi, T. Y. Gan, M. Gomis, E. Hawkins, R. Jones, R. Kopp, K. Leitzell, E. Lonnoy, D. Maraun, V. Masson-Delmotte, T. Maycock, A. Pirani, R. Ranasinghe, J. Rogelj, A. C. Ruane, S. Szopa, and P. Zhai. Climate change 2021: Summary for all, 2021.

Copernicus EMS/ECMWF. River discharge - 2021, 2021. URL https://climate.copernicus.eu/esotc/2021/river-discharge. Accessed on 7 October, 2023.

C. Deser, J. W. Hurrell, and A. S. Phillips. The role of the north atlantic oscillation in european climate projections. *Climate Dynamics*, 49(9):3141–3157, 2017. doi: 10.1007/s00382-016-3502-z.

A. Dhinakaran. Understanding kl divergence. Online, 2023. URL https://towardsdatascience.com/understanding-kl-divergence-f3ddc8dff254.

S. Diress and T. Bedada. Precipitation and temperature trend analysis by mann kendall test: The case of addis ababa methodological station, addis ababa, ethiopia. *African Journal on Land Policy and Geospatial Sciences*, 4(4):517–526, 2021. ISSN 2657-2664. doi: 10.48346/IMIST.PRSM/ajlp-gs.v4i4.24086. URL https://revues.imist.ma/index.php/AJLP-GS/article/view/24086.

European Environment Agency. Landscapes in transition: An account of 25 years of land cover change in europe. EEA Report 10/2017, 2017.

European Environment Agency. Global and european temperatures, 2023a. URL https://www.eea.europa.eu/ims/global-and-european-temperatures.

European Environment Agency. Land cover and land cover changes in european countries in 2000-2018 - land monitoring service. Online, 2023b. URL https://www.eea.europa.eu/data-and-maps/dashboards/land-cover-and-change-statistics.

A. K. Georgoulias, D. Akritidis, A. Kalisoras, J. Kapsomenakis, D. Melas, C. S. Zerefos, and P. Zanis. Climate change projections for greece in the 21st century from high-resolution euro-cordex rcm simulations. *Atmospheric Research*, 271:106049, 2022. ISSN 0169-8095. doi: https://doi.org/10.1016/j.atmosres.2022.106049. URL https://www.sciencedirect.com/science/article/pii/S0169809522000357.

K. H. Hamed. Trend detection in hydrologic data: The mann–kendall trend test under the scaling hypothesis. *Journal of Hydrology*, 349(3):350–363, 2008. ISSN 0022-1694. doi: https://doi.org/10.1016/j.jhydrol.2007.11.009. URL https://www.sciencedirect.com/science/article/pii/S0022169407006865.

K. H. Hamed and A. Ramachandra Rao. A modified mann-kendall trend test for autocorrelated data. *Journal of Hydrology*, 204(1):182–196, 1998. ISSN 0022-1694. doi: https://doi.org/10.1016/S0022-1694(97)00125-X. URL https://www.sciencedirect.com/science/article/pii/S002216949700125X.

S. Hanus, M. Hrachowitz, H. Zekollari, G. Schoups, M. Vizcaino, and R. Kaitna. Timing and magnitude of future annual runoff extremes in contrasting alpine catchments in austria. *Hydrology and Earth System Sciences Discussions*, 2021:1–35, 2021a.

S. Hanus, M. Hrachowitz, H. Zekollari, G. Schoups, M. Vizcaino, and R. Kaitna. Future changes in annual, seasonal and monthly runoff signatures in contrasting alpine catchments in austria. *Hydrology and Earth System Sciences*, 25(6):3429–3453, 2021b. doi: 10.5194/hess-25-3429-2021. URL https://hess.copernicus.org/articles/25/3429/2021/.

M. Heberger. delineator.py: Fast, accurate watershed delineation using hybrid vector- and raster-based methods and data from merit-hydro.

IPCC. Climate change widespread, rapid, and intensifying – ipcc, 2022. URL https://www.ipcc.ch/2021/08/09/ar6-wg1-20210809-pr/. Last modified 13 December 2020.

G. James, D. Witten, T. Hastie, and R. Tibshirani. Step by step to understanding k-means clustering and implementation with sklearn. Online, 2023. URL https://towardsdatascience.com/understanding-kl-divergence-f3ddc8dff254.

M. G. Kendall. *Rank correlation methods.* Griffin, London, 1975.

L. S. Kuchment. The hydrological cycle and human impact on it. *Water resources management*, 40, 2004.

Z. Kundzewicz. Climate change impacts on the hydrological cycle. *Ecohydrology and Hydrobiology*, 8:195–203, 12 2008. doi: 10.2478/v10104-009-0015-y.

Landesamt für Umwelt, Naturschutz und Geologie Mecklenburg-Vorpommern. Pegelportal mecklenburg-vorpommern, n.d. URL https://pegelportal-mv.de/pegel_mv.html. Accessed on 26 September, 2023.

B. Lehner, P. Döll, J. Alcamo, et al. Estimating the impact of global change on flood and drought risks in europe: A continental, integrated analysis. *Climatic Change*, 75:273–299, 2006. doi: 10.1007/s10584-006-6338-4. URL https://doi.org/10.1007/s10584-006-6338-4.

C. Linares, J. Díaz, M. Negev, G. S. Martinez, R. Debono, and S. Paz. Impacts of climate change on the public health of the mediterranean basin population - current situation, projections, preparedness and adaptation. *Environmental research*, 182:109107, 2020a. URL https://api.semanticscholar.org/CorpusID:211192333.

C. Linares, J. Díaz, M. Negev, G. S. Martínez, R. Debono, and S. Paz. Impacts of climate change on the public health of the mediterranean basin population - current situation, projections, preparedness and adaptation. *Environmental Research*, 182: 109107, 2020b. ISSN 0013-9351. doi: https://doi.org/10.1016/j.envres.2019.109107. URL https://www.sciencedirect.com/science/article/pii/S001393511930903X.

H. B. Mann. Nonparametric tests against trend. *Econometrica*, 13:245–259, 1945.

Matthew Heberger. Global watersheds, n.d. URL https://mghydro.com/. Accessed on 7 October, 2023.

S. I. McClean. Data mining and knowledge discovery. In R. A. Meyers, editor, *Encyclopedia of Physical Science and Technology (Third Edition)*, pages 229–246. Academic Press, New York, third edition edition, 2003. ISBN 978-0-12-227410-7. doi: https://doi.org/10.1016/B0-12-227410-5/00845-0. URL https://www.sciencedirect.com/science/article/pii/B0122274105008450.

Ministry for the Ecological Transition, France. Eaufrance hydro, n.d. URL https://hydro.eaufrance.fr/. Accessed on 26 September, 2023.

Ministère de l'Environnement, du Climat et du Développement durable, Luxembourg. Inondations luxembourg, n.d. URL https://www.inondations.lu/. Accessed on 26 September, 2023.

G. Okafor, O. Jimoh, and K. Larbi. Detecting changes in hydro-climatic variables during the last four decades (1975-2014) on downstream kaduna river catchment, nigeria. *Atmospheric and Climate Sciences*, 7:161–175, 2017. doi: 10.4236/acs.2017.72012.

W. M. Organisation. Temperatures in europe increase more than twice global average, 2022. URL https://public.wmo.int/en/media/press-release/temperatures-europe-increase-more-twice-global-average.

T. Petrow and B. Merz. Trends in flood magnitude, frequency and seasonality in germany in the period 1951–2002. *Journal of Hydrology*, 371(1):129–141, 2009. ISSN 0022-1694.

doi: https://doi.org/10.1016/j.jhydrol.2009.03.024. URL https://www.sciencedirect.com/science/article/pii/S0022169409001917.

Rijkswaterstaat, Ministry of Infrastructure and Water Management, Netherlands. Rijkswaterstaat, n.d. URL https://www.rijkswaterstaat.nl/. Accessed on 26 September, 2023.

J. Roger A. Pielke. What is climate change? *Energy & Environment*, 15(3):515–520, 2004. doi: 10.1260/0958305041494576. URL https://doi.org/10.1260/0958305041494576.

E. Rottler, T. Francke, G. Bürger, and A. Bronstert. Long-term changes in central european river discharge for 1869–2016: impact of changing snow covers, reservoir constructions and an intensified hydrological cycle. *Hydrology and Earth System Sciences*, 24(4): 1721–1740, 2020. doi: 10.5194/hess-24-1721-2020. URL https://hess.copernicus.org/articles/24/1721/2020/.

B. Santer et al. Contributions of anthropogenic and natural forcing to recent tropopause height changes. *Science*, 301(25 July):479–483, 2003. doi: 10.1126/science.1084123. URL https://doi.org/10.1126/science.1084123.

P. K. Sen. Estimates of the regression coefficient based on kendall's tau. *Journal of the American Statistical Association*, 63(324):1379–1389, 1968. doi: 10.1080/01621459.1968.10480934. URL https://www.tandfonline.com/doi/abs/10.1080/01621459.1968.10480934.

Service Public de Wallonie. Hydrometrie wallonie, n.d. URL https://hydrometrie.wallonie.be/home.html. Accessed on 26 September, 2023.

L. Terray and J. Boé. Quantifying 21st-century france climate change and related uncertainties. *Comptes Rendus Geoscience*, 345(3):136–149, 2013. ISSN 1631-0713. doi: https://doi.org/10.1016/j.crte.2013.02.003. URL https://www.sciencedirect.com/science/article/pii/S1631071313000357.

A. J. Teuling, E. A. G. de Badts, F. A. Jansen, R. Fuchs, J. Buitink, A. J. Hoek van Dijke, and S. M. Sterling. Climate change, reforestation/afforestation, and urbanization impacts on evapotranspiration and streamflow in europe. *Hydrology and Earth System Sciences*, 23(9):3631–3652, 2019. doi: 10.5194/hess-23-3631-2019. URL https://hess.copernicus.org/articles/23/3631/2019/.

A. A. Torres-García, O. Mendoza-Montoya, M. Molinas, J. M. Antelis, L. A. Moctezuma, and T. Hernández-Del-Toro. Chapter 4 - pre-processing and feature extraction. In A. A. Torres-García, C. A. Reyes-García, L. Villaseñor-Pineda, and O. Mendoza-Montoya, editors, *Biosignal Processing and Classification Using Computational Learning and Intelligence*, pages 59–91. Academic Press, 2022. ISBN 978-0-12-820125-1. doi: https://doi.org/10.1016/B978-0-12-820125-1.00014-2. URL https://www.sciencedirect.com/science/article/pii/B9780128201251000142.

R. Twardosz, A. Walanus, and I. Guzik. Warming in europe: Recent trends in annual and seasonal temperatures. *Pure and Applied Geophysics*, 178(10):4021–4032, 10 2021. ISSN 1420-9136. doi: 10.1007/s00024-021-02860-6. URL https://doi.org/10.1007/s00024-021-02860-6.

United Nations. United nations framework convention on climate change (unfccc). Online,

1992. URL https://unfccc.int/files/essential_background/background_publications_htmlpdf/application/pdf/conveng.pdf.

G. Villarini, J. A. Smith, F. Serinaldi, and A. A. Ntelekos. Analyses of seasonal and annual maximum daily discharge records for central europe. *Journal of Hydrology*, 399 (3):299–312, 2011. ISSN 0022-1694. doi: https://doi.org/10.1016/j.jhydrol.2011.01.007. URL https://www.sciencedirect.com/science/article/pii/S0022169411000321.

E. Vyshkvarkova and O. Sukhonos. Compound extremes of air temperature and precipitation in eastern europe. *Climate*, 10(9), 2022. ISSN 2225-1154. doi: 10.3390/cli10090133. URL https://www.mdpi.com/2225-1154/10/9/133.

P. Ward, H. Renssen, and J. e. a. Aerts. Sensitivity of discharge and flood frequency to twenty-first century and late holocene changes in climate and land use (river meuse, northwest europe). *Climatic Change*, 106:179–202, 2011. doi: 10.1007/s10584-010-9926-2. URL https://doi.org/10.1007/s10584-010-9926-2.

P. J. Ward, H. Renssen, J. C. J. H. Aerts, R. T. van Balen, and J. Vandenberghe. Strong increases in flood frequency and discharge of the river meuse over the late holocene: impacts of long-term anthropogenic land use change and climate variability. *Hydrology and Earth System Sciences*, 12(1):159–175, 2008. doi: 10.5194/hess-12-159-2008. URL https://hess.copernicus.org/articles/12/159/2008/.

R. Weigel, B. Bat-Enerel, C. Dulamsuren, L. Muffler, G. Weithmann, and C. Leuschner. Summer drought exposure, stand structure, and soil properties jointly control the growth of european beech along a steep precipitation gradient in northern germany. *Global change biology*, 29, 11 2022. doi: 10.1111/gcb.16506.

R. Wicklin. The kullback–leibler divergence between discrete probability distributions. Online, 2020. URL https://blogs.sas.com/content/author/rickwicklin/.

R. R. Wilcox. Chapter 10 - robust regression. In R. R. Wilcox, editor, *Introduction to Robust Estimation and Hypothesis Testing (Fifth Edition)*, pages 577–651. Academic Press, fifth edition edition, 2022. ISBN 978-0-12-820098-8. doi: https://doi.org/10.1016/B978-0-12-820098-8.00016-6. URL https://www.sciencedirect.com/science/article/pii/B9780128200988000166.

K. Winkler, R. Fuchs, M. Rounsevell, et al. Global land use changes are four times greater than previously estimated. *Nature Communications*, 12:2501, 2021. doi: 10.1038/s41467-021-22702-2. URL https://doi.org/10.1038/s41467-021-22702-2. Online; accessed on September 12, 2023.

J. Zeder and E. M. Fischer. Observed extreme precipitation trends and scaling in central europe. *Weather and Climate Extremes*, 29:100266, 2020. ISSN 2212-0947. doi: https://doi.org/10.1016/j.wace.2020.100266. URL https://www.sciencedirect.com/science/article/pii/S2212094719301720.

Appendix

A1 Changes in Magnitude

A1.1 Yearly Average mean daily flow

A1.1.1 Average mean daily flow - DEM and trends of the stations:

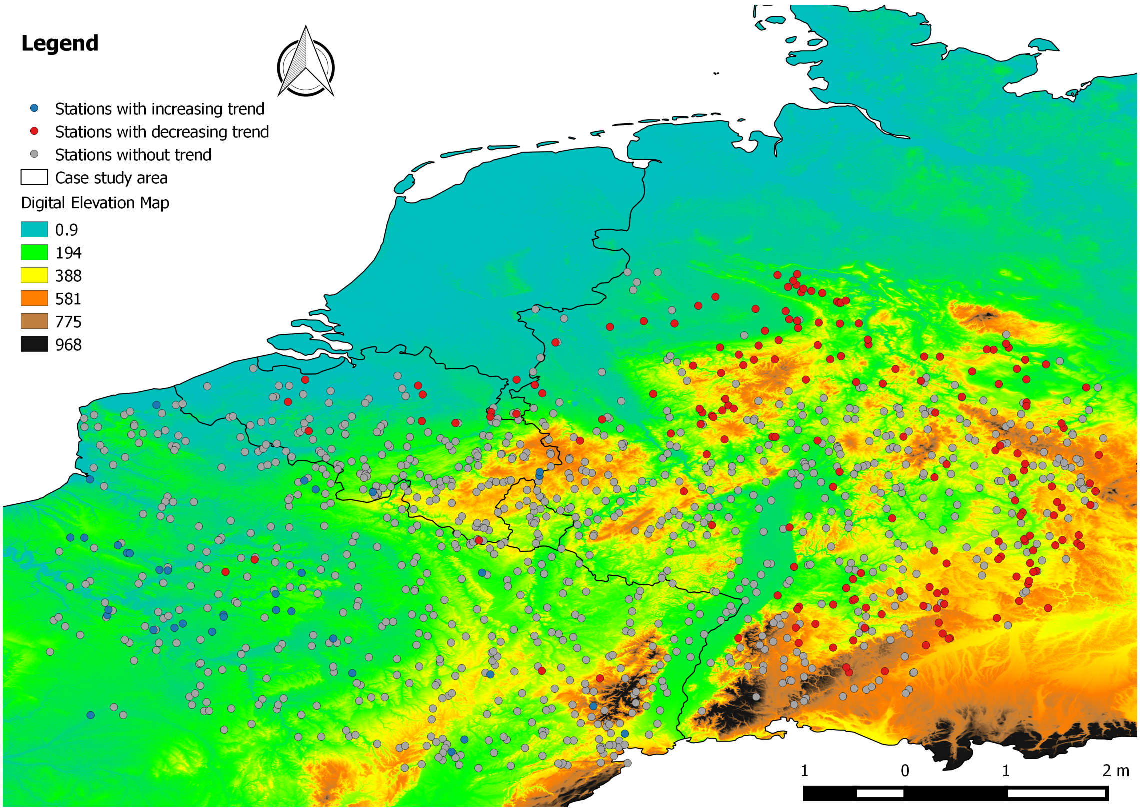

Figure A1.1: 2002-2021 Average mean daily flow - Stations with increasing, decreasing trend or no trend - Digital Elevation Map (DEM).

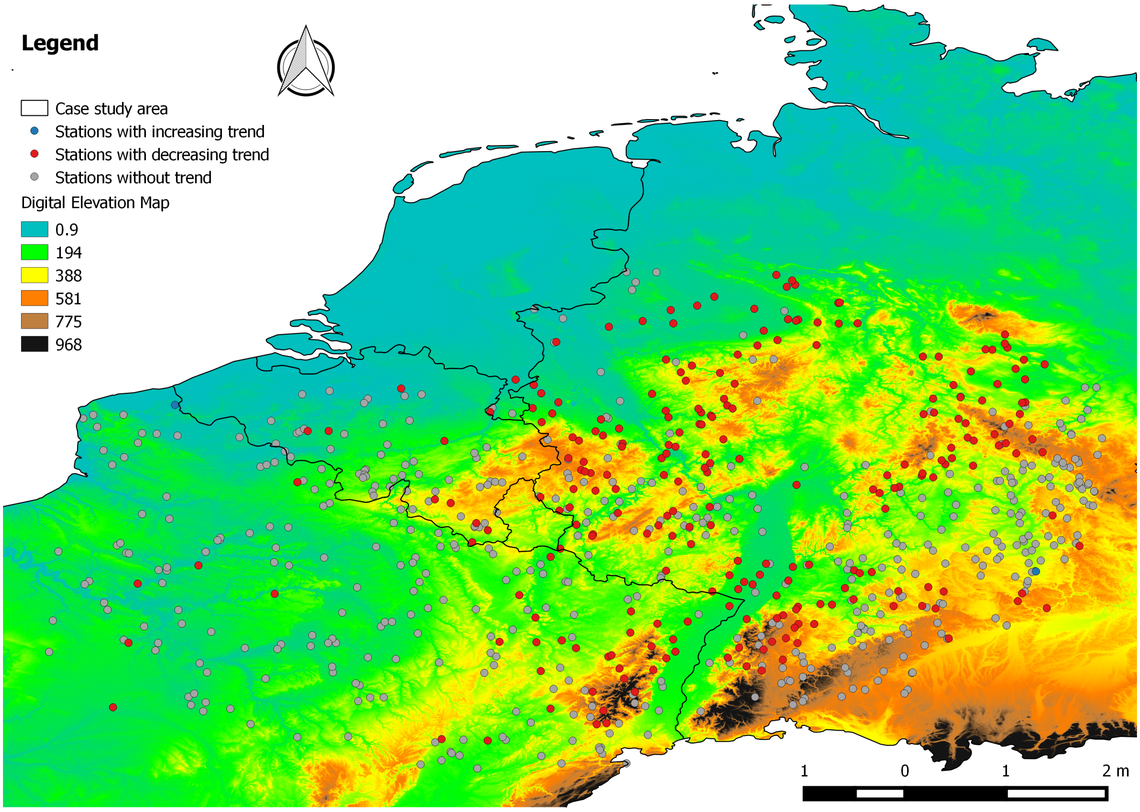

Figure A1.2: 1982-2021 Average mean daily flow - Stations with increasing, decreasing trend or no trend - Digital Elevation Map (DEM).

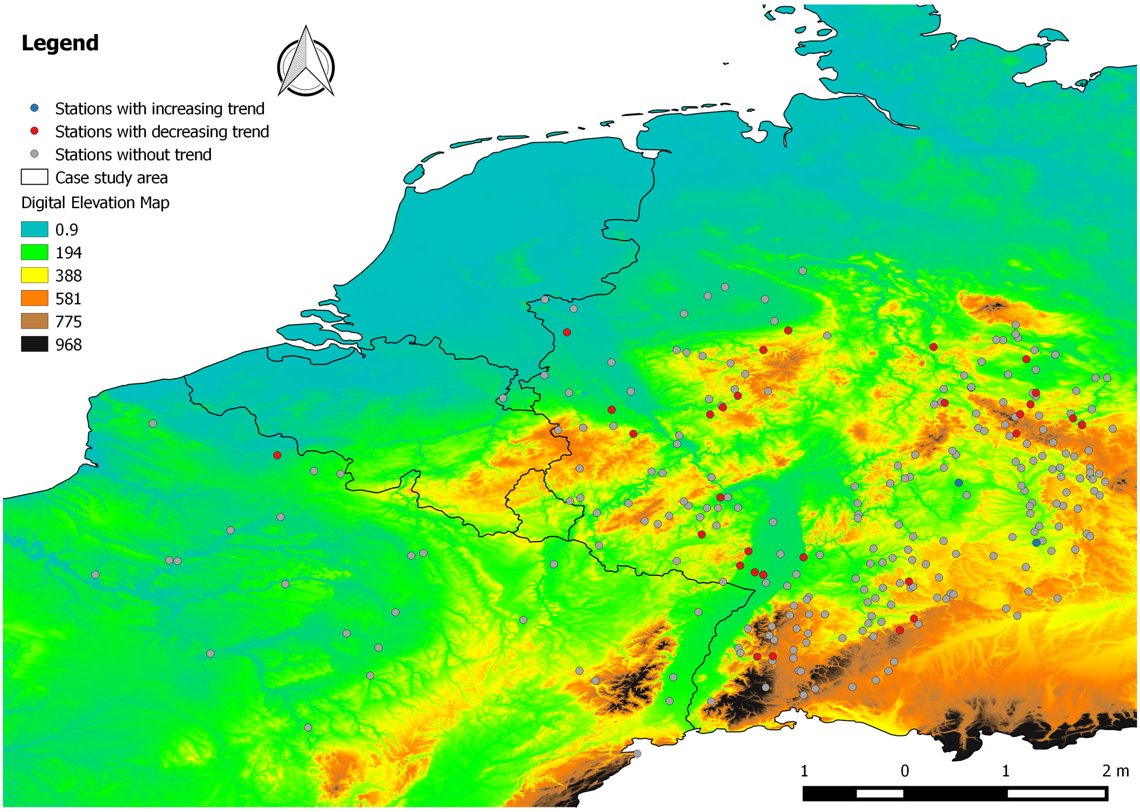

Figure A1.3: 1962-2021 Average mean daily flow - Stations with increasing, decreasing trend or no trend - Digital Elevation Map (DEM).

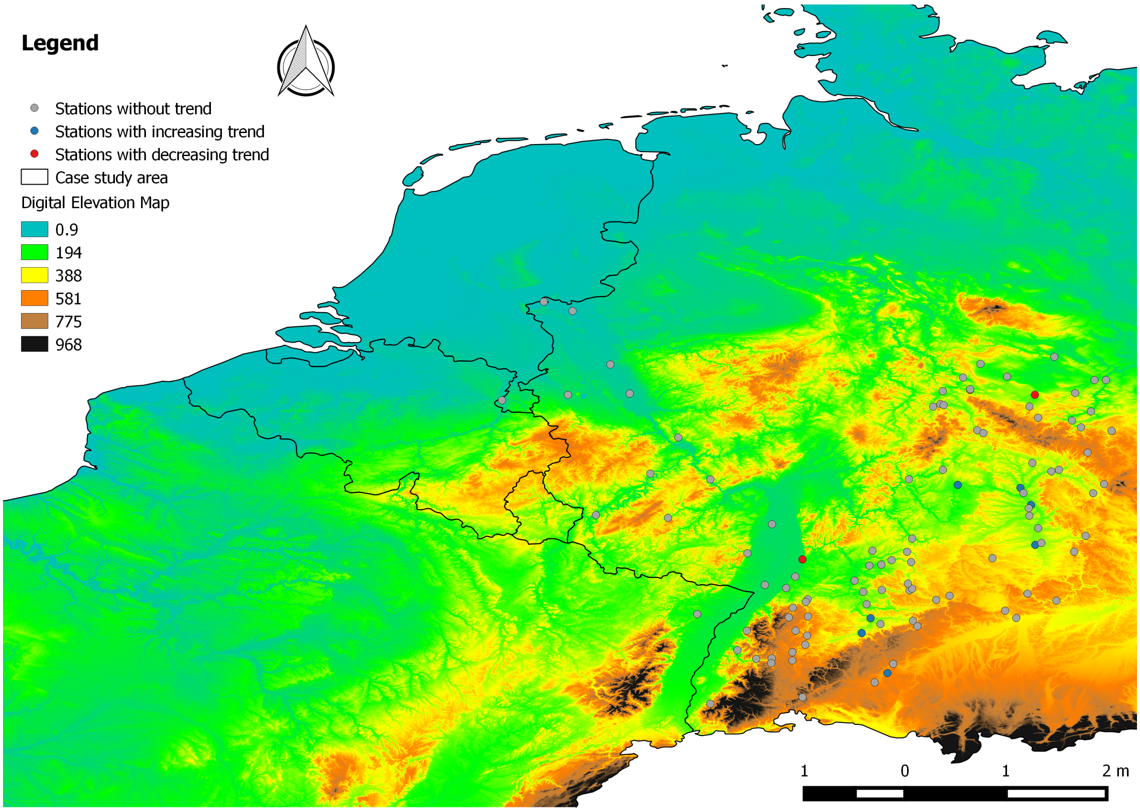

Figure A1.4: 1942-2021 Average mean daily flow - Stations with increasing, decreasing trend or no trend - Digital Elevation Map (DEM).

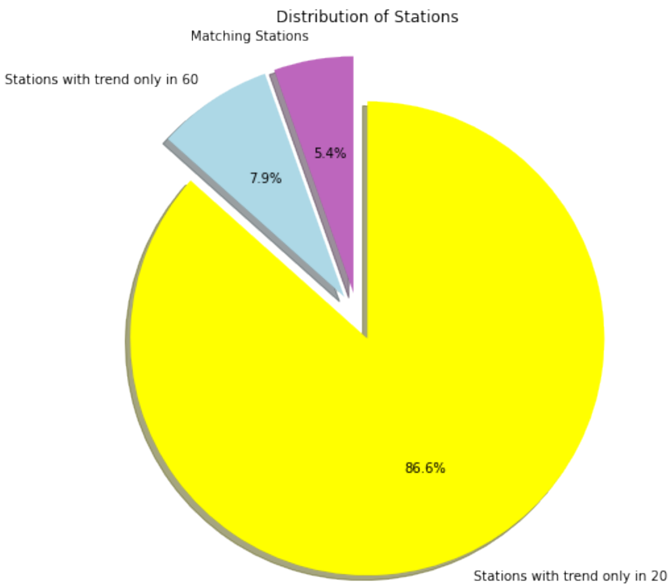

Figure A1.5: 2002-2021 & 1962-2021 Average mean daily flow - Matching stations.

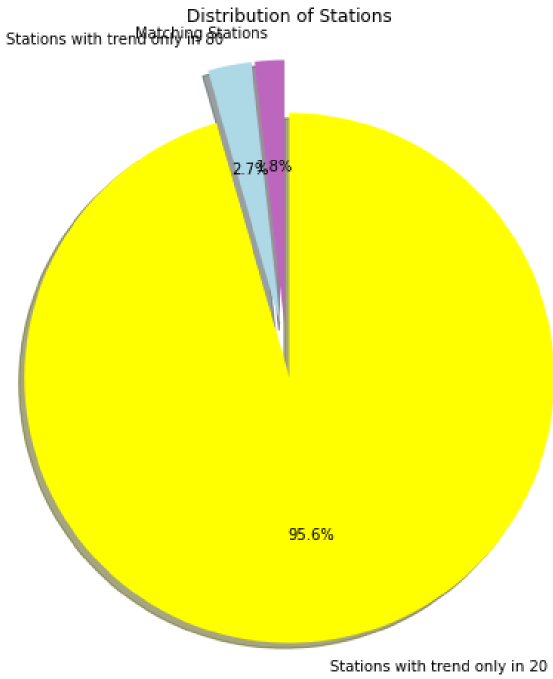

Figure A1.6: 2002-2021 & 1942-2021 Average mean daily flow - Matching stations.

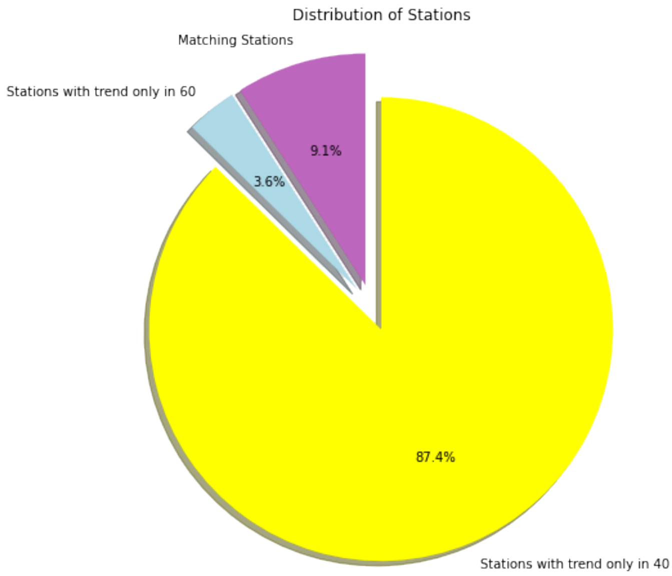

Figure A1.7: 1982-2021 & 1962-2021 Average mean daily flow - Matching stations.

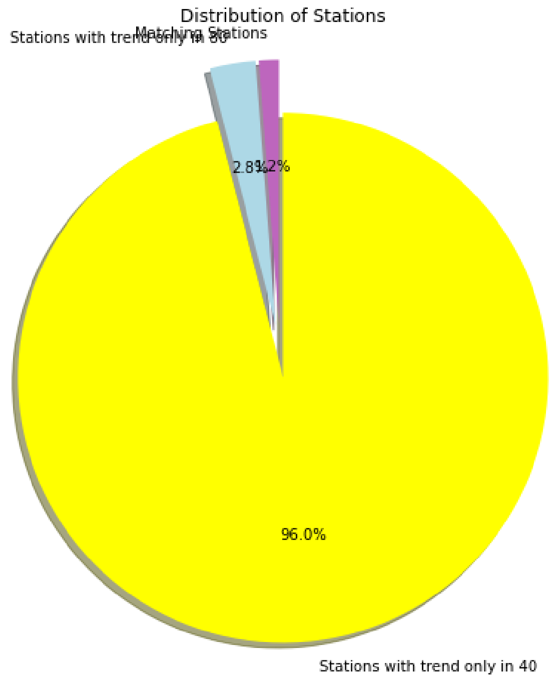

Figure A1.8: 1982-2021 & 1942-2021 Average mean daily flow - Matching stations.

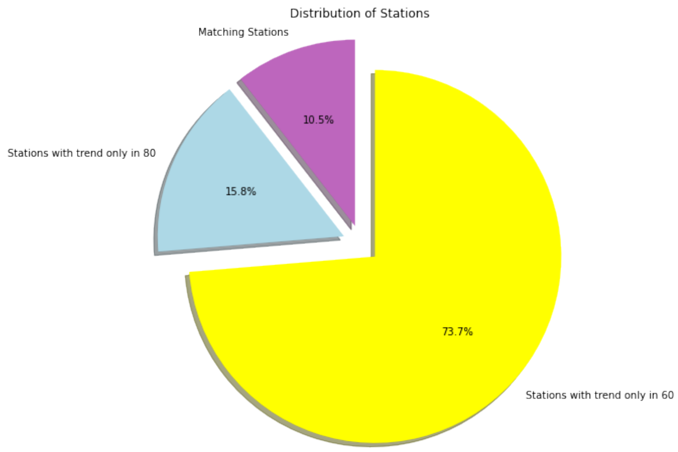

Figure A1.9: 1962-2021 & 1942-2021 Average mean daily flow - Matching stations.

A1.1.2 Maximum mean daily flow - DEM and trends of the stations:

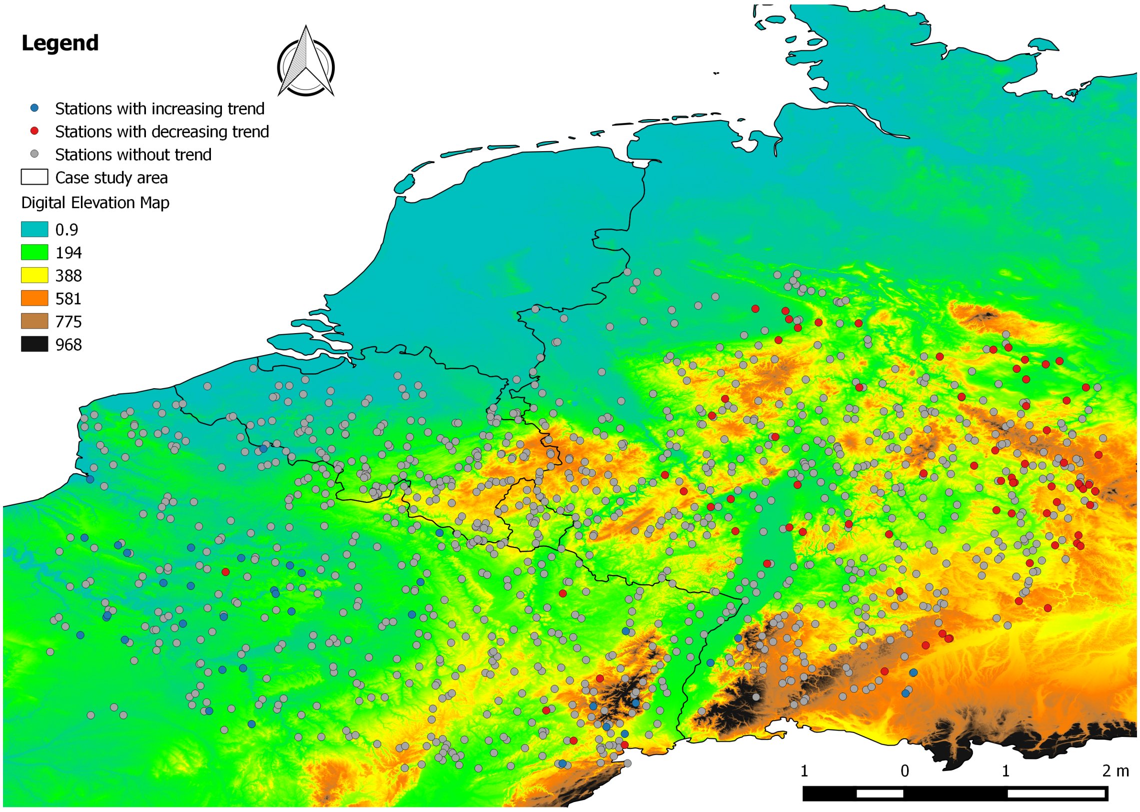

Figure A1.10: 2002-2021 Maxima mean daily flow - Stations with increasing, decreasing trend or no trend - Digital Elevation Map (DEM).

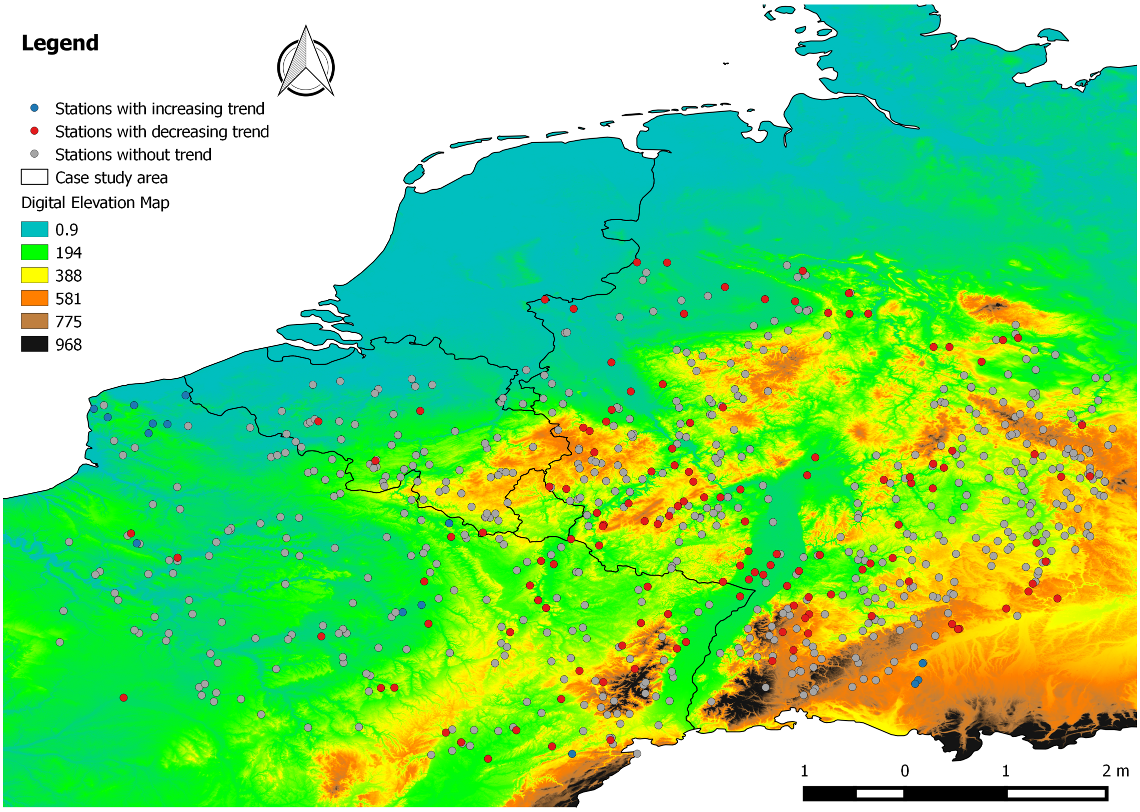

Figure A1.11: 1982-2021 Maxima mean daily flow - Stations with increasing, decreasing trend or no trend - Digital Elevation Map (DEM).

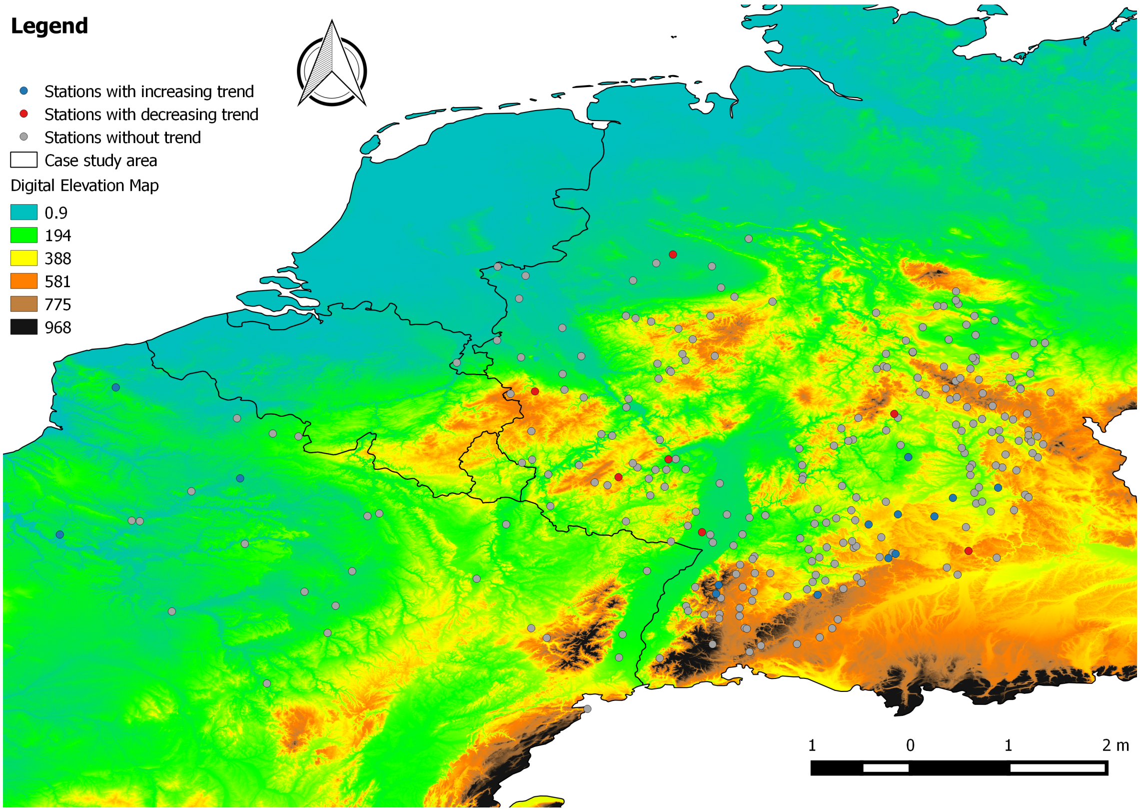

Figure A1.12: 1962-2021 Maxima mean daily flow - Stations with increasing, decreasing trend or no trend - Digital Elevation Map (DEM).

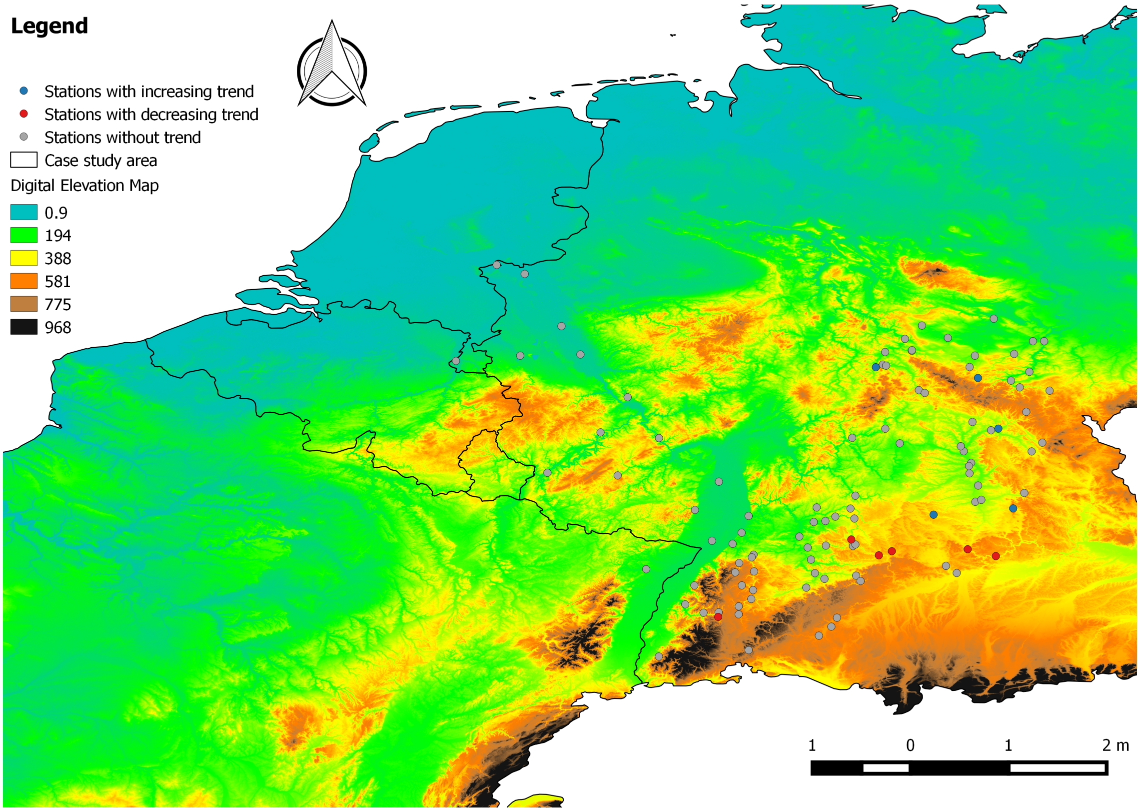

Figure A1.13: 1942-2021 Maxima mean daily flow - Stations with increasing, decreasing trend or no trend - Digital Elevation Map (DEM).

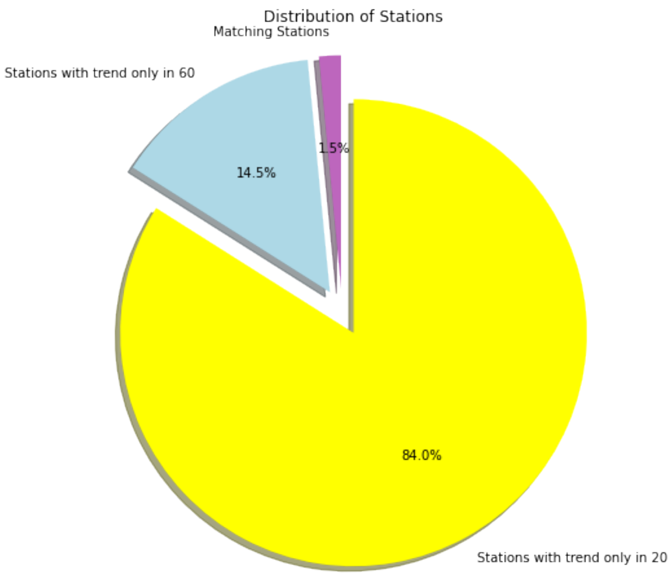

Figure A1.14: 2002-2021 & 1962-2021 Maxima mean daily flow - Matching stations.

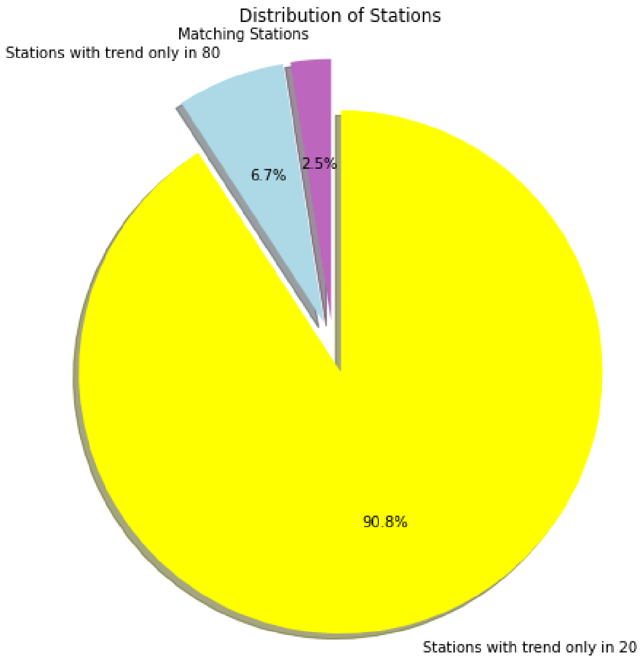

Figure A1.15: 2002-2021 & 1942-2021 Maxima mean daily flow - Matching stations.

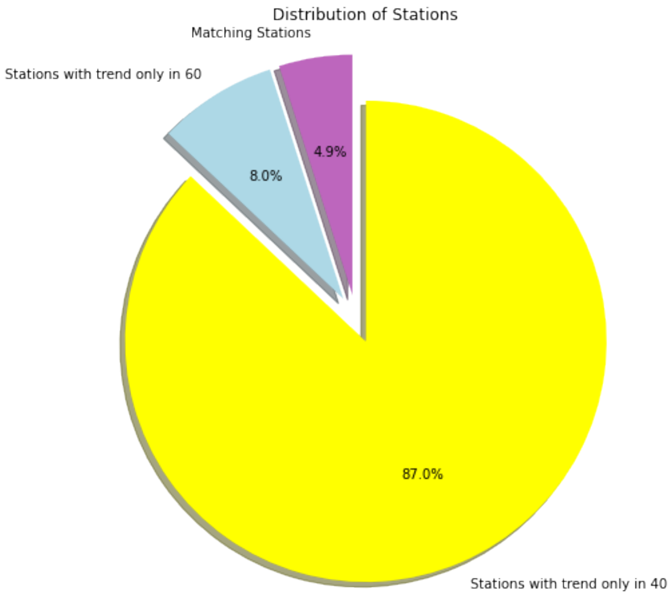

Figure A1.16: 1982-2021 & 1962-2021 Maxima mean daily flow - Matching stations.

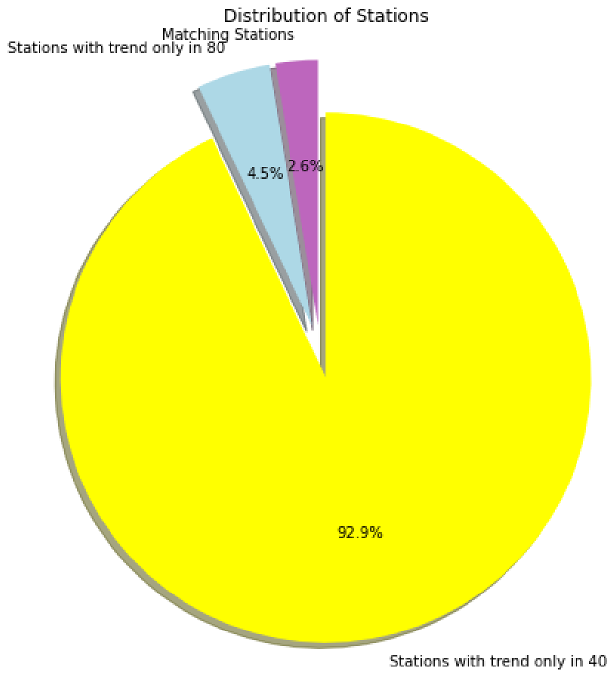

Figure A1.17: 1982-2021 & 1942-2021 Maxima mean daily flow - Matching stations.

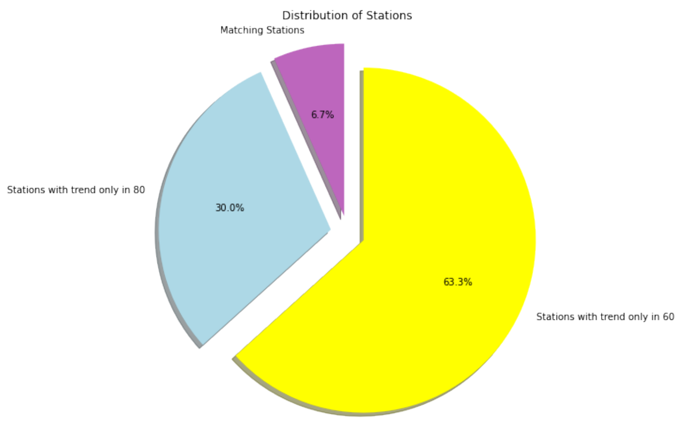

Figure A1.18: 1962-2021 & 1942-2021 Maxima mean daily flow - Matching stations.

A1.1.3 Minimum mean daily flow - DEM and trends of the stations:

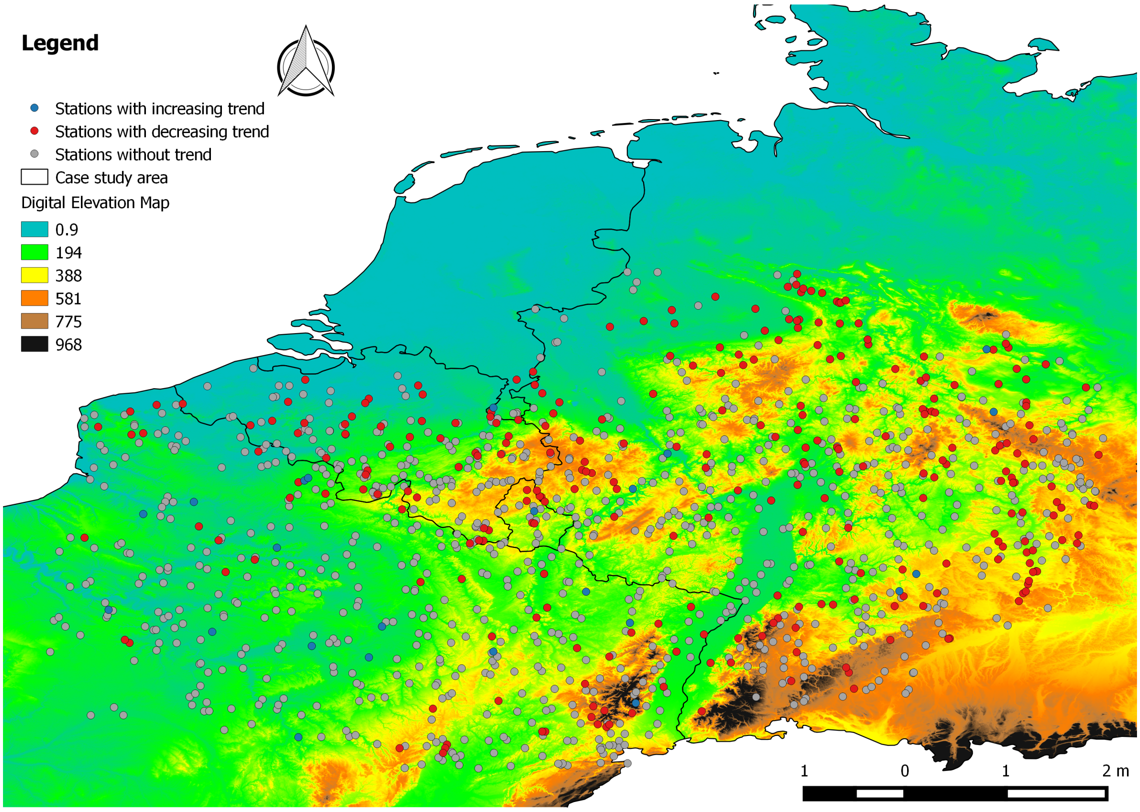

Figure A1.19: 2002-2021 Minima mean daily flow - Stations with increasing, decreasing trend or no trend - Digital Elevation Map (DEM).

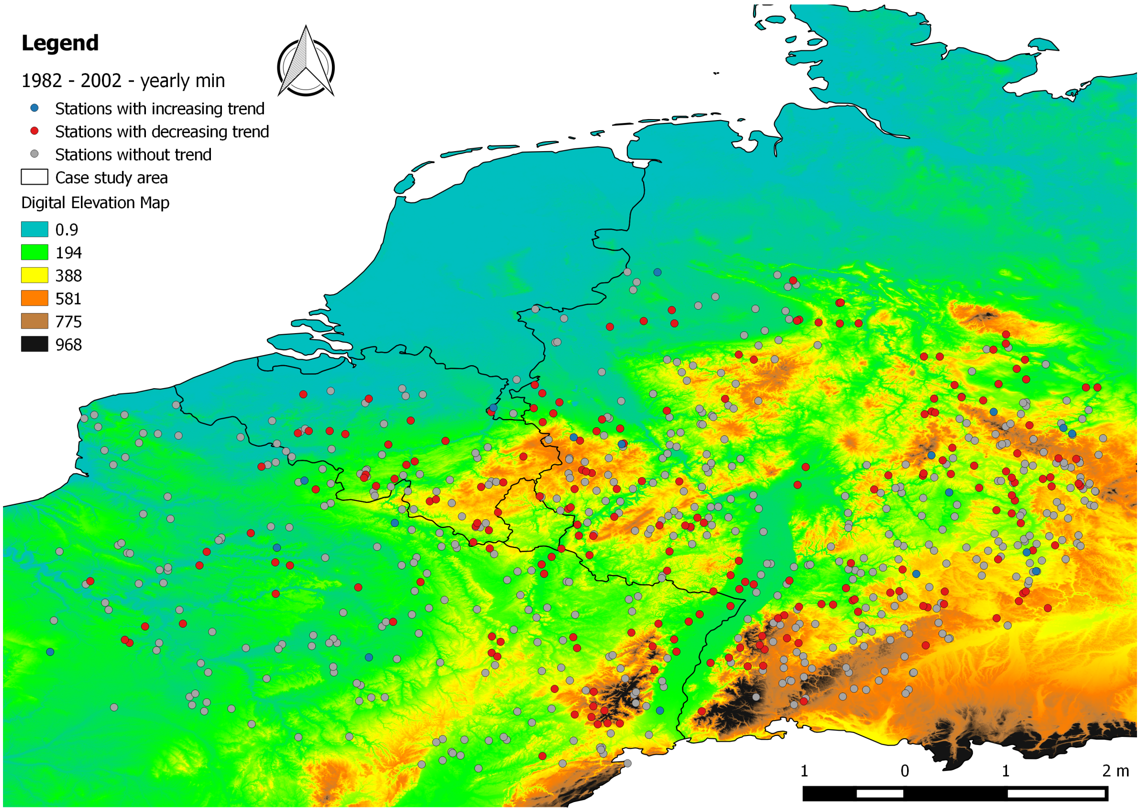

Figure A1.20: 1982-2021 Minima mean daily flow - Stations with increasing, decreasing trend or no trend - Digital Elevation Map (DEM).

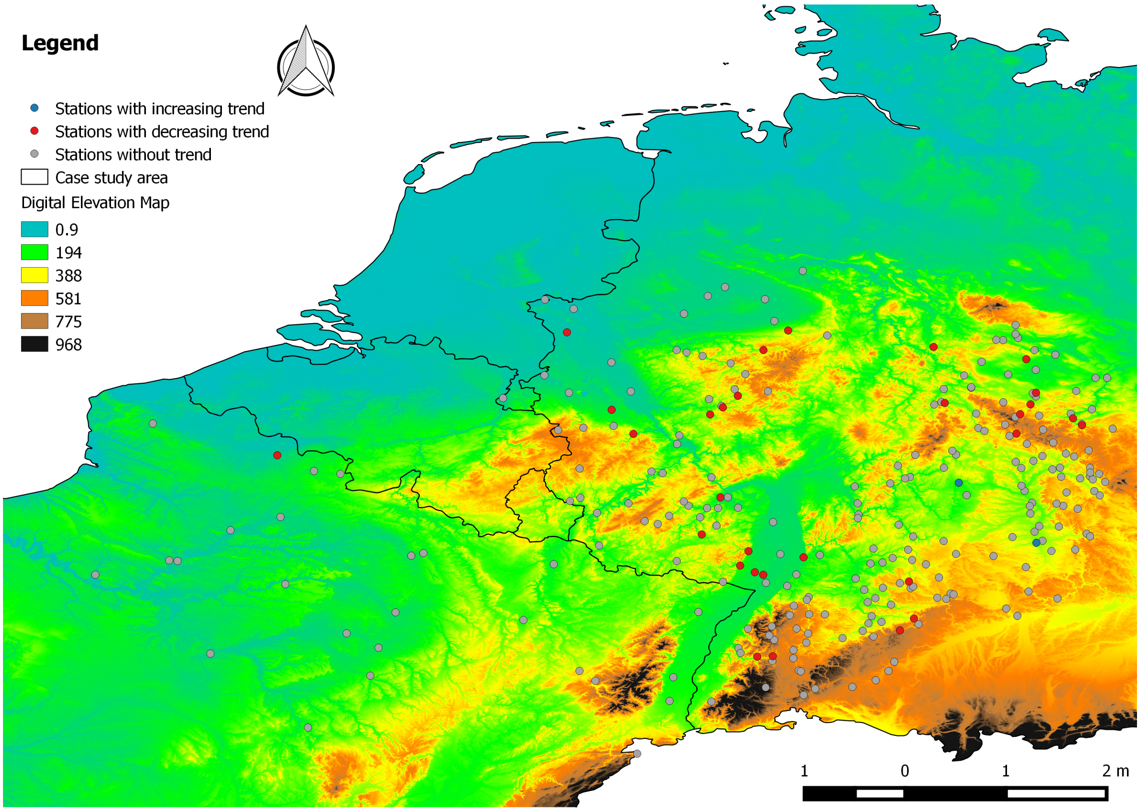

Figure A1.21: 1962-2021 Minima mean daily flow - Stations with increasing, decreasing trend or no trend - Digital Elevation Map (DEM).

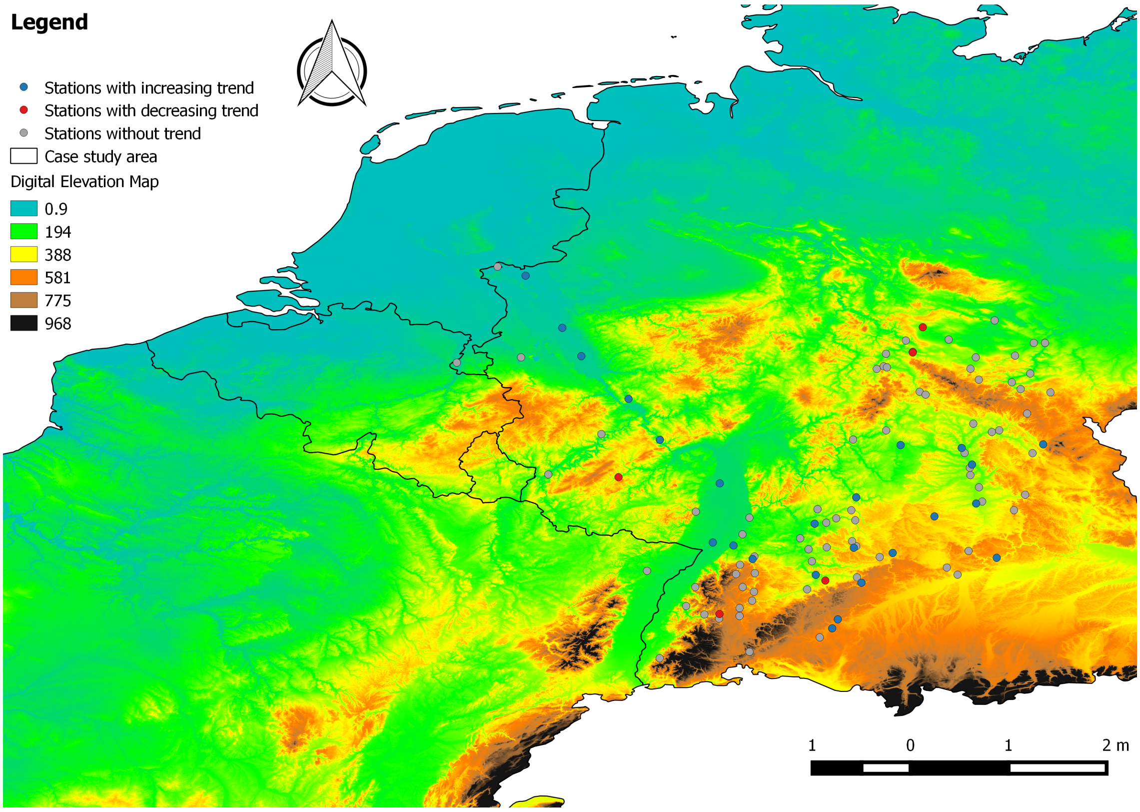

Figure A1.22: 1942-2021 Minima mean daily flow - Stations with increasing, decreasing trend or no trend - Digital Elevation Map (DEM).

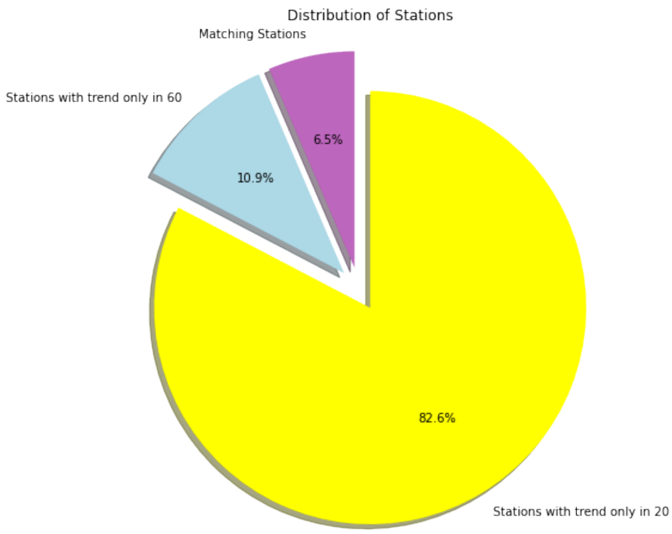

Figure A1.23: 2002-2021 & 1962-2021 Minima mean daily flow - Matching stations.

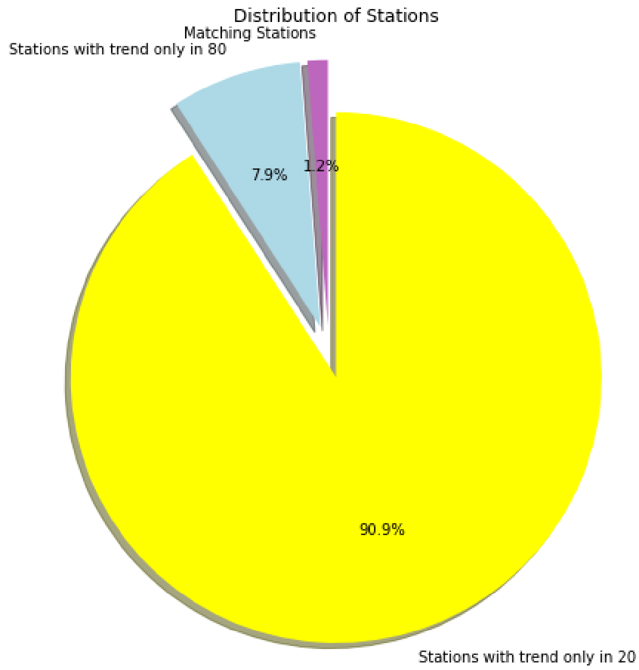

Figure A1.24: 2002-2021 & 1942-2021 Minima mean daily flow - Matching stations.

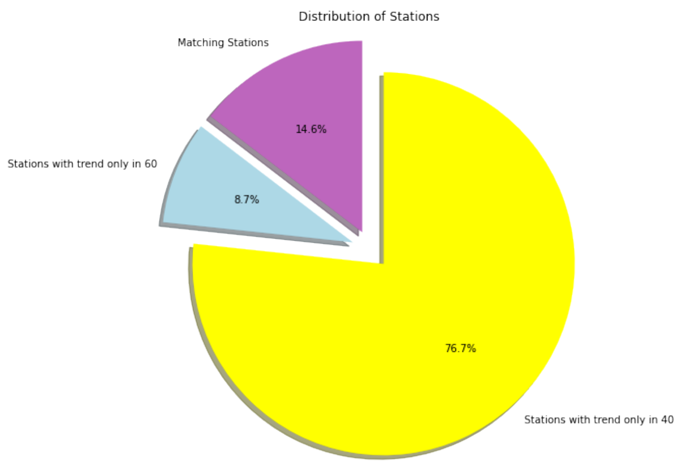

Figure A1.25: 1982-2021 & 1962-2021 Minima mean daily flow - Matching stations.

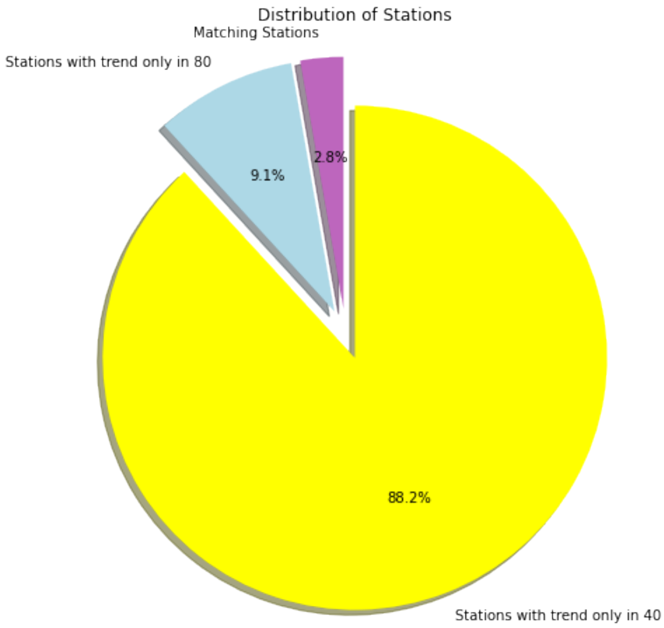

Figure A1.26: 1982-2021 & 1942-2021 Minima mean daily flow - Matching stations.

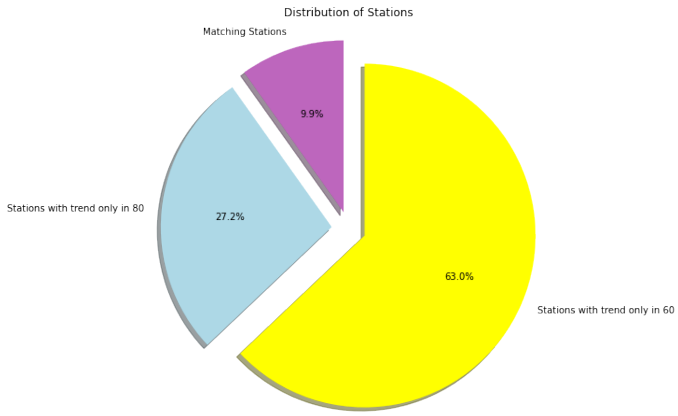

Figure A1.27: 1962-2021 & 1942-2021 Minima mean daily flow - Matching stations.

A1.2 Monthly analysis

To gain a deeper understanding of how to interpret the cluster plot's cube, the following explanation is provided. This cube vividly illustrates the precise locations of the North coordinate and the remaining coordinates.

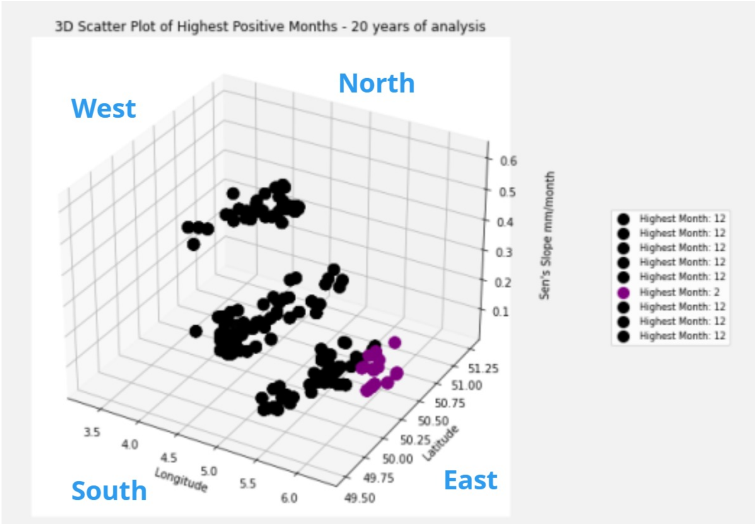

Figure A1.28: Cluster plot - Explanation of the cube.

Additionally, all the cluster plots, encompassing various time spans and covering different analyses, including average, maximum, and minimum discharges, are presented below:

A1.2.1 Average Discharges Analyses

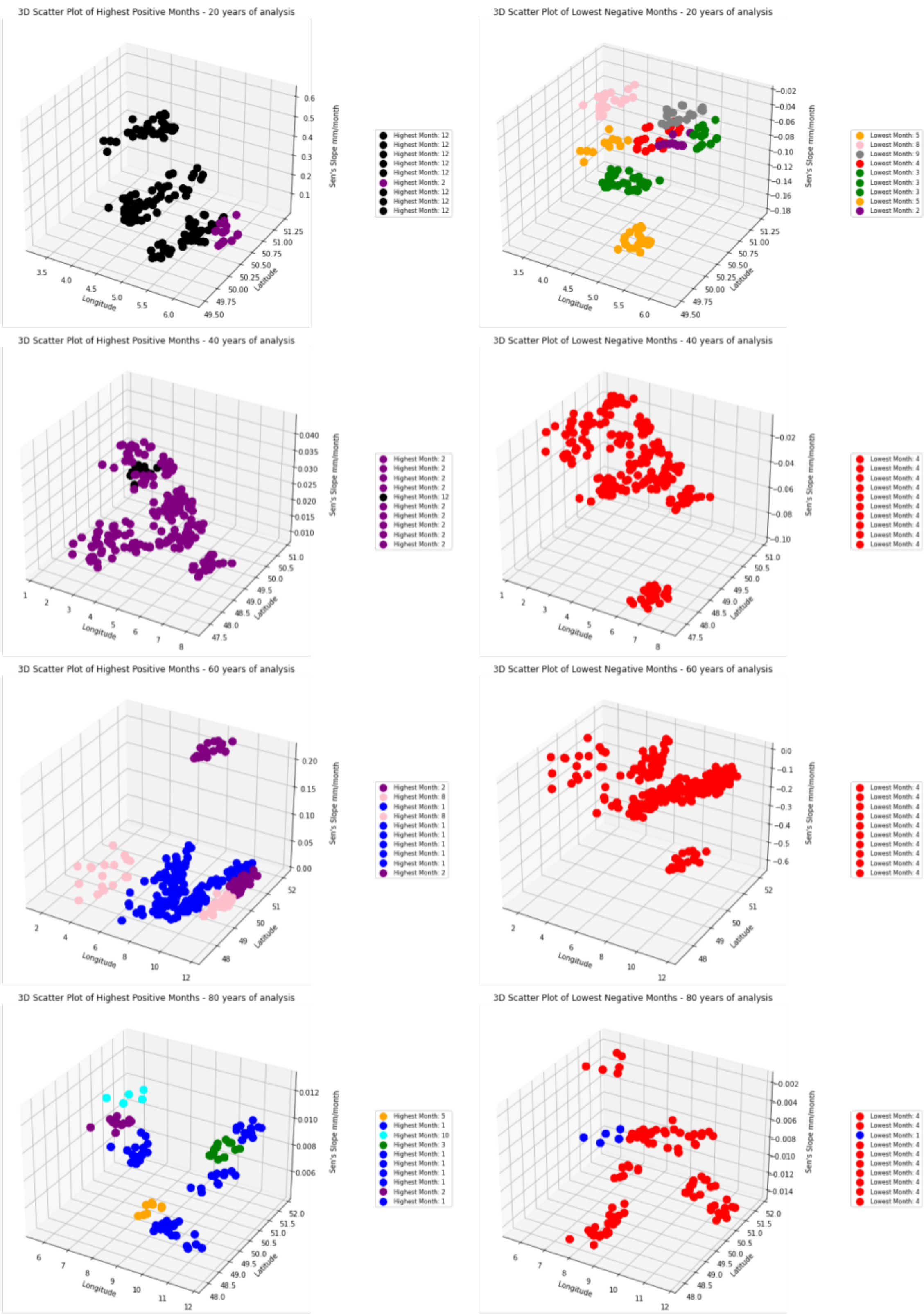

Figure A1.29: Cluster plot for highest and lowest trends through the years - Average trends of each month for the groups of the stations.

A1.2.2 Maximum Discharges Analyses

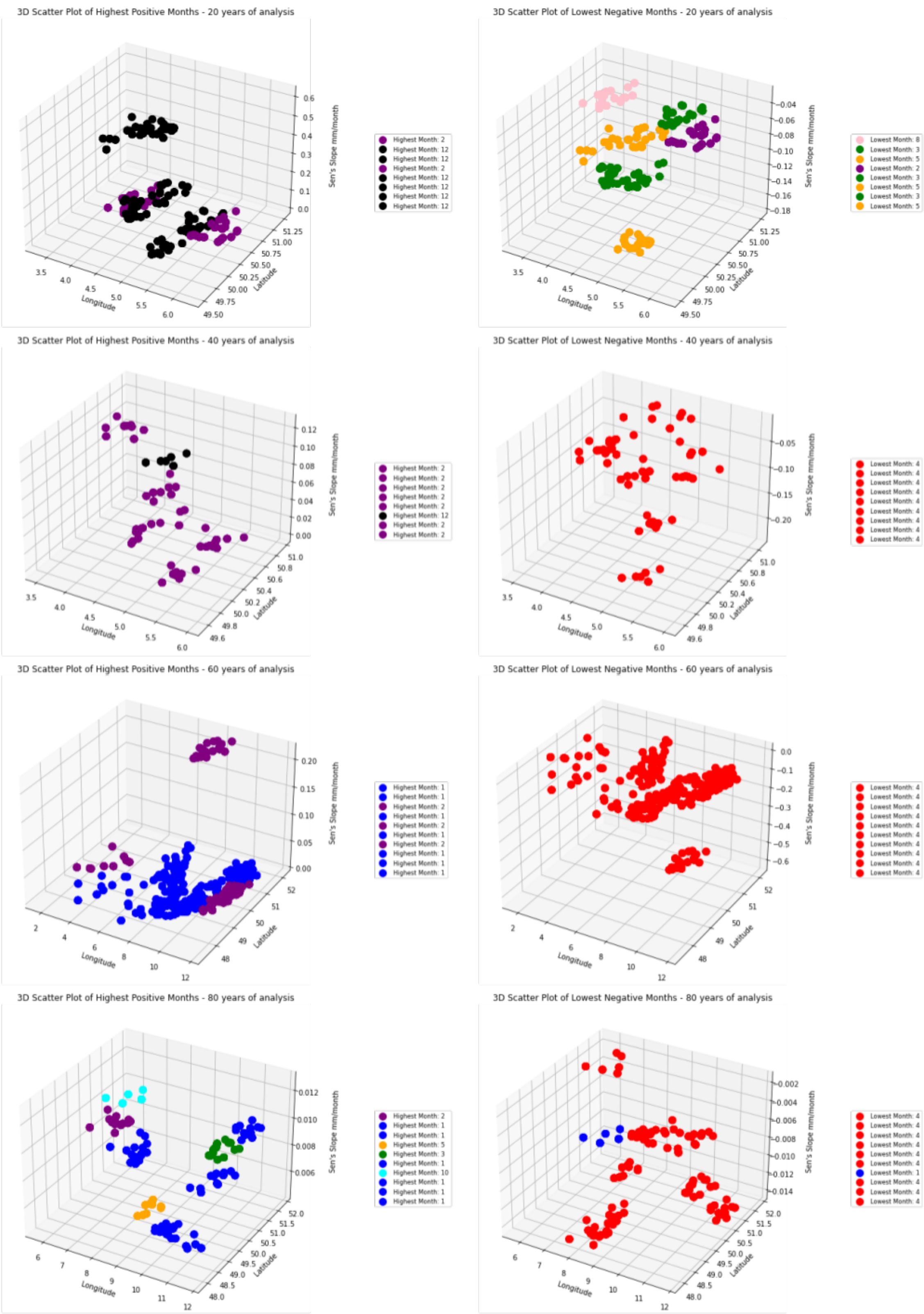

Figure A1.30: Cluster plot for highest and lowest trends through the years - Maxima trends of each month for the groups of the stations.

A1.2.3 Minimum Discharges Analyses

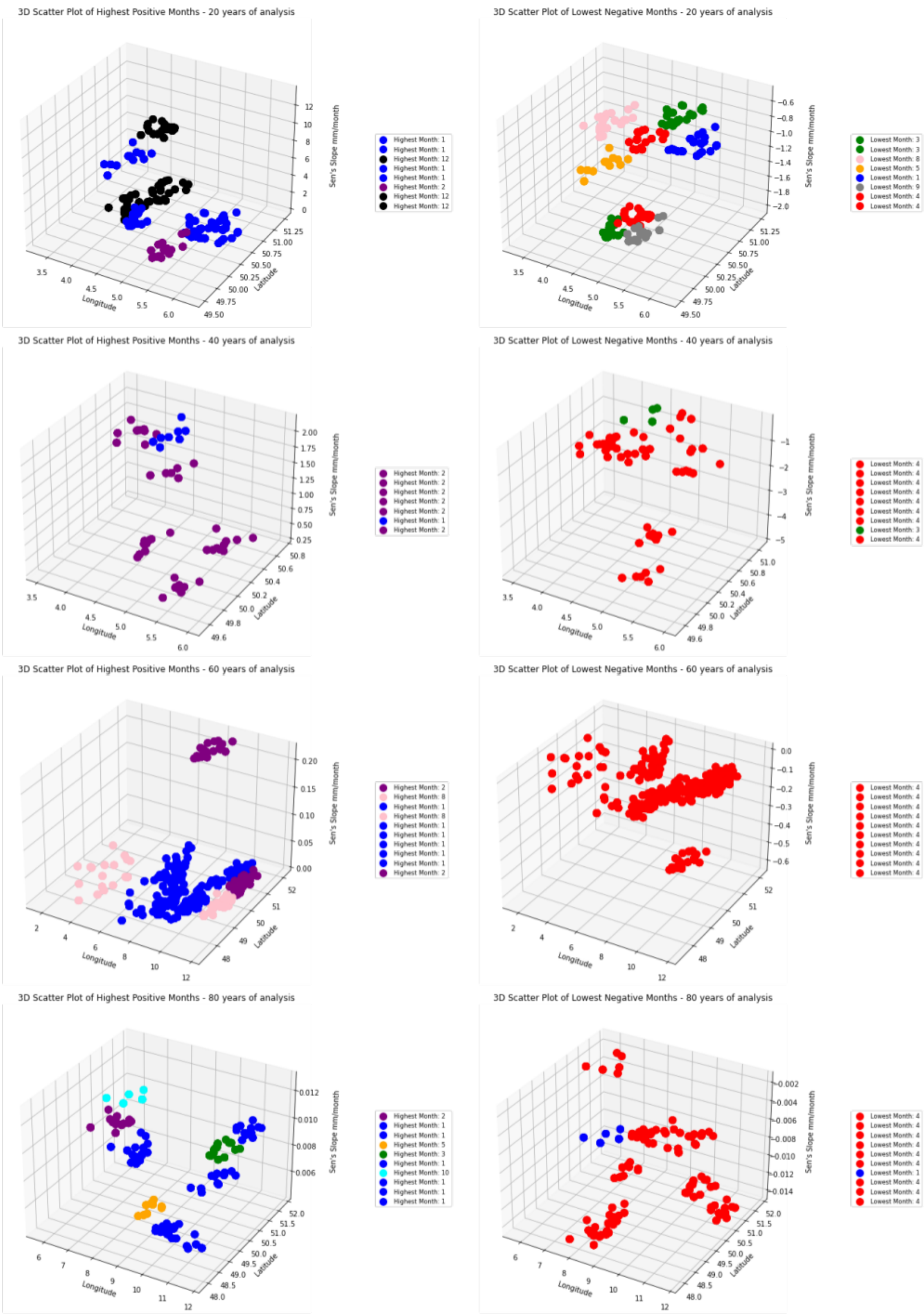

Figure A1.31: Cluster plot for highest and lowest trends through the years - Minima trends of each month for the groups of the stations.

A2 Changes in Timing

A3 Maxima analysis

The figure presents a concentration map derived from 60 and 80 years of data analysis. In this visualization, the length of the arrows corresponds to the degree of concentration. Longer arrows indicate a consistent dominant month over the years, while shorter arrows suggest variability in the dominant month. Each arrow is color-coded to represent specific months. This color scheme helps identify the corresponding dominant month for a given concentration value.

Additionally, a histogram accompanying the map illustrates the distribution of concentration values. A concentration value of 0 signifies that multiple months have discharge values close to the maximum, indicating high variability. Conversely, concentrations near 1 indicate that one month consistently experiences the maximum discharge over the years.

Upon examining Figure A3.1, it becomes evident that a majority of the stations exhibit concentrations ranging from 0.8 to 0.9. This implies a low degree of variability regarding the months in which the highest flow occurs. A similar pattern is observed in the analysis spanning 80 years, as depicted in Figure A3.2.

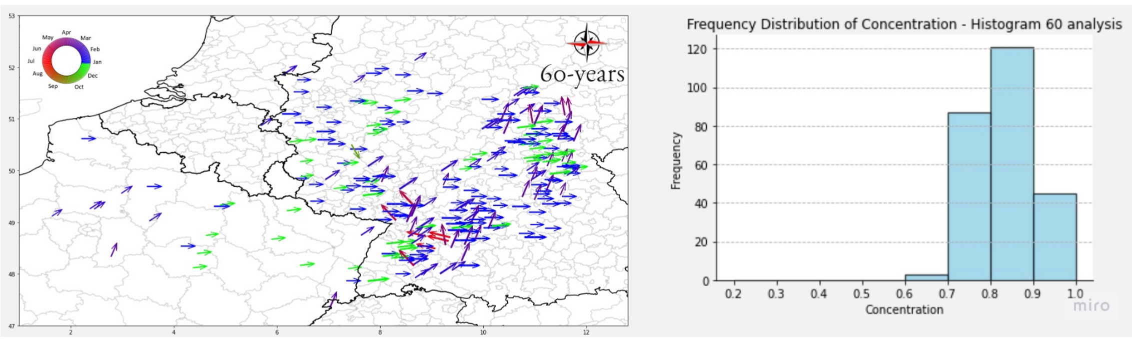

Figure A3.1: Concentration map for the 60 years of analysis (1962 - 2021) - Dominant month of the Maxima discharges.

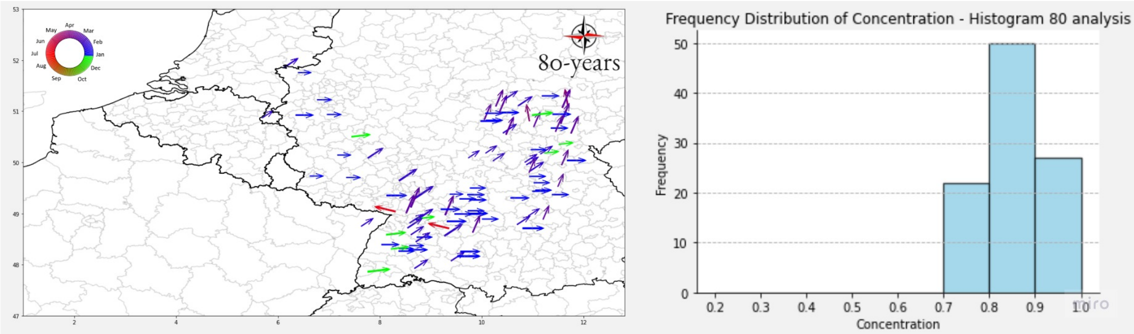

Figure A3.2: Concentration map for the 80 years of analysis (1942 - 2021) - Dominant month of the Maxima discharges.

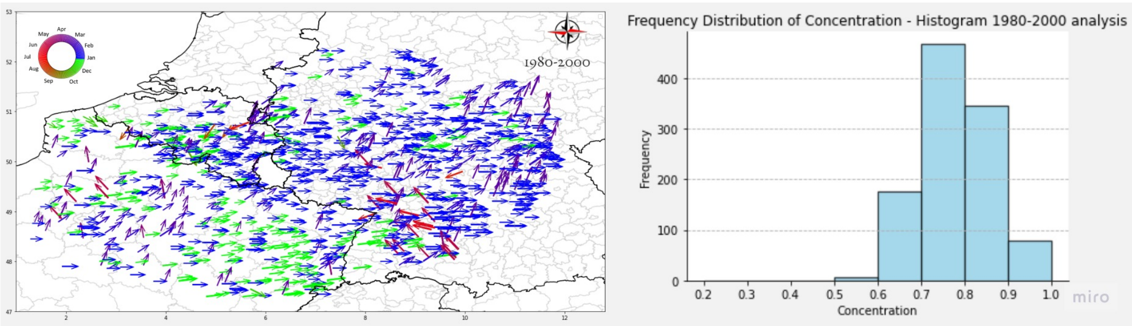

Figure A3.3: Concentration map for the time period from 1980-2000 - Dominant month of the Maxima discharges.

A4 Minima analysis

Respectively, the concentration maps were created for 60 and 80 years of analysis.

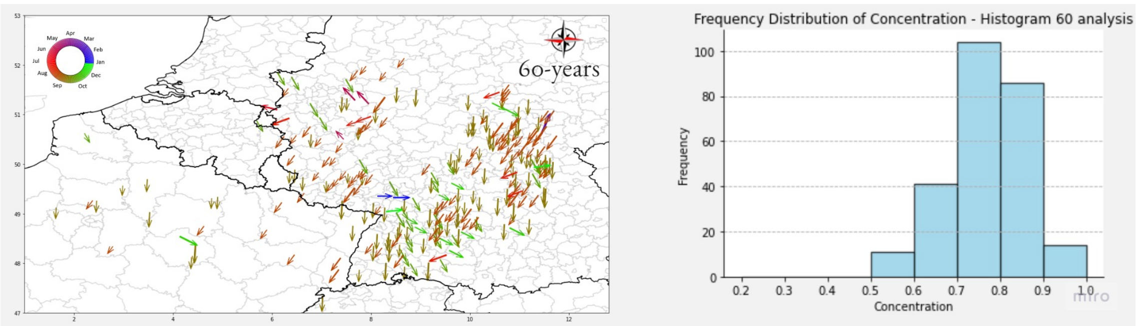

Figure A4.1: Concentration map for the 60 years of analysis (1962 - 2021) - Dominant month of the Minima discharges.

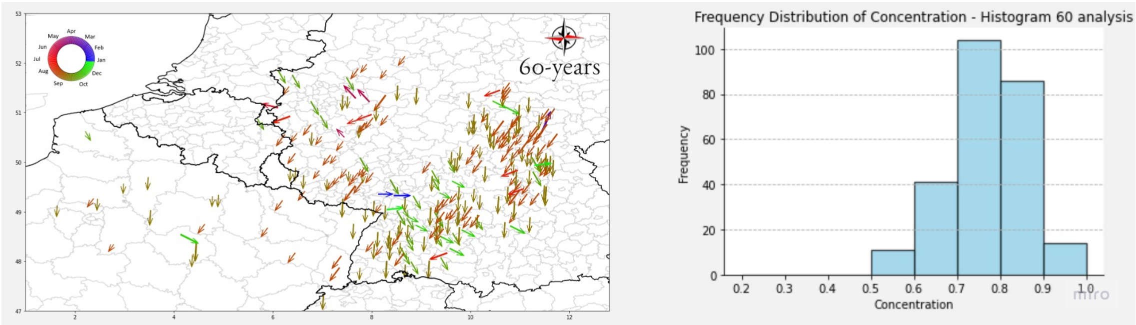

Figure A4.2: Concentration map for the 80 years of analysis (1942 - 2021) - Dominant month of the Minima discharges.

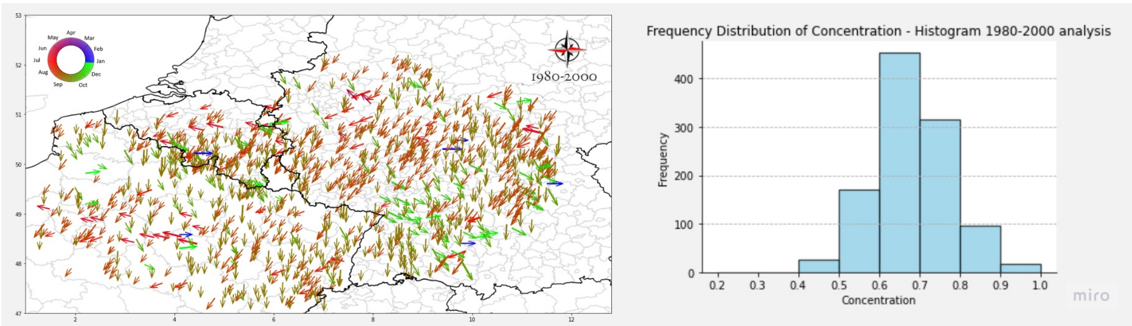

Figure A4.3: Concentration map for the time period from 1980-2000 - Dominant month of the Minima discharges.